SEPARATION OF MACROMOLECULES FROM AQUEOUS SYSTEMS USING ELECTROSPUN FIBERS

A Thesis Submitted to
the Graduate School of Engineering and Sciences of
İzmir Institute of Technology
in Partial Fulfilment of the Requirements for the Degree of

DOCTOR OF PHILOSOPHY

in Materials Science and Engineering

by
Tuğba ISIK

November 2018
İZMİR

We approve the thesis of **Tuğba ISIK**

Examining Committee Members:

Prof. Dr. Mustafa M. DEMİR
Department of Materials Science and Engineering, İzmir Institute of Technology

Prof. Dr. Sacide ALSOY ALTINKAYA
Department of Chemical Engineering, İzmir Institute of Technology

Assoc. Prof. Dr. Ümit Hakan YILDIZ
Department of Chemistry, İzmir Institute of Technology

Assist. Prof. Dr. Erdal EROĞLU
Department of Bioengineering, Manisa Celal Bayar University

Assist. Prof. Dr. Ozan KARAMAN
Biomedical Engineering, İzmir Katip Çelebi University

30 November 2018

Prof. Dr. Mustafa M. DEMİR
Supervisor, Department of Materials Science and Engineering
İzmir Institute of Technology

Prof. Dr. Mustafa M. DEMİR
Head of the Department of Materials Science and Engineering

Prof. Dr. Aysun SOFUOĞLU
Dean of the Graduate School of Engineering and Sciences

ACKNOWLEDGEMENTS

I would never have been able to finish my thesis without the guidance of my committee members, help from friends, and support from my family.

Firstly, I would like to express my gratitude to my advisor, Prof. Mustafa M. Demir, for his instructive comments, patience, confidence and providing me with a suitable atmosphere for doing this research.

Dr. Nesrin Horzum Polat, *my academic sister*, is not only my co-advisor with her great comments and suggestions to this thesis, but also she is like a sister for her friendly, warm and emotional supports during this research.

Besides my advisors, I would like to thank the rest of my thesis committee: Prof. Sacide Alsoy Altınkaya and Dr. Ü. Hakan Yıldız for accepting to be in my committee, and also for their insightful comments, feedback and encouragements for this thesis. I also want to thank to Prof. Yusuf Yağcı and Prof. Tamer Uyar because of their collaborations.

I am as well thankful to the specialists at İYTE-Environmental Research Center for the ICP-MS analysis, at Izmir Institute of Technology Biotechnology and Bioengineering Research and Application Centre for UV analysis, and at İYTE-Center of Materials Research for the material characterization.

I also thank to the members of Demir Research Group for their supports during this research. A special thanks to faculty members of Materials Science and Engineering and research assistants of Chemistry Department for sharing their knowledge.

I owe very special thanks to Yekta Arya Ölçer for being my sister and my best friend from high school years. I also thank to my best friends Öykü Mehrioğlu, Gözde Duman, Zekiye Bayındır and Özgü Yıldırım even if we are away from each other. I also thank to my other friends that I could not count their name here, sincerely.

Most importantly, I would like to thank my lovely family: my parents and my brother for supporting me spiritually throughout writing this thesis and my life in general. This thesis is dedicated to them who have given me their unconditional support, both financially and emotionally throughout my degree.

Finally, but in the first place of my mind, I would like to thank the man who always supports and motivates me in my decisions: my love and my *'future husband'* Ali Kandemir for his warm love and for being always on my side during this thesis process.

ABSTRACT

SEPARATION OF MACROMOLECULES FROM AQUEOUS SYSTEMS USING ELECTROSPUN FIBERS

Electrospinning has been recognised as a versatile method for the fabrication of continuous polymeric fibers with various type of morphology. Since it allows changing the fiber diameter, surface morphology and porosity by adjusting the solution and instrumental parameters, electrospun fibers present a wide range of properties that cannot be found in bulk materials. Through this thesis, removal of several types of pollutants from the aqueous systems was studied by using the electrospun fibers fabricated from both virgin and waste polymers.

The first part of the dissertation deals with the removal of macromolecular pollutants from aqueous systems by using waste-based electrospun fibers. Electrospun fibers fabricated from CD cover and expanded polystyrene wastes were utilized for the *protein-rich medical waste treatment* by using Bovine Serum Albumin, Myoglobin and Trypsin as protein models. Electrospun fibers from expanded polystyrene wastes were utilized for the *remediation of oily wastewaters*.

The second part of the dissertation deals with the *polyatomic nuclear waste removal* using uranyl ions as analyte and amidoxime functionalized PIM-1 electrospun fibers.

The last part of this dissertation describes an approach for the *fabrication of fluorine-free hydrophobic surfaces* by electrospraying of methacrylate based linear and hyperbranched copolymers.

ÖZET

ELEKTROEĞİRME LİFLERİ KULLANARAK MAKROMOLEKÜLLERİN SULU SİSTEMLERDEN AYRILMASI

Elektrodokuma, çeşitli morfolojiye sahip polimerik liflerin üretilmesi için çok yönlü bir yöntemdir. Çözelti ve enstrümantal parametrelerin değiştirilmesiyle lif çapı, yüzey morfolojisi ve gözeneklilik gibi çeşitlendirilmesine izin verdiğinden, elektrodokuma lifler yığın malzemelerde bulunamayan çok çeşitli özellikler sunarlar. Bu tezde, hem ticari hem de atık polimerler kullanılarak üretilen elektrodokuma lifler kullanılarak sulu sistemlerden çeşitli kirletici türlerinin uzaklaştırılması incelenmiştir.

Tezin ilk kısmı, atık bazlı elektrodokuma lifler ile makromolekül yapıdaki kirletici maddelerin sulu sistemlerden uzaklaştırılması ile ilgilidir. CD kapağı ve strafor atıklarından üretilen elektrodokuma lifler ile Bovin Serum Albümin, Miyoglobin ve Tripsin model proteinleri kullanılarak hazırlanan protein zengini tıbbi atıklar temizlendi. Strafor atıklardan üretilen elektrodokuma lifler ile yağlı atık sular iyileştirildi.

Tezin ikinci kısmı, amidoksim grubu kullanılarak fonksiyonel hale getirilmiş PIM-1 lifleriyle radyoaktif uranyum iyonlarının sulu sistemlerden giderilmesiyle ilgilidir.

Bu tezin son kısmı, metakrilat bazlı lineer ve dallanmış kopolimerlerden elektrodokuma ile hidrofobik yüzeylerin üretilmesine yönelik bir yaklaşımı anlatmaktadır.

Dedicated to my family and Ali

TABLE OF CONTENTS

LIST OF FIGURES x

LIST OF TABLES xv

LIST OF ABBREVIATIONS xvi

CHAPTER 1. INTRODUCTION 17

1.1. Motivation 17

1.2. Scope of thesis 17

1.3. Electrospinning 18

1.4. Recycling of plastics for adsorbent fabrication 22

CHAPTER 2. PROTEIN-RICH MEDICAL WASTE TREATMENT VIA WASTE ELECTROSPINNING 25

2.1. Introduction 26

2.2. Experimental Section 28

2.3. Results and Discussion 30

2.4. Conclusion 42

CHAPTER 3. OIL REMOVAL EFFICIENCY OF PS FIBERS WITH VARIOUS MORPHOLOGIES 43

3.1. Introduction 43

3.2. Experimental 45

3.3. Effect of Solvent Composition on The Oil Adsorption Capacity of PS Fibers. 46

3.3.1. Results and Discussion 48

3.4. Recycling of Expanded Polystyrene by Electrospinning: Instead of Landfill Remediate Oily Wastewaters 56

3.4.1. Results and Discussion 57

3.5. Conclusion 73

CHAPTER 4. REMOVAL OF URANIUM IONS FROM AQUEOUS SYSTEMS VIA AMIDOXIMATED PIM-1 FIBERS 75

4.1. Introduction 75

4.2. Experimental 77

4.3. Results and Discussion 80
4.4. Conclusion 87

CHAPTER 5. HYDROPHILIC TO HYDROPHOBIC CONVERSION OF PHOTOCHEMICALLY PREPARED METHACRYLATE-BASED POLYMERS WITH VARIOUS CHAIN ARCHITECTURES 88
5.1. Introduction 89
5.2. Experimental 91
5.3. Results and Discussion 91
5.4. Conclusion 98

CHAPTER 6. EVALUATION AND OVERALL CONCLUDING REMARKS 100

REFERENCES 102

LIST OF FIGURES

Figure **Page**

Figure 1.1. Schematic representation of electrospinning set up 20

Figure 1.2. SEM micrograph of (a) Linear poly(hydroxyethyl methacrylate-co - methylmethacrylate) beads from DMF solution, (b) beads-on-string polystyrene fibers from DMF solution, (c) ribbon-like polystyrene fibers from THF solution, and (d) uniform gelatine fibers in acetic acid solution. 21

Figure 1.3. Schematic representation of Taylor cone at low and high level voltages during the electrospinning process. 21

Figure 1.4. Potential applications of electrospun nanofibers 22

Figure 2.1. Schematic representation of the purpose of the study 25

Figure 2.2. SEM micrographs of electrospun fibers fabricated from vir-PS, f-PS and CD-PS from 10, 15 and 20 wt% polymer solutions. Insets show higher magnification image of the electrospun fibers 32

Figure 2.3. AFD of the electrospun fibers obtained at different polymer solution concentration 33

Figure 2.4. BET nitrogen adsorption results of vir-PS-10, f-PS-10 and CD-PS-10 electrospun fibers. 34

Figure 2.5. TGA curves of virgin and waste PS fibers 35

Figure 2.6. XPS spectra of vir-PS, f-PS and CD-PS electrospun fibers. Inset indicates Ca (2p) spectra of CD-PS fibers 35

Figure 2.7. FTIR-ATR spectra of com-PS, f-PS and CD-PS electrospun fibers 36

Figure 2.8. XRD profiles of com-PS, f-PS and CD-PS electrospun fibers 37

Figure 2.9. Calibration graphs of BSA, MYO, and TRY solutions. 37

Figure 2.10. Quantity of adsorbed **(a)** BSA, **(b)** MYO, and **(c)** TRY molecules at pH 7.4 on vir-PS, f-PS, and CD-PS electrospun fibers fabricated at different PS concentration in DMF:THF 38

Figure 2.11. BSA adsorption at various concentrations on the adsorption capacity of the PS fibers**.** Inset shows the SEM micrograph of PS/$CaCO_3$ fibers prepared in the lab for comparison 39

Figure 2.12. The size distributions of PS/$CaCO_3$ **(a)** beads and **(b)** fibers prepared by PS solution with 10 wt% polymer content and 10 wt% of $CaCO_3$ filler 40

Figure 3.1. SEM micrographs of vir-PS fibers with respect to different solvent compositions and vir-PS solution concentrations (Scale bar is 10 μm). 48

Figure 3.2. Schematic representation of phase separation that solvent-rich domain consists of a small amount of polymer and polymer-rich domain consists of small portion of solvent 50

Figure 3.3. AFD of vir-PS fibers with respect to various solvent compositions and PS concentrations. 51

Figure 3.4. Dependence of vir – PS fiber morphology on DMF: THF composition versus PS concentration. 52

Figure 3.5. WCA of vir-PS fibers from various compositions. 54

Figure 3.6. (a) Oil adsorption performance of vir-PS electrospun fibers with respect to solvent composition and initial PS concentration, SEM micrographs that show intrinsic porosity of vir-PS fibers fabricated from (b) 3:1 and (c) 1:3 DMF to THF ratio. 55

Figure 3.7. Oil separation efficiency of vir-PS fibers from oil contaminated water mixtures with respect to sunflower oil concentration. 55

Figure 3.8. SEM micrographs of f-PS fibers with respect to different solvent compositions and f-PS solution concentrations (Scale bar is 10 μm). 59

Figure 3.9. Dependence of surface texture on DMF:THF composition versus f-PS solution concentration (solid lines were estimated by using the SEM micrographs in Figure 3.8). 62

Figure 3.10. Cross-sectional SEM micrographs of the fibers fabricated from 20 wt% f-PS solutions with various solvent compositions of DMF:THF ratio **(a)** 1-0, **(b)** 3-1, **(c)** 1-1, **(d)** 1-3, and **(e)** 0-1. 63

Figure 3.11. (a) Water contact angle comparison of the f-PS adsorbents fabricated from different solvent combinations with 20wt% solution concentration, photographic images of water and oil droplets on (b) pristine foam and (c) f-PS fiber. (The numbers in parenthesis indicate the solvent composition, DMF-THF ratio.)..... 64

Figure 3.12. WCA hysteresis of f-PS fibers and their comparison with foam. 65

Figure 3.13. Oil adsorption variation of electrospun f-PS fibers with respect to (a) contact time and (b) drain out time..... 66

Figure 3.14. Pseudo first order plots of f-PS-10 and f-PS-20 adsorbents..... 66

Figure 3.15. Vegetable oil adsorption capacity of f-PS electrospun fibers with respect to solvent composition and initial PS concentration. The letters '**xx**' refer to the absence of data points in the dataset probably due to the polymer cup formation and beads on string instead of fibers..... 68

Figure 3.16. Comparison of the vegetable oil adsorption capacity of pristine foam, commercial adsorbent and f-PS fibers fabricated from 1:3 (DMF:THF) solvent system. Insets show the SEM micrographs of pristine foam and commercial adsorbent..... 69

Figure 3.17. The adsorption processes of (a) vegetable oil and (b) engine oil using the as-prepared f-PS adsorbent with 5% oil-polluted water. 70

Figure 3.18. (a) Oil separation efficiency of electrospun fibers using vegetable oil, photographs of oil-water mixture (b-c) before adsorption, (d) after

adsorption, optical micrographs of mixture (e) before adsorption, and (f) after adsorption of 5 % oil polluted water. 71

Figure 3.19. Oil separation efficiency comparison of pristine foam, commercial adsorbent and proposed f-PS fiber (1:3) by using vegetable oil, engine oil, and real oily wastewater sample. 72

Figure 4.1. The photographic representation of experimental set-up. 78

Figure 4.2. Speciation diagram of U(VI) between a pH range (a) 2.0 to 14.0 and (b) 3.0 to 7.0 79

Figure 4.3. SEM micrographs of (a-b) PIM-FM and (c-d) AF-PIM-FM fibers (insets show the fiber diameter distributions). 81

Figure 4.4. Structure of fibrous membranes before and after functionalization and their speculative binding mechanism to uranyl ions. 81

Figure 4.5. Batch adsorption study of amidoxime functionalized PIM-1 powder (blue) and membrane (green) using stirrer and shaker. Red dashed lines show the initial uranyl solution concentration. 82

Figure 4.6. Column adsorption study of U(VI) as a function of pH. 83

Figure 4.7. Column adsorption study of U(VI) as a function of initial concentration in terms of (a) µg U(VI) / g fiber and (b) % sorption. 84

Figure 4.8. Variation of percentage sorption of uranyl ions with the number of repetitive uses of the same fibrous sorbent at 5 ppm U(VI) concentration. 85

Figure 4.9. Percentage uranyl desorption as a function of time for PIM-FM and AF-PIM-FM. 85

Figure 4.10. Consecutive sorption / desorption cycles of fibrous membranes for 5 ppm U(VI) solution using 1 M $NaHCO_3$ as the desorbing agent. 86

Figure 5.1. Schematic representation of the purpose of the study 88

Figure 5.2. SEM micrographs of copolymers (a) Lin-PH1 drop cast, (b) Hyp-PH1 drop cast, (c) Lin-PH1 electrospray, and (d) Hyp-PH1 electrospray samples. Insets show profiles of water droplets with their water contact angles. (e) Water contact angle comparison of Lin-PH1 and Hyp-PH1 samples. 92

Figure 5.3. Bead size distributions of (a) Lin-PH1, (b) Lin-PH2, (c) Lin-PD1, (d) Lin-PD2, (e) Hyp-PH1, (f) Hyp-PH2, and (g) Hyp-PD2 electrospray samples. 93

Figure 5.4. SEM micrographs of co-polymers **(a)** Lin-PD2 drop cast, **(b)** Hyp-PD1 drop cast, **(c)** Lin-PD2 electrospray, and **(d)** Hyp-PD1 electrospray samples. Insets show profiles of water droplets with their water contact angles. **(e)** Water contact angle comparison of Lin-PD2 and Hyp-PD1 samples..... 94

Figure 5.5. SEM micrographs and WCA profiles of **(a)** Lin-PH1, (**b)** Lin-PH2, **(c)** Hyp-PH1 and **(d)** Hyp-PH2 copolymers. 95

Figure 5.6. XPS spectra of **(a)** Lin-PH1 and **(b)** Hyp-PH1 copolymers. Insets show (1) drop cast and (2) electrospray samples. 96

Figure 5.7. SEM micrographs and water contact angle profiles of Lin-PH2 coatings prepared by **(a)** drop casting, **(b)** 45 w/v% and **(c)** 15 w/v% electrospraying. 98

LIST OF TABLES

Table **Page**

Table 2.1. The solution properties (conductivity and viscosity) of PS samples at different concentrations 31

Table 2.2. BET surface area of com-PS, f-PS, CD-PS and PS/$CaCO_3$ electrospun fibers extracted from BET isotherms 34

Table 2.3. Energy Dispersive X-Ray Spectroscopy (EDX) results of electrospun fibers 36

Table 2.4. Analytically calculated Langmuir and Freundlich adsorption isotherm constants for BSA adsorption on PS fibers [a] 41

Table 3.1. Properties and oil adsorption capacities of vir-PS fibers. 53

Table 3.2. The characteristics of PS solutions and the resulting electrospun PS fibers. 58

Table 3.3. Analytically calculated Pseudo first order constants for oil adsorption on PS fibers. 67

Table 3.4. Comparison of oil adsorption capacities of polymeric electrospun fibers. ... 73

Table 4.1. ICP-MS operation parameters. 79

Table 5.1. Surface chemical compositions of linear and hyperbranched copolymers calculated from C(1s) and O(1s) XPS spectra. 97

LIST OF ABBREVIATIONS

AFD	average fiber diameter
BET	Brunauer-Emmett-Teller
BSA	Bovine Serum Albumin
CD-PS	CD waste polystyrene
DMF	*N,N*-dimethylformamide
EDX	energy dispersive X-ray
EPS	expanded polystyrene
FTIR	Fourier transform infrared spectrometer / spectrometry
f-PS	foam waste polystyrene
Hyp-PD1	hyperbranched P(DMAEMA-*co*-MMA
Hyp-PH1	hyperbranched P(HEMA-*co*-MMA)
ICP-MS	inductively coupled plasma-mass spectrometer / spectrometry
Lin-PD1	linear P(DMAEMA-*co*-MMA
Lin-PH1	linear P(HEMA-*co*-MMA)
Mw	Molecular weight
MYO	myoglobin
NMR	nuclear magnetic resonance
PEG	polyethylene glycol
PIM-1	polymers of intrinsic microporosity
PS	polystyrene
RH	relative humidity
SEM	scanning electron microscope / microscopy
TGA	thermogravimetric analysis
THF	Tetrahydrofuran
TRY	Trypsin
TIPS	thermally induced phase separation
VIPS	vapour induced phase separation
vir-PS	virgin polystyrene
XPS	X-ray photoelectron spectroscopy
XRD	X-ray diffraction
WCA	Water contact angle

CHAPTER 1

INTRODUCTION

1.1. Motivation

Water pollution is a global threat and its significance is increasing gradually due to the anthropogenic activities, urbanization, and industrialization. By virtue of the dispensability of water, remediation of the water sources from pollutants becomes a challenging task. Today's technology offers the opportunity for the design and fabrication of desired adsorbent materials with high surface area and these materials take place in various environmental remediation applications such as treatment of oily waters, removal of heavy metal ions, and elimination of biological pollutants from wastewaters. Recently, electrospun nanofibrous membranes have gained a great attention due to their high surface area, diversified morphology, and durability. The interconnected webs and porosity of electrospun fibers create a suitable media for the filtration and adsorption applications (Gopal et al. 2006, Horzum et al. 2010, Horzum et al. 2013, Horzum et al. 2012, Isik and Demir 2018, Isik et al. 2016, Lalia et al. 2013, Yoon, Hsiao, and Chu 2008, Yoon et al. 2006). On the other hand, plastic pollution is another environmental concern that plastic consumption increases dramatically. Plastic wastes are discarded generally after their first usage and caused to overflow in the landfill sites (MacArthur 2017a, Hopewell, Dvorak, and Kosior 2009). Thus, recycling of the daily waste plastics requires a significant attention. Through this thesis, the main motivation is based on the development and fabrication of electrospun fibrous adsorbents for the remediation of wastewaters from organic and inorganic pollutants. Additionally, recycling of plastic wastes and fabrication of adsorbent materials for polluted water remediation were handled as another point of motivation.

1.2. Scope of thesis

The first (*Chapter 1*) part of thesis comprises a general introduction to the subject, which describes the general equipment of the thesis (electrospinning) and the

perspective of plastic recycling in terms of adsorbent fabrication for remediation of wastewaters. The following parts of the thesis were organized in the same manner starting with a theoretical section and following by experimental details, discussion of the results and main conclusion of the chapter.

The second part of the study (*Chapter 2*) deals the disposal of medical wastes by using electrospun adsorbents, which were fabricated from waste CD covers. The adsorption capacity of adsorbents was compared with virgin polystyrene and waste expanded polystyrene by using Bovine Serum Albumin (BSA), Myoglobin and Trypsin. The fabricated adsorbents provide an efficient separation tool for BSA molecules due to the calcium carbonate moieties in CD cover wastes. In *Chapter 3*, by changing the solvent composition of polymer solution, the porosity of polystyrene fibers is enhanced. Moreover, porous expanded polystyrene fibers were obtained by electrospinning of polystyrene in different solvent compositions. All of the resulting adsorbents were used for the remediation of oily wastewater systems. In *Chapter 4*, PIM-1 polymer was modified with amidoxime groups and the sorption efficiency of modified fibers were determined for the removal of radioactive U(VI) ions from aqueous systems. In *Chapter 5*, the methacrylate based linear and hyperbranched copolymer solutions were subjected to electrospraying process for the generation of hydrophobic surfaces. The last (*Chapter 6*) part of the thesis is a conclusive chapter that summarizes the purpose and results.
The main purpose of this study is to show the pollutant removal application of electrospun polymers from both virgin and waste polymers with different morphology and investigate the influence of surface texture on the sorption efficiency of resulting materials.

1.3. Electrospinning

The basis of electrospinning, which dates back to early 1700's that the generation of aerosols under high electrical potential to drops, was described and studies followed by the investigation of required amount of charge to overcome the surface tension of a drop by Lord Rayleigh (Rayleigh 1882). In the early 1900's, the first devices were patented to spray liquids through the electrical field and artificial silk was fabricated in 1929 by using electrical charge (Kiyohiko 1929). In 1934, electrospinning of plastics was described first time and Simm *et al.* patented the

fabrication of fibers with diameters less than 1 μm in 1972 (Anton 1929, Simm et al. 1972). Then, a substantial attention have been gained by electrospinning in 1990's by Reneker group that fundamental and application based researches from different disciplines was combined (Zacharides et al. 1995). Electrospinning provides ultrathin and continuous fibers from solutions, suspensions and melts from a variety of materials and can be applied to both synthetic and natural polymers. Firstly, polymers were employed as fiber forming materials and then materials like metals, ceramics, and glasses were considered as fiber precursors. Moreover, it is an easily controlled process for the fabrication of nanostructured systems with specific surface topographies (Demir et al. 2002). The characteristics of polymers significantly change by tuning the diameter of fibers from micrometer to nanometer due to the large surface area to volume ratio, flexibility and mechanical performance. Electrospinning could be performed with not only polymer-based sources but also inorganic, metal and ceramic fibers could be fabricated (Greiner and Wendorff 2007). Furthermore, the process gives access to functionalize the fibers with several functionalization agents via pre / post modification methods. Due to its versatility, the applications of electrospinning have been expanded to the fields of energy storage, biomedicine, tissue engineering, cell adhesion, sensor applications, catalytic applications and filtration (Wu et al. 2013, Berber et al. 2016, Celik et al. 2017, Demirkurt et al. 2018, Guner et al. 2018, Horzum et al. 2016, Incel et al. 2017, Boyaci et al. 2013, Horzum et al. 2014).

Figure 1.1 shows the typical electrospinning set up with a horizontal arrangement of electrodes. There are three basic components to complete the set-up: a high voltage power supply generally with a direct current (DC) potential, a capillary tube with a pipette or conductive needle of small diameter, and a metal collecting screen. The polymer solution is pumped through the capillary nozzle, which serves as an electrode, and a high voltage is applied to create charged jet on the tip of the needle. Generally, a high electric field of 1.0 – 5.0 kV cm^{-1} is applied and tip to collector distance is settled as 10 – 25 cm in the set-up. The flowing current ranges from a few hundred nanoamperes to microamperes. Then, the polymer solution evaporates and solidifies throughout the electric field and electrospun fibers are collected on the grounded collector (Huang et al. 2003).

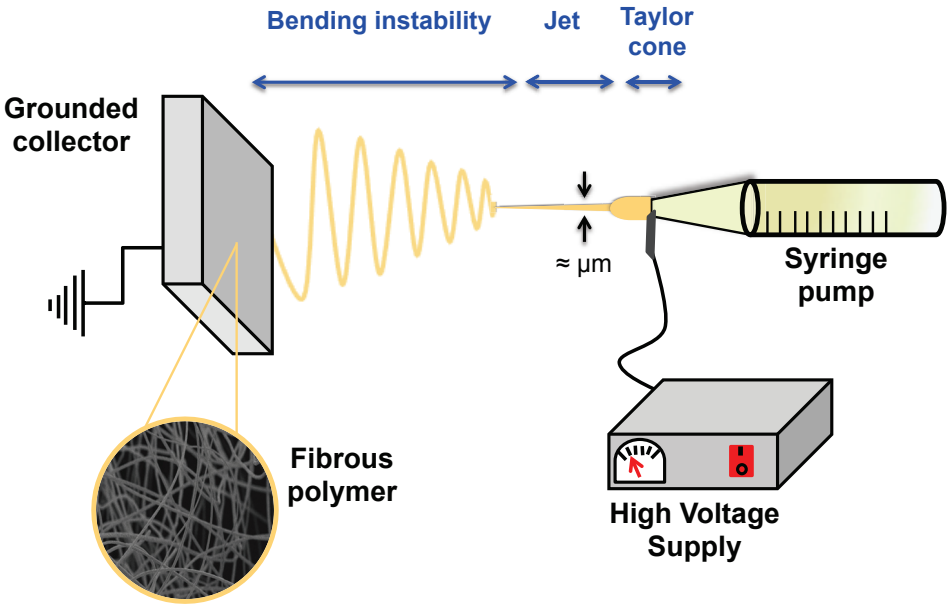

Figure 1.1. Schematic representation of electrospinning set up

Properties of the polymer solution (concentration, viscosity, vapour pressure, and surface tension) have the biggest influence on the morphology of the fibers during the electrospinning. Formation of beads or bead-on-string structures rather than fibers has been observed occasionally during the electrospinning process (Figure 1.2a-b). Many authors describe that the presence of bead or bead-on-string structures is an undesirable condition but Isık *et al.* proposed that presence of these characteristics enhances the roughness of the surfaces by showing more hydrophobic behaviour (Isik et al. 2017). The reason of this bead formation is based on the instability of the jet of polymer solution. Rutledge and his colleagues investigated the mechanism of instabilities during the electrospinning and predicted three different instabilities: two axisymmetric and one non-axisymmetric modes (Shin et al. 2001b, a, Hohman et al. 2001a, b). The axisymmetric modes are responsible for the bead formation that Rayleigh instability is the most likely reason. Rayleigh instability is dominated by the surface tension and increasing surface tension favours the instability. The bead formation is favoured by high surface tension of polymer solution that surface tension tries to make the area per unit mass smaller by changing the jet into spheres (Zuo et al. 2005). In some instances, the fibers could be observed as ribbon-like structures due to the rapid drying and collapse of jet (Liu, Huang, and Jin 2015) (Figure 1.2c). Moreover, the uniform and thin fibers could be fabricated by choosing the suitable solvent and concentration combination for each polymer type (Figure 1.2d).

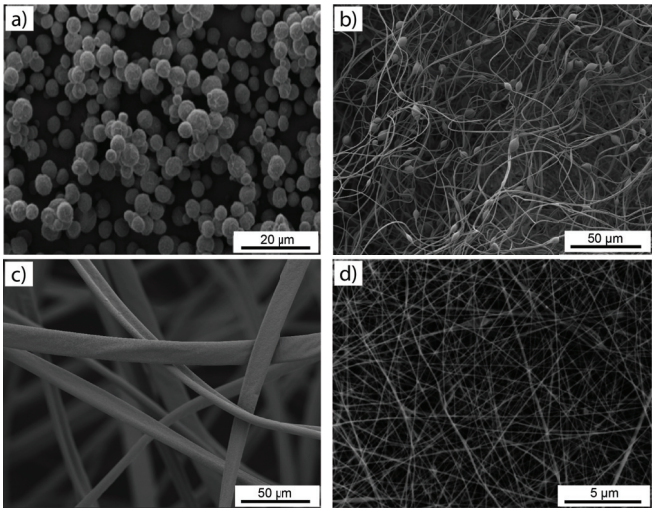

Figure 1.2. SEM micrograph of (a) Linear poly(hydroxyethyl methacrylate-co - methylmethacrylate) beads from DMF solution, (b) beads-on-string polystyrene fibers from DMF solution, (c) ribbon-like polystyrene fibers from THF solution, and (d) uniform gelatine fibers in acetic acid solution

During the electrospinning process, the applied electrical field results in the formation of a cone-shaped deformation of the polymer drop on the tip of the needle. At appropriate voltage, the shape of the cone changes and the jet formation occurs. When the voltage excesses the required value for process conditions, the multiple jets are formed (Korycka et al. 2018) (Figure 1.3). On the way to the grounded collector, the solvent of the polymer solution evaporates and solid fibers are precipitated while the velocity of jet reaches up to 40 m s^{-1} (Greiner and Wendorff 2007).

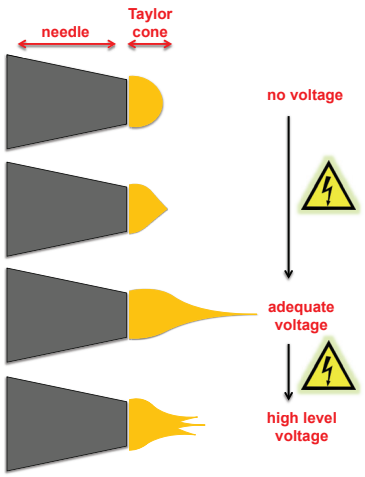

Figure 1.3. Schematic representation of Taylor cone at low and high level voltages during the electrospinning process

Electrospinning technique is a considerably simple route for the generation of fibers with diversified morphology and properties. Thanks to the unique and practical features of electrospun fibers, they are attractive for the numerous applications as shown in Figure 1.4. Filtration and adsorption applications of electrospun fibers were focused on throughout the thesis.

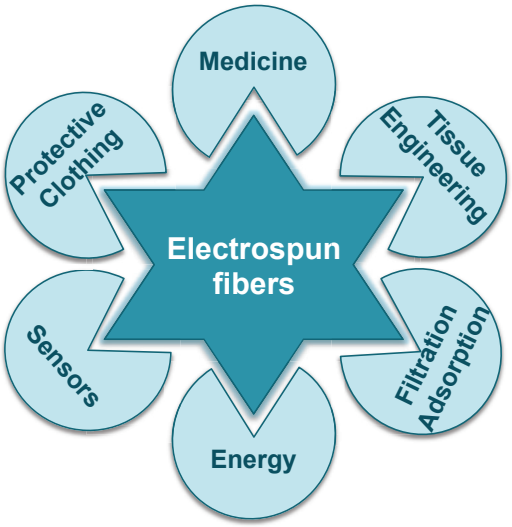

Figure 1.4. Potential applications of electrospun nanofibers

1.4. Recycling of plastics for adsorbent fabrication

When the limited availability of finite sources on earth was concerned, recycling of discarded waste products becomes crucial and plastics are the main targets due to their pollution problem and slow degradation under natural conditions (Teo 2018). Among the various recycling methods, electrospinning is a feasible and facile method for the fabrication of fibrous materials from feed materials with impurities. This method abolishes the obstacles of traditional methods such as purification of feed material before usage. Moreover, the resulting fibrous materials could be used in several applications due to the diversified process parameters following by a large variety of material properties. Esmaeili *et al.* reported the recycling of PET, PS and PC wastes by changing various operational parameters and demonstrated the significant effect of applied voltage on average fiber diameter (Esmaeili, Deymeh, and Rounaghi 2017). Moreover, recycling of PS wastes has been shown by several studies in the literature

and useful products could be easily converted from waste products (Shin and Chase 2005, Shin 2005, Munir et al. 2014, Zulfi et al. 2017). Beside the synthetic polymers, natural polymers have also been recycled that chicken feathers have been used for the extraction of keratin protein. However, blending the keratin with other biodegradable polymers is required due to the low molecular weight of keratin itself (S.K., , and Krati 2013). Cellulose is another abundant biopolymer in the nature and electrospun fibers fabricated from cellulose have been gaining attention due to its unique structure (Kalaoglu, Unlu, and Atici 2016).

Oil-spills, heavy metals, dyes and other hazardous chemicals contaminate the water sources rapidly due to the growing urbanization in recent decade. Thus, removal of these pollutants becomes crucial to protect the environment and maintain the sustainability of world. Water remediation could be carried out by adsorption, biotechnology, catalytic processes, membrane processes, and magnetically assisted processes (Khin et al. 2012). However, adsorption based processes are the most frequently studied ones for the water remediation and various types of these materials have been used in the literature such as beads, granules, powders, fibers and flakes (Santhosh et al. 2016). Simply, adsorption process is a kind of mass transfer that pollutants from the solution are transferred onto the sorbent surface. The most important key factors that play significant role in suitable adsorbent selection are their cost effectiveness and applicability. Thus, adsorbent fabrication from the waste materials has been gaining attention that low cost adsorbents could be fabricated while the waste materials could be reused. On the other hand, application of nanoparticles or powders is difficult during the adsorption process because separation of the adsorbent materials after remediation requires another process. Therefore, electrospun fibers are encouraging materials for water remediation applications.

PET bottles are the most common waste plastics and they are discarded after their single usage. When the contamination level of waste plastics is considered, PET bottles are extremely clean wastes among the others. In literature, large quantities of PET fibers were fabricated to filter the polycyclic aromatic compounds in tobacco smoke. (Strain et al. 2015) Zander *et al* have also demonstrated the filtration efficiency of PET bottles with 99% efficiency (Zander et al. 2015). After modification of PET fibers with chitosan, removal of Cr (VI) ions from wastewaters were studied by Khorram *et al*. (Khorram, Mousavi, and Mehranbod 2017). Separation of oil-water mixtures by using glass fiber media supplemented recycled PS fibers was demonstrated

by Shin *et al*. (Shin 2006, Shin, Chase, and Reneker 2005). Also, recycling of High Impact PS (CD case) and EPS electrospun fibers for the removal of infectious clinical wastes was reported by Isık *et al.* that the additives found in waste CD cases enhanced protein adsorption capacity (Isık and Demir 2018). In another study, keratin / polyamide 6 blend nanofibers were fabricated by Aluigi *et al.* that their water and air cleaning ability were investigated with chromium ions and airborne formaldehyde (Aluigi et al. 2009). Bio-based functional fibers were also fabricated by Woranuch *et al.* that starch blended polyvinyl alcohol electrospun fibers were used for volatile organic compound adsorption (Woranuch et al. 2017).

CHAPTER 2

PROTEIN-RICH MEDICAL WASTE TREATMENT VIA WASTE ELECTROSPINNING

Medical wastes are infectious clinical wastes (blood, saliva, urine) due to their high pathogenic content. Incineration is the most commonly used method in waste management that possess high water content along with molecularly dissolved species such as proteins. The process is costly; so that the removal of solid content dissolved in aqueous part by preliminary filtration can reduce the volume of the waste material. In this study, fibrous mats were prepared by electrospinning of PS wastes from DMF and THF solutions (Figure 2.1). Then they are employed in the removal of protein-based solid contents of medical wastes before their disposal.

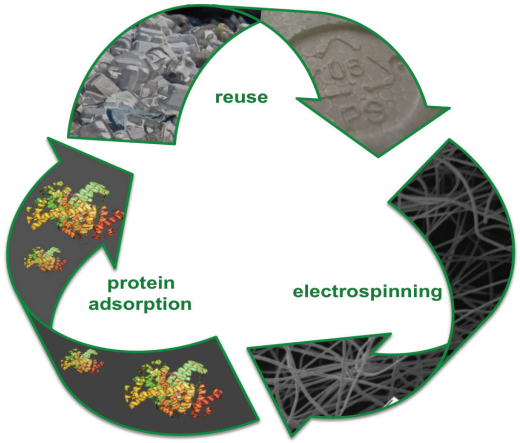

Figure 2.1. Schematic representation of the purpose of the study

Two sources of PS waste (CD cover and Styrofoam) were employed along with virgin PS for comparison. The adsorption capacity of as-prepared electrospun fibers was examined for three model proteins: Bovine Serum Albumin (BSA), Myoglobin (MYO), and Trypsin (TRY). The fibers obtained from PS CD wastes have remarkably larger protein sorption capacities (particularly BSA) than the fibers obtained from virgin PS. XPS reveals the presence of $CaCO_3$ domains in CD covers added into PS during their production steps to increase mechanical properties. There may be an electrostatic

interaction between Ca^{2+} and the negatively charged groups of the protein. In this way, PS wastes could be converted to a beneficial secondary product by electrospinning and also resulting materials promises for the disposal of medical wastes. This may be one of the frontiers study on the removal of medical wastes from adsorbents produced by electrospinning of waste polymers.

2.1. Introduction

The management of the medical wastes is one of the demanding challenges humanity facing as population increases. When these wastes are not properly handled, they represent a high risk of infection or injury to healthcare personnel and also to the general public. Because of these concerns, there is a worldwide awareness about the effective control and safe handling of these wastes (Park et al. 2009, WHO 2015, Hossain et al. 2013, Windfeld and Brooks 2015, WHO 2005). Over the total amount of medical wastes, 85% of them are non-hazardous while 15% of them are considered hazardous that might be infectious, toxic or radioactive. However, both hazardous and non-hazardous wastes were generally mixed and disposed together so that the hazardous waste amount increases (WHO 2015). Among the various types of medical wastes, blood wastes come in to prominence due to their enormous generation and the presence of appropriate nature for the growth of pathogens (Hossain et al. 2016). Landfilling, steam autoclave sterilization, and incineration are the main methods currently being used and considered technologies for the disposal of medical wastes (Zhao et al. 2009). Landfilling of medical wastes with large amounts is not recommended, because the hazardous substances could contaminate the groundwater and they require large empty spaces (Pruss, Giroult, and Rushbrook 1999). In sterilization, the volume of wastes is limited with the size of autoclave, i.e. it requires running the system many times one after the other suggesting a tedious process. Incineration, on the other hand, appears out the unavoidable solution for the management of medical disposal. However, medical waste contains about 92% water that increases the cost of this process (WHO 2005, Pruss, Giroult, and Rushbrook 1999). The isolation of solid content of fluid wastes prior to dispose may remarkably reduces the volume and accordingly the cost of the disposing process. Thereafter, the non-hazardous liquid part (mainly water) could be

disposed by spilling into sanitary sewer (Rutala and Weber 2010, Pruss, Giroult, and Rushbrook 1999).

Polystyrene (PS) is a commodity polymer used in various applications such as packaging, insulation, CD / DVD cases, containers, and various single-use accessories. The disposal and degradation of these plastics are not only harmful to the environment, but it also represents missed economic opportunities. If the current trend in plastic consumption continues, more plastic wastes by weight could be than fish in the oceans in 2050 (MacArthur 2017b). In addition, recycling and reuse approaches save remarkable amount of energy when compared with the virgin material production that ~130 million kJ of energy could be saved for each ton of recycled plastic (Jeannette M. Garcia and Robertson 2017). Plastics can be widely recycled, both in waste treatment and in the production of secondary products. The recycled PS has been employed for various applications as secondary products. Zare *et al.* discussed the comprehensive applications of nanofillers in the recycling process of polymer composites (Zare 2013). Chaukura *et al.* presented an overview on the production and potential uses of current waste PS, and also employed waste PS precursors for the synthesis of porous and functionalized conjugated microporous polymers for the removal of dye from wastewaters (Chaukura et al. 2016, Chaukura, Mamba, and Mishra 2017). Recently, Ruziwa *et al.* reported the utilization of sulphonated waste PS for the removal of heavy metal ions from water. Another example for the usability of waste PS materials as sorbent for the separation of $O_2/N_2$and CO_2/N_2 gases was reported by Zhuang *et al.* (Zhuang, Tseng, and Wey 2016). Fibrous materials prepared by electrospinning are commonly used as adsorbents in adsorption studies because of their large specific surface area, mechanical integrity, and ease of functionalization (Gopi et al. 2017, Isik et al. 2016, Zhang, Menkhaus, and Fong 2008). These materials could be utilized for the adsorption of heavy metal ions, proteins, dyes or cells; however, the application of the electrospun PS wastes has not been reported according to the best of authors' knowledge. The attachment, proliferation, and differentiation of the epithelial cells to form the stratified epithelium using electrospun poly(D,L-lactide) fibrous scaffold membranes were reported by Leong *et al.* (Leong et al. 2009). For the protein adsorption studies, dye immobilized polyacrylonitrile nanofiber membranes have potential for bromelain adsorption with high capture capacity (Zhang et al. 2010). Also, cellulose acetate membranes were demonstrated to capture BSA and bilirubin after regeneration and functionalization with a protein specific ligand (Ma, Kotaki, and

Ramakrishna 2005). Electrospun PS fibers are excellent candidates for the adsorption due to their large surface area, superior hydrophobicity, and micrometer level roughness (Miyauchi, Ding, and Shiratori 2006, Demir 2010). Electrospinning is a convenient method for the fabrication of adsorbent materials due to its several advantages such as high surface to volume ratio and high porosity. Also, the solution and process parameters could be easily manipulated to get desired fiber morphology (Bhardwaj and Kundu 2010). Haridas *et al.* fabricated submicron PS fibers by modifying the morphology of fibers from smooth to rough, and altered the resulting fibers from hydrophobic to hydrophilic (Haridas et al. 2014). This study aims to use electrospinning to recycle urban PS waste from different sources (CD cases and foam) to fabricate protein adsorbents, which can then be used as a separation tool for protein-rich medical waste disposal. The adsorption capacity of fibrous PS adsorbents is examined using three commonly used model proteins: Bovine Serum Albumin (BSA), Myoglobin (MYO), and Trypsin (TRY). Their adsorption performances are then compared in fibrous adsorbents fabricated from virgin PS. This approach is promising for the removal of solid components of protein-rich medical wastes and attains the ability to recycle composites with more than one type of material.

2.2. Experimental Section

Waste PS materials were subjected to a sterilization process prior to experimentation. Waste samples (CD case and foam) were initially rinsed with 70% ethanol and then autoclaved by steam sterilization at 121 °C for 30 min. The molecular weight of PS samples was determined using a Dynamic Light Scattering (DLS) instrument (Malvern Nano ZS, Worcestershire, UK). Refractive indices of PS solutions (150, 100, 50, and 25 $g \cdot L^{-1}$) were determined using a manual Abbe Refractometer, and the refractive index increment ($dn \cdot dc^{-1}$) of each PS sample was calculated. These records were then entered in Malvern Nano ZS software, the scattering Rayleigh ratio of DMF was taken as 9.82×10^{-6}, and the weight-averaged molecular weight of samples was calculated. This procedure was conducted for virgin polystyrene (vir-PS), waste foam PS (f-PS), and waste CD case PS (CD-PS). Conductivity of polymer solutions was measured using a multi-parameter (VWR Collection MU6100 L); viscosity measurements of all samples were conducted using a rotational viscometer (Thermo

Scientific HAAKE Viscotester C, Massachusetts, USA) with a L1 spindle, where the rotational velocity of the spindle was 6 rpm for 20 wt% solution and 30 rpm for 10 and 15 wt% solutions.

The solutions used in electrospinning (vir-PS, f-PS, and CD-PS with different solid contents of 10–15–20 wt%) were prepared in an equivolume mixture of DMF and THF. Electrospun fibers of vir-PS with a calcium carbonate ($CaCO_3$) additive were fabricated by adding 10 wt% $CaCO_3$ into 10 wt% PS solution from DMF:THF blend. Each solution was then transferred into a 20 mL plastic syringe using a stainless-steel needle (18 gauges); the needle was connected horizontally to a high voltage supply under 15 kV (Gamma High Voltage Research Ormond Beach, FL, US). A micro-infusion pump (New Era NE300 Infusion Pump, Farmingdale, NY, USA) was used to fix the flow rate at 1.0 mL · h^{-1} and the tip to collector distance was set at 15 cm; therefore, the potential difference was 0.8 kV · cm^{-1}. Humidity and temperature were 43% and 24 °C, respectively. Nonwoven electrospun fibers were collected on aluminum foil, and the morphology of fibers was examined using a Scanning Electron Microscope (SEM, FEI Quanta250 FEG, Oregon, USA); surface chemistry of fibers was studied using an X-ray Photoelectron Spectrometer (XPS, Thermo Scientific K-Alpha Surface Analysis, Massachusetts, USA); the thermal degradation profile was determined by Perkin–Elmer Diamond TG/DTA; the surface area of the electrospun mats was measured using the Brunauer–Emmett–Teller (BET) gas adsorption method (Micromeritics Gemini V, GA, USA); and Fourier Transform Infrared Spectroscopy (FTIR) measurements were conducted using an Attenuated Total Reflection (ATR) attachment (Perkin Elmer FT-IR System Spectrum BX, Waltham, MA).

To examine their adsorption capacity, PS fiber mats were treated with protein solutions. All protein solutions were prepared at pH 7.4 in PBS buffer. BSA and MYO were dissolved separately in PBS solution to give 10^{-6} M, and TRY solution was dissolved in 5×10^{-6} M using PBS buffer. The calibration curves of all protein solutions were prepared within a range of 1×10^{-7} and 1×10^{-3} M, and the linear region of the curves was selected for extrapolation of unknown concentrations. Plastic syringes (2 mL volume; diameter 11 mm) were used to prepare the filtration set-up, and fibers (5 mg) were weighed and placed in the syringes. Approximately 1 mL of PBS solution was passed through each syringe to soak the filters and provide easy filtration. After all the PBS solution was drained out of the syringe, 500 μL each of BSA, MYO, and TRY solution was passed through clean filters, and the filtered solution was collected in

centrifuge tubes. To calculate the adsorption capacity of the filters, the absorbance spectra of filtered solutions was taken between 200 to 800 nm. The adsorption capacity of fibers was then determined with the equation,

$$q = \left[\left(c_i - c_f\right) \cdot V\right] / m \tag{1}$$

where q is the adsorption capacity (mg/g); V is the volume (mL) of solution passed through the syringe; $c_i$and c_f are initial and final BSA concentrations (mg/ml); and m is the mass of the fiber (mg). Optical absorbance measurements were made using a UV-Vis spectrophotometer (SHIMADZU, UV 2550, Japan). The decrease in the absorption intensity of protein solutions was attributed to the adsorption of proteins on the electrospun fibers because protein solutions did not demonstrate any absorbance lost in the absence of fibers. The effect of initial BSA concentration (10^{-7} and 10^{-4} M) on adsorption capacity was investigated by filtration of BSA solutions.

2.3. Results and Discussion

Conductivity and viscosity are two important solution parameters of electrospinning process. Table 2.1 presents the properties of the electrospinning precursor solution. The solution conductivity of the equivolume mixture of DMF:THF was 1.9 μS · cm^{-1}. Then, it is reduced to 1.7 for 10% vir-PS solution and further reduced to 1.2 μS · cm^{-1} with a concentration of 20 wt%. Increasing the amount of non-conductive polymer reduces the conductivity of the solution; i.e. a higher polymer concentration yields a lower conductivity. A similar decrease in conductivity was also seen for f-PS and CD-PS solutions; although CD-PS solutions have a strictly larger conductivity most probably due to the presence of ionic $CaCO_3$ additive (this point will be given further in the text). M_w of the PS was found to be 322, 40, and 880 kDa for vir-PS, f-PS, and CD-PS, respectively. CD-PS is composed of General Purpose Polystyrene (GPPS) that has been employed for the fabrication of various goods. It has higher molecular weight compared to other PS samples so that it provides superior mechanical performance due to having high M_W (Fornes et al. 2001). It is well established that viscosity of polymer solution strongly depends on concentration and molecular weight of the constituent chains. Chain entanglement is the crucial factor; the increase in either

of these parameters triggers the increase of viscosity. Three concentrations of the polymer have been prepared: 10, 15, and 20wt%. Nothing surprise, independent of the PS type, increasing the concentration of the solutions increases the viscosity of solutions. When the viscosity of PS solutions those having the same concentrations were compared, this general rule is not fulfilled. For instance, CD-PS cases have the lowest viscosity although it has the highest molecular weight, which seems against common sense. However, it needs to be noted that they are industrial products, which may potentially have some other additives (for instance lubricants and plasticizers) to facilitate their fabrication process, accordingly change their flow properties (Xie et al. 2004).

Table 2.1. The solution properties (conductivity and viscosity) of PS samples at different concentrations.

Sample Name	**Solution Conductivity ($\mu S \cdot cm^{-1}$)**	**Solution Viscosity (cP)**
vir-PS-10	1.4	48
vir-PS-15	1.1	140
vir-PS-20	0.7	560
f-PS-10	1.7	50
f-PS-15	1.6	134
f-PS-20	1.2	400
CD-PS-10	18.3	35
CD-PS-15	13.6	111
CD-PS-20	12,4	480

The PS samples were dissolved in an equivolume mixture of DMF:THF at different concentrations (10, 15, and 20 wt%). Sub-micron PS fibers were fabricated by electrospinning. Figure 2.2 shows the SEM micrographs of the fibers obtained from vir-PS, f-PS, and CD-PS. Although the three samples can be readily processed by electrospinning and yield sub-micrometer diameter fibers, they differ in the morphology of both the individual electrospun fibers and electrospun fiber mats. The viscosity of the polymer solution is the dominant parameter involved in the electrospinning process (Demir et al. 2002). It is well established that low viscosity yields atomization of the feeding solution (electrospraying) (Isık et al. 2017), whereas a higher viscosity induces

entanglement of the constituent chains, thereby enabling formation of continuous fibers (electrospinning). The influence of viscosity can be remarkably seen for fibers prepared from 10wt% solution. The electrospun mat obtained from vir-PS-10 and f-PS-10 exhibit straight bead-free fibers.

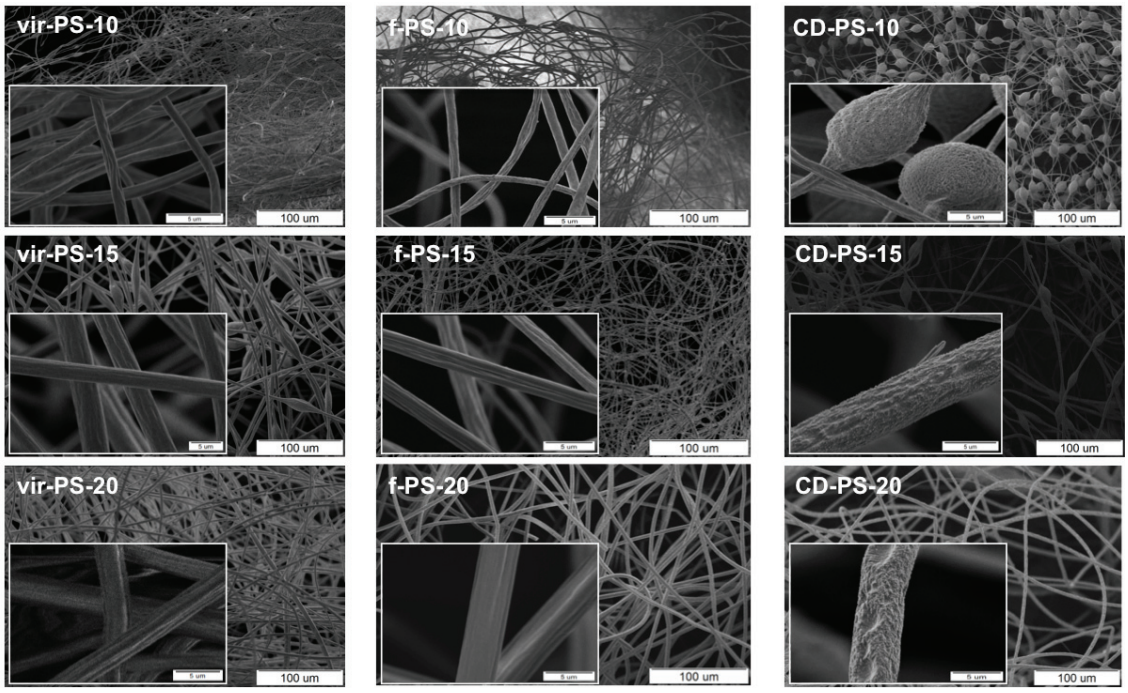

Figure 2.2. SEM micrographs of electrospun fibers fabricated from vir-PS, f-PS and CD-PS from 10, 15 and 20 wt% polymer solutions. Insets show higher magnification image of the electrospun fibers.

On the other hand, CD-PS-10 presents beads-on-string morphology. It is well established that the beads appear out for electrospinning of low viscosity solutions (Gupta et al. 2005). Indeed, the viscosity of CD-PS solution is the lowest compared to other two samples (see Table 1). These fibers have been used in adsorption of proteins so that the surface feature is extremely important. Vir-PS and f-PS fibers have a smooth surface; however, the inset of CD-PS fibers shows remarkable surface roughness at high magnifications. This roughness may be originated from the presence of $CaCO_3$ domains on fiber surface.

Figure 2.3 shows the effect of polymer solution concentration, namely viscosity, on average fiber diameter (AFD). An increase in concentration from 10 to 20 wt% enhances the AFD up to 6 times, most probably due to the increase in viscoelastic forces that makes stretching of jet difficult (Demir et al. 2002). Fiber diameter

distributions were obtained from SEM micrographs and measured by Image J (Schneider 2012) (Figure 2.3). The 10wt% solution of CD-PS provides the thinnest electrospun fibers with beads; because it has the lowest viscosity out of all solutions prepared from other PS sources.

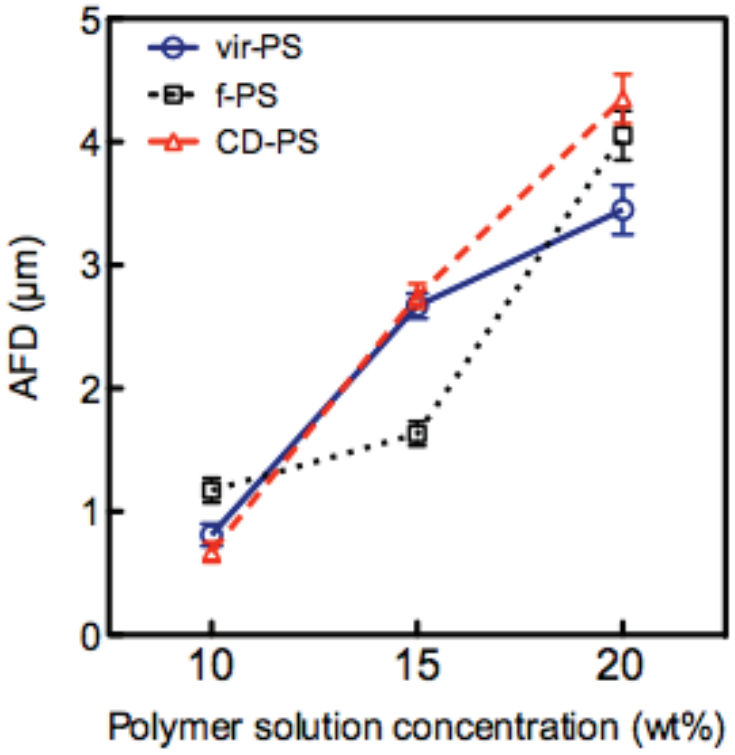

Figure 2.3. AFD of the electrospun fibers obtained at different polymer solution concentration

Nitrogen adsorption / desorption measurements were conducted to determine the BET surface area of electrospun fibers. Figure 2.4 shows the nitrogen adsorption isotherms used to calculate surface area of the fibers obtained from vir-PS-10, f-PS-10, and CD-PS-10. The amount of gas adsorbed onto vir-PS and CD-PS is 110 cm^3/g (surface area: 42 m^2/g) and 254 cm^3/g (surface area: 35 m^2/g), respectively. Isotherms of f-PS-10 fibers have the largest surface area out of all other samples (67 $m^2 \cdot g^{-1}$). AFD seems to be the strongest parameter in determination of surface area. BET results also indicate that the increase in AFD reduces the surface area of fibers (Table 2.2).

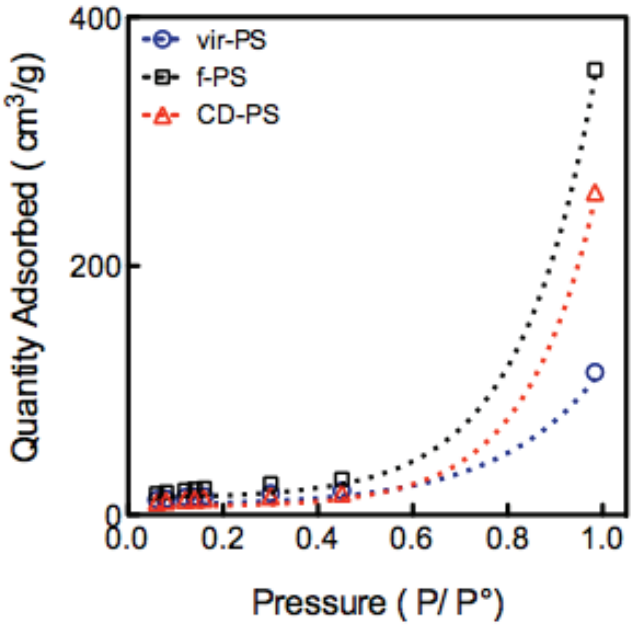

Figure 2.4. BET nitrogen adsorption results of vir-PS-10, f-PS-10 and CD-PS-10 electrospun fibers

Table 2.2. BET surface area of com-PS, f-PS, CD-PS and PS/$CaCO_3$ electrospun fibers extracted from BET isotherms

wt %	vir-PS	f-PS	CD-PS
	(m^2 / g)		
10	42	67	35
15	21	24	21
20	19	26	14

To determine the inorganic content, a thermogravimetric analysis was conducted for all PS systems under identical conditions. Regardless of the source of PS, Figure 2.5 shows that all fiber mats were decomposed at nearly 400 °C. This one-stage decomposition of fibers may be attributed to scission of the backbone. Although both fibers undergo almost complete degradation, it can be seen that CD-PS fibers with 10 % inorganic inclusion remain and resist higher temperatures than parent PS, and this result validates the presence of inorganic species in CD-PS fibers.

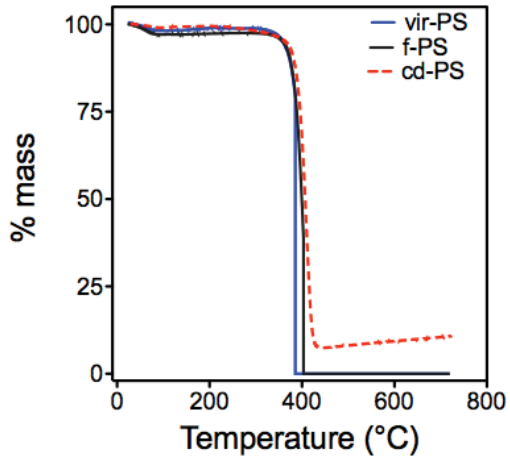

Figure 2.5. TGA curves of virgin and waste PS fibers

X-ray Photoelectron Spectra (XPS) demonstrate the presence of calcium carbonate ($CaCO_3$) domains in CD-PS fibers (Figure 2.6). The Ca (2p) signals with binding energies between 345 – 355 eV can be assigned to $CaCO_3$ molecules found in the CD-PS fibers, and the weight percentage of Ca was estimated 4.2 % from the area under the signal. Because TGA result gave the overall inorganic content in the CD-PS fiber, the residual $CaCO_3$ percentage was found as 10 % and Ca percentage within the molecule can be calculated as around 4 %. Consequently, TGA results are in coherence with XPS results.

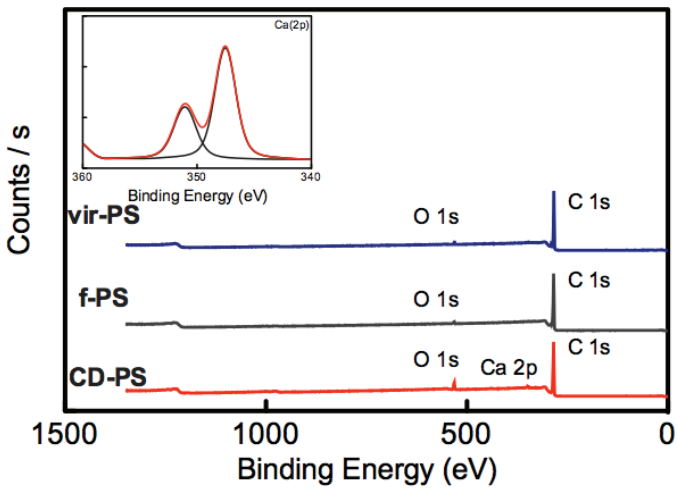

Figure 2.6. XPS spectra of vir-PS, f-PS and CD-PS electrospun fibers. Inset indicates Ca (2p) spectra of CD-PS fibers.

When EDX (Table 2.3) and XPS results were considered, the residual 10 % mass of CD-PS fibers in TGA thermogram can be attributed to the presence of $CaCO_3$ inclusions. It is well established that inorganic fillers have a wide range of applications in the plastic industry for improving mechanical and optical properties (Demir and Wegner 2012). As it is globally abundant, $CaCO_3$ is one of the most commonly used inorganic fillers for polymers (Chan et al. 2002).

Table 2.3. Energy Dispersive X-Ray Spectroscopy (EDX) results of electrospun fibers

Element	vir-PS	f-PS	CD-PS
	(atom %)		
C	100,0	98,8	98,5
O	0,0	1,2	1,4
Na	0,0	0,0	0,0
Mg	0,0	0,0	0,0
Si	0,0	0,0	0,0
Ca	0,0	0,0	0,1

FTIR-ATR spectra show remarkable vibrational signals at around 1390 cm^{-1} and 1680 cm^{-1}, indicating the presence of C=O stretching bands (Figure 2.7). Both spectroscopic techniques validate the presence of $CaCO_3$ in the CD-PS unlike to the other sources of PS.

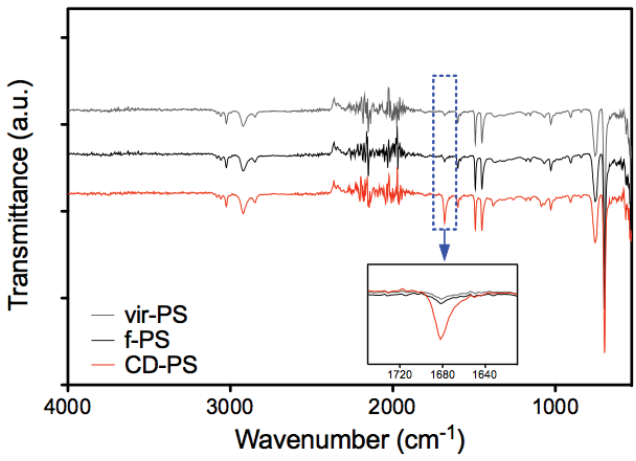

Figure 2.7. FTIR-ATR spectra of com-PS, f-PS and CD-PS electrospun fibers

The diffraction patterns in XRD profiles indicate broad peaks around $2\theta = 20°$, which reveals the amorphous nature of polystyrene fibers. Further, Figure 2.8 confirms the absence of any detectable ordered crystalline structure in vir-PS, f-PS, and CD-PS.

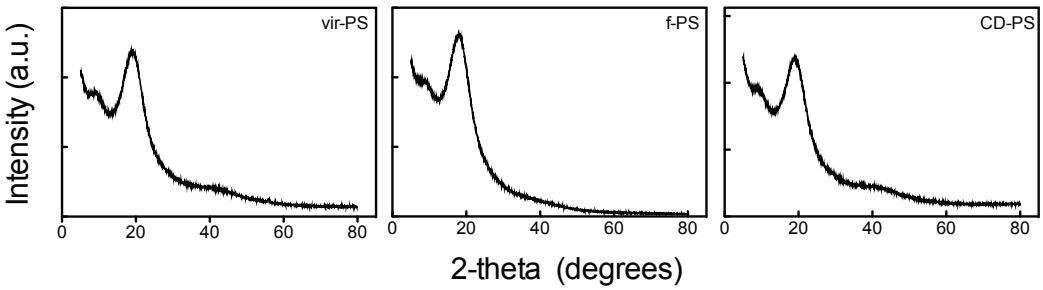

Figure 2.8. XRD profiles of com-PS, f-PS and CD-PS electrospun fibers

The main objective of this work is to use electrospun mats from waste PS as a separation tool for protein-rich medical waste disposal. Protein adsorption capacities of fibers were examined using Bovine Serum Albumin (BSA, 66 kDa, IEP ~ 5.4), Myoglobin (MYO, 17 kDa, IEP ~ 7.0), and Trypsin (TRY, 23 kDa, IEP ~ 10) as model proteins. These three proteins were selected for both their different molecular weights and isoelectric point. For the quantitative determination of adsorbed amounts, calibration graphs of these solutions were generated and used for further calculations (Figure 2.9).

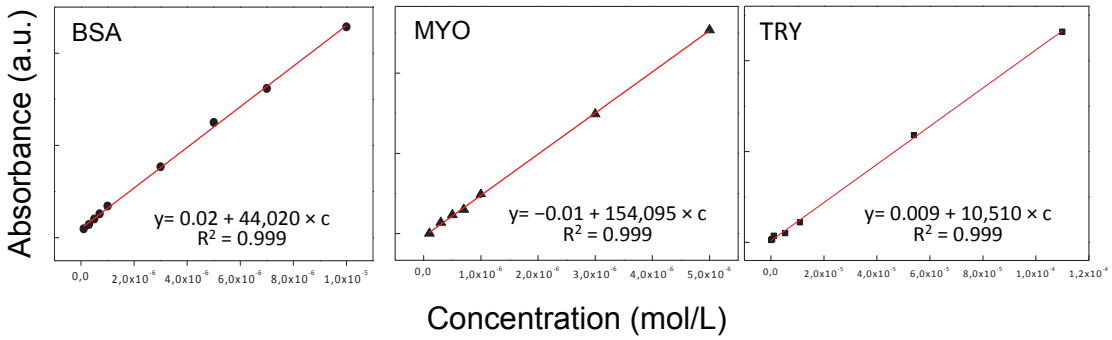

Figure 2.9. Calibration graphs of BSA, MYO, and TRY solutions

Figure 2.10 shows the protein adsorption capacities of fibers in moles ($\times 10^8$) of adsorbed analyte per gram fiber. The results do not correspond to maximum adsorption capacity. They refer to the adsorption capacities of fibers while the protein solutions are

passing through the syringe columns that the duration of process was around 30 sec. The sieving property of fibers was investigated by using different sized proteins. Independent of the PS source, electrospun fibers enable the adsorption of BSA molecules in larger amounts than MYO and TRY.

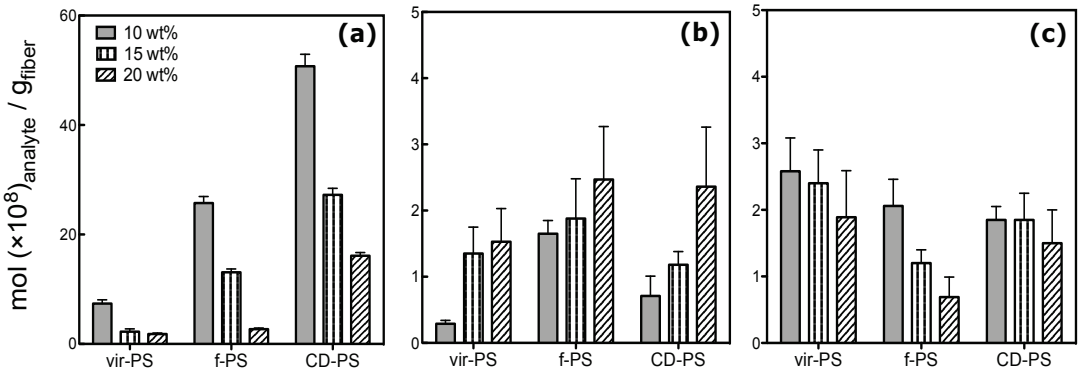

Figure 2.10. Quantity of adsorbed **(a)** BSA, **(b)** MYO, and **(c)** TRY molecules at pH 7.4 on vir-PS, f-PS, and CD-PS electrospun fibers fabricated at different PS concentration in DMF:THF

Figure 2.10a shows that thin fibers have the highest BSA adsorption capacity when each PS source was considered in itself, i.e., the high surface area of the fibers with thin AFD enhances the BSA adsorption. The source of PS waste also has an effect on the adsorption performance. The BSA adsorption capacity of CD-PS fibers was strikingly larger than that of vir-PS and f-PS fibers, although the BET surface area of CD-PS fibers was smaller than the other ones. It is considered that the high affinity of BSA molecules to CD-PS surfaces most probably originates from the interaction between $CaCO_3$ domains, which are found originally as an additive in CD case wastes. Isoelectric point of BSA is around 4.8; at pH=7.4 the charge of the molecule is negative. The electrostatic interaction between positively-charged Ca^{2+} ions and negatively-charged BSA (at pH 7.4) may thus be the driving force for the enhanced adsorption capacity of CD-PS fibers (Lima et al. 2001).

MYO was used as another blood protein to investigate the adsorption capacity of PS fibers. In contrast to BSA, MYO demonstrated almost non-binding behaviour toward the PS fibers from all samples (Figure 2.10b). CD-PS-10 and f-PS-10 fibers have nearly 70 and 25 folds lower adsorption capacity for MYO, respectively.

Similarly, fabricated PS fibers do not have tendency to hold TRY. CD-PS-10 and f-PS-10 fibers have ≈ 15 times less adsorption of TRY compared to one of BSA (Figure 2.10c). Consequently, PS fibers were found to be more selective to BSA than the other model proteins. There may be both physical and chemical reasons. BSA has hydrophobic groups that may improve the interaction with PS. Moreover, the addition of $CaCO_3$ may arise electrostatic interaction between Ca^{2+} and negatively charged groups of BSA. From the physical point of view, the reason could also be the sieving effect of electrospun fibers because BSA has higher molecular weight accordingly larger size than other two proteins. Thus, it can be readily be stuck onto fibers due to internal and external pores and also interfibrillar spacing between fibers.

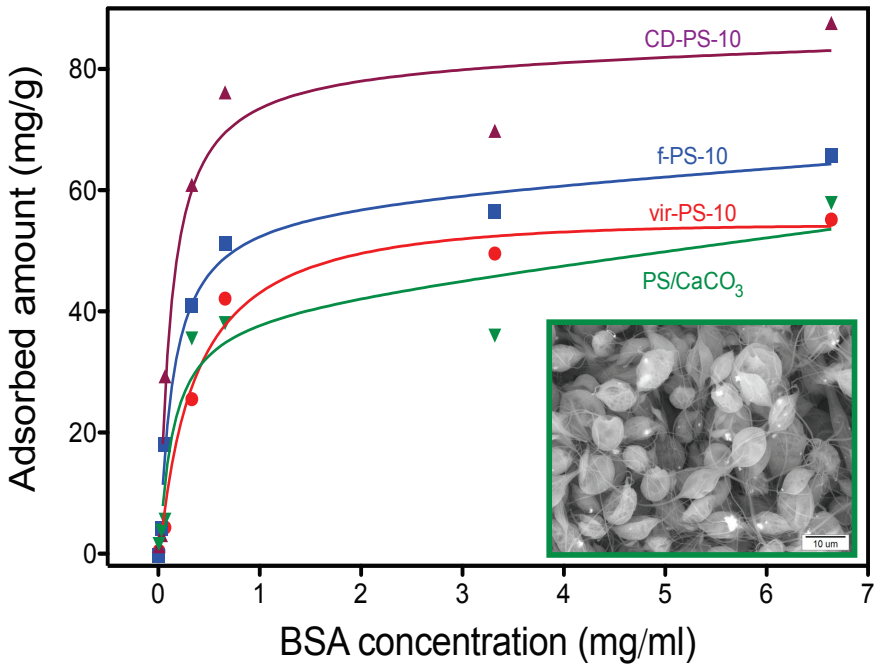

Figure 2.11. BSA adsorption at various concentrations on the adsorption capacity of the PS fibers**.** Inset shows the SEM micrograph of $PS/CaCO_3$ fibers prepared in the lab for comparison.

Adsorption experiments were conducted to reveal the effect of the initial concentration on the adsorption of BSA by the fibers obtained from waste PS. Throughout these experiments, a fixed amount of adsorbent (5.0 mg of PS fibers) was employed, and the initial concentration of BSA solution varied in the range of 6 to 6500 ppm at a fixed pH of 7.4. Figure 2.11 shows BSA adsorption as a function of initial concentration. An increasing concentration of BSA results in a gradual increase in the

adsorption capacity up to a plateau, which implies that there are available sites to adsorb BSA molecules up to that value. However, the adsorption sites reach saturation state at higher initial concentrations of BSA when all sites are occupied. Out of all the waste samples, the largest BSA adsorption capacity (81.5 $mg \cdot g^{-1}$) was ascertained for CD-PS-10 sample.

To get further insight about the role of $CaCO_3$ domains of waste PS-CD cases in protein adsorption, PS/$CaCO_3$ composite fibers were prepared for comparison from virgin PS and commercial $CaCO_3$ powder. The concentration of $CaCO_3$ was fixed to 10% as in the case of CD cover. No surface modification was applied to $CaCO_3$ to increase the compatibility with PS matrix. Its adsorption capacity was then compared with that of CD-PS-10. The inset shows the beady nature of the resulting PS/$CaCO_3$ fibers prepared at identical conditions. Although vir-PS-10 has smooth fibers, the composite sample shows beads-on-string morphology consisting of an excess amount of beads (≈ 5.5 μm) and thin fibers with diameters of 0.4 μm connecting the beads (Figure 2.12). The highest BSA adsorption capacity (53.9 $mg \cdot g^{-1}$) occurred that was nearly the same as that of vir-PS fibers (without $CaCO_3$). It may be reason that the formation of beads reduces the effective surface area of the fibers, i.e. the less surface area, the less sorption capacity is. On the other hand, $CaCO_3$ may have positive effect for adsorption because of electrostatic interaction between Ca^{2+} and negatively charged BSA. Both effect may be balanced and the similar adsorption of protein is observed from both virgin PS and PS/ $CaCO_3$ composite fibers prepared in the lab for comparison with CD-PS. The higher adsorption capacity of CD-PS can be attributed to the homogeneous dispersion of $CaCO_3$ moiety compared to PS/$CaCO_3$, even though they contain identical amounts of $CaCO_3$.

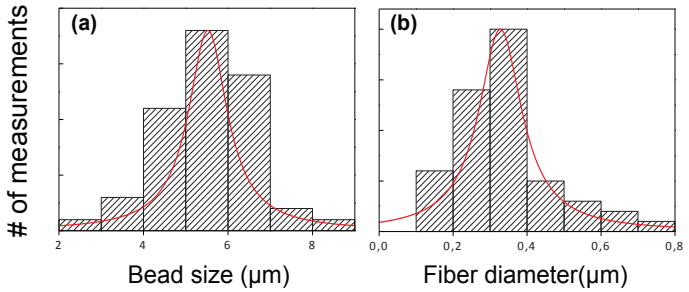

Figure 2.12. The size distributions of PS/$CaCO_3$ **(a)** beads and **(b)** fibers prepared by PS solution with 10 wt% polymer content and 10 wt% of $CaCO_3$ filler

The Langmuir (2) and Freundlich (3) models are common isotherm models that were used to fit the experimental data. Langmuir model describes monolayer adsorption on a surface through homogeneous site within the adsorbent. On the other hand, Freundlich model assumes that adsorption occurs on a heterogeneous surface by multilayer sorption. The values of Langmuir and Freundlich constants were obtained from linear fits of the adsorption data are given in Table 2.4.

$$\frac{c_e}{q_e} = \frac{1}{q_m \cdot b_L} + \frac{1}{q_m} \cdot c_e \quad (2)$$

$$lnq_e = lnK_F + \frac{1}{\eta_F} \cdot lnc_e \quad (3)$$

Table 2.4. Analytically calculated Langmuir and Freundlich adsorption isotherm constants for BSA adsorption on PS fibers [a]

Adsorption model	Parameter	vir-PS	f-PS	CD-PS	PS/$CaCO_3$
Langmuir	R^2	0.863	0.995	0.986	0.775
	Q_0	27,1	76,9	158,7	23,3
	b	0,13	0,05	0,02	0,19
Freundlich	R^2	0.882	0.918	0.824	0.884
	K_f	0,58	1,58	5,99	0,66
	1/n	0,57	0,48	0,35	0,55

[a] Solution volume, solution pH, sorbent amount and reaction temperature were 1.0 mL, pH 7.4, 5.0 mg, and 25 °C, respectively.

The adsorption isotherms consider the equilibrium conditions that could be generally achieved in batch sorption (Horzum et al. 2013). This filtration system is based on the column sorption and the required time to reach the equilibrium could not be provided through the experiments. Thus, adequate linear correlations were not observed for all fittings. The theoretical adsorption capacities (Q_0) of BSA on PS fibers have been evaluated and the highest Q_0 was found for CD-PS fibers, which is 158.7 mg $\cdot g^{-1}$, due to the beforementioned reasons. PS/$CaCO_3$ fibers have the lowest Q_0, which is close to the com-PS. The K_f values of Freundlich model show the affinity of adsorption process and unsurprisingly, CD-PS fibers show the highest affinity toward BSA adsorption among the other fibers.

2.4. Conclusion

Two sources of urban PS waste (CD cover and styrofoam) are converted into a protein adsorbent via electrospinning that can be used to filter solid content of the protein-rich medical wastes before their disposal. Although they may contain some ingredients employed during their production such as lubricants and plasticizers, they can readily be processed by electrospinning. Electrospun mats obtained from the PS wastes show remarkable adsorption capacity for three model proteins as following order: BSA > MYO > TRY. The mats consisting of thin fibers show higher adsorption capacity due to both having large surface area that increases the available binding sites for the protein and sieving effect of interfibrillar spacing. Although f-PS fibers have the largest BET surface area, the BSA adsorption capacity is highest in CD-PS. The presence of $CaCO_3$ already dispersed in the PS volume most probably to increase final product features may show high affinity to the proteins. The electrostatic interactions between the Ca^{2+} and negatively charged BSA may override the high adsorption capacity. To approve the role of $CaCO_3$ on adsorption study, PS/$CaCO_3$ composite fibers were fabricated synthetically for comparison. The inclusion of $CaCO_3$ improves the adsorption of proteins compared to parent PS; however, the result appears worse than the one obtained from CD-PS probably having better dispersion of $CaCO_3$ domains. In conclusion, this approach presented in this study may represent a successful way of making valuable products from waste PS to get rid of protein-rich solid content of the medical wastes accumulated from hospitals. There have been other researches about the adsorption application of waste polymers but this study is the first that aims the protein adsorption application of polystyrene wastes. Future studies will be focused on using same approach to process other commodity waste plastics produced in larger volumes such as polypropylene and polyethylene terephthalate.

CHAPTER 3

OIL REMOVAL EFFICIENCY OF PS FIBERS WITH VARIOUS MORPHOLOGIES

3.1.Introduction

The significant increase in the generation of oily wastewater brings front several problems that threaten human life and ecological systems. The oil-water emulsions have been emitted from both domestic sources and also industrial activities (petrochemical, leather, etc.) into the sea, sewages or water sources by causing a wide range of impacts on social and economic activities (Feng et al. 2004, Chaudhary et al. 2014, Wang et al. 2015, Zhou et al. 2016, Shannon et al. 2008). Conventional oil-water separation methods vary from gravity separation, centrifugal settling, air flotation, and chemical demulsification but they have inherent drawbacks such as low efficiency, requirement of large footprint, and consumption of high energy, equipment corrosion, high equipment cost and secondary pollution (Xu et al. 2015, Xiao et al. 2016, Padaki et al. 2015, Ou et al. 2016, Mullin and Champ 2003, Margesin and Schinner 1999). Thus, there is an outgrowth environmental demand for the investigation of oily wastewater treatment systems, which are highly selective, efficient and effortless to apply. In recent years, filtration membranes have been developed for the remediation of oily wastewaters. However, membrane-fouling problems, which reduce the separation efficiency, and high cost of proposed membranes, limit the application range of these materials (Xue et al. 2014). Therefore, the fabrication of novel oil adsorbent materials that show special wettable properties arouses a significant attention in recent years (Li et al. 2017, Chu, Feng, and Seeger 2015, Wang et al. 2015). The special wettability determines the relation between liquid and solid surface and wettable properties come from the oleo-philic / phobic and hydro-philic / phobic characteristics of surfaces. In comparison with the superhydrophilic / superoleophobic materials (water-removing type), superhydrophobic / superoleophilic materials (oil-removing type) are more convenient because it is difficult to get a material having larger surface energy than water and smaller than oil. Oil removing type of adsorbents can selectively adsorb oil

from oil / water mixtures and this property is ascribed to their superhydrophobic / superoleophilic nature (Xue et al. 2014). This type of adsorbents can convert liquid state oily wastes into semisolid state and enable the removal of oil from the medium (Tan et al. 2013, Li, Zeng, et al. 2014). Diverse methods have been proposed for the fabrication of these kind of novel materials by rational combination of surface composition and rough structure such as sol-gel (Xu, Wang, and Sanderson 2010), salt induced phase inversion (Zhang et al. 2015), layer-by-layer assembly (Manna and Lynn 2015, Li, Li, and Sun 2010), chemical or plasma etching (Jiang et al. 2017, Song et al. 2015), and electrochemical processes (Qing et al. 2016). Silica aerogels, zeolites and clays have been widely used materials after modification with several functional groups to improve the oil adsorption ability of materials (Xue et al. 2014). In addition to the abovementioned inorganic adsorbents, synthetic polymers adsorbents have also been attracted more and more attention. Wang *et al.* fabricated 3D polycarbonate monolith by thermally impacted non-solvent induced phase separation and as-prepared monolith could adsorb various types oils 4 times its pristine weight (Wang et al. 2017). Copper coated polyurethane sponges were fabricated by Zhu *et al.* and these sponges adsorbs various kinds of oils 13 times of their weight (Zhu, Pan, and Liu 2011). Polystyrene (PS) is known its low cost, high chemical resistance as well as its hydrophobicity. The hydrophobic property brings about the oleophilic characteristic for PS adsorbents, which makes them suitable for oil spill clean-up. There are numerous routes for the fabrication of PS adsorbents in oil spill clean-up applications but many of existing routes challenge for easy to use due to the multistep procedures (Wu et al. 2012). Among all of the current techniques, electrospinning is one of the most versatile techniques used to roughen surfaces, which is required to enhance the hydrophobic property of surfaces (Al-Qadhi et al. 2015). It is a straightforward technique for the fabrication of micro- / nanoscale fibers and utilization of the as-prepared fibers as adsorbents in various media (Celik et al. 2017, Demir et al. 2002, Horzum et al. 2010, Horzum et al. 2013, Horzum et al. 2012, Isik et al. 2016). The structural advances of electrospun fibers stem from their enhanced surface area, high porosity, ease of surface functionalization, high mechanical integrity and tunable surface features (Greiner and Wendorff 2007, Feng et al. 2004, Reneker and Chun 1996). The hydrophobic behaviour of electrospinning surfaces result from the high surface roughness, and diversified surface topography and trapped air could minimize the interfacial energy between solid and liquid (Zhou and Wu 2015, Isik et al. 2017). The purpose of this study is to enhance

the oil adsorption capacity - porosity - of PS adsorbents by changing the morphology of fibers. Porosity in electrospun polymer fibers has been demonstrated generally by involving the utilization of high vapour pressure solvents (Bognitzki et al. 2001, Megelski et al. 2002) or the inclusion of dopants in the solutions (Gupta et al. 2009, Zhang et al. 2006).

Therefore, we followed a path for the fabrication of porous PS fibers that the solvent composition (THF and DMF amounts) of PS fibers was changed in electrospinning solutions. Then, expanded PS waste (f-PS) fibers were recycled by electrospinning and the resulting fibers with various morphologies were achieved. Further, the oil adsorption and oil / water separation efficiencies of fibrous materials were evaluated.

3.2. Experimental

The molecular weight of PS samples was determined by applying Rayleigh equation in the Static Light Scattering mode of Dynamic Light Scattering (DLS) instrument (Malvern Nano ZS, Worcestershire, UK). Conductivity of polymer solutions was measured using a multi-parameter (VWR Collection MU6100 L); viscosity measurements of all samples were conducted using a rotational viscometer (Thermo Scientific HAAKE Viscotester C, Massachusetts, USA) with a L1 and R2 spindles, where the rotational velocity of the spindle was 2 rpm for 30 wt%, 6 rpm for 20 wt% and 30 rpm for 10 wt% solutions.

Virgin PS (vir-PS) and expanded PS waste (f-PS) solutions, which were prepared in an equivolume mixture of DMF and THF with different solid contents of 10-15–20-25-30 wt%, were used in electrospinning. Each solution was then transferred into a 20 mL plastic syringe using a stainless-steel needle (18 gauges); the needle was connected horizontally to a high voltage supply under 12 kV (Gamma High Voltage Research Ormond Beach, FL, US). A micro-infusion pump (New Era NE300 Infusion Pump, Farmingdale, NY, USA) was used to fix the flow rate at 2.0 mL $\cdot$ h^{-1} and the tip to collector distance was set at 12 cm; therefore, the potential difference was 1.0 kV $\cdot$ cm^{-1}. Humidity and temperature were 52% and 24 °C, respectively. Nonwoven electrospun fibers were collected on aluminium foil.

The morphology of fibers was examined using a Scanning Electron Microscope (SEM, FEI Quanta250 FEG, Oregon, USA) after sputtering by gold using ion sputter. The average diameters of the fibers were estimated by statistically from SEM micrographs using ImageJ software. Contact angle measurements were achieved with Contact Angle Meter (Attension Lite, Biolin Scientific, Stockholm, Sweden) for both water and oil contact angles. The surface area of the electrospun mats was measured using the Brunauer–Emmett–Teller (BET) gas adsorption method (Micromeritics Gemini V, GA, USA).

For the comparison of the oil adsorption performance of as-fabricated adsorbents, the oil adsorption capacities of each type of fibers were investigated. A sample of 25 mg of each fiber mat was immersed in 10 mL of sunflower oil, which is stained with red oil paint. After treating the fiber with oil for 60 seconds, the fiber was removed and drained out for 30 seconds. Then, the adsorbed oil amount was determined by measuring the difference between initial and final weight of fiber with an analytical balance. All experiments were repeated 3 times to evaluate the repeatability. The results were given as adsorbed oil amount (g) per gram fiber with their standard deviations.

The removal efficiency of oil from the aqueous mixtures was investigated by preparing different concentrations of oily water mixtures with sunflower oil. 2, 5, 10 and 15% oily mixtures were prepared in 20 mL water by adding oil droplets. 25 mg of fiber were immersed in oily water and mixed for 60 seconds. Then, the difference between initial and final weight of fiber was measured with an analytical balance. All experiments were repeated 3 times to evaluate the repeatability. The results were given as percentage oil separation efficiency with their standard deviations. The oil adsorption capacity and oil water separation efficiency were examined for foam (expanded PS) itself and the commercial adsorbent, which was supplied by Municipality of İzmir, for the comparison of as-fabricated fibers with the existing products.

3.3. Effect of Solvent Composition on The Oil Adsorption Capacity of PS Fibers

Electrospinning technique is a straightforward method to produce micro to nanoscale fibers. Note that electrospinning of PS allows controlling both surface and internal porosity of an individual fiber along with the roughness of electrospun mat

(assembly of the nonwoven individual fibers) (Demir 2010). In the field of fibrous polymers, phase separation is a common strategy adopted to produce porous structures. During the electrospinning of polymer solutions, solvent evaporation occurs rapidly and thermodynamically driven events dominantly come into play (Megelski et al. 2002). Phase separation is a common, inevitable particularly in humid environments, strategy for the development of porosity inside of the fiber and on the fibers surface. Vapor-induced phase separation (VIPS) and thermal-induced phase separation (TIPS) are the most pertinent phase separation mechanisms that cause to the development of porosity formation on PS fibers (Arnauts and Berghmans , Casper et al. 2004, Lin et al. 2010, Kongkhlang et al. 2008). In the former, moisture plays a significant role due to the non-solvent / solvent interaction that water acts as a non-solvent. This process is induced by penetration of non-solvent from vapour phase into the polymer solution and non-solvent (water) precipitates the polymer out of the solution by generating a solid matrix from polymer-rich phase and porous region from solvent-rich phase. In the latter, liquid-liquid disintegration has significant importance that at low temperatures, a phase separation takes place in polymer rich and solvent rich regions (vandeWitte et al. 1996). Phase separation in TIPS mechanism occurs by lowering the surface temperature of fibers due to the rapid evaporation of solvent and the system passes through the binodal curve to enter the metastable region. The porous structure of amorphous polymers comes from the liquid-liquid phase separation following by gelation of the polymer (Laxminarayan et al. 1994). Moreover, rapid evaporative cooling on the surface of fibers could lead to the formation of the breath figure on the surface that cools the moisture in air and condenses by following the growth of droplets. As the jet dries, the water droplets leave imprints on the surface in the form of pores (Lu and Xia 2013, Srinivasarao et al. 2001). It can be claimed that neither the phase separation theory nor the formation of breath figures alone fully explains the phenomena of pore formation in electrospun PS fibers. Rather, the combination of both phase separation mechanisms (VIPS and TIPS) and breath figure formation simultaneously play active role in the structural development of electrospun fibers.

Herein, we reported a simple and low-cost method for the fabrication of hydrophobic oil adsorbent fibers from waste PS sources by electrospinning in DMF / THF mixture. The fibers were investigated in terms of surface topography by changing the pore structure and different solvent combinations were examined to find the optimum parameters for highest oil adsorption capacity. The morphology of the

adsorbents was characterized by scanning electron microscopy (SEM). Contact angle measurements were employed to demonstrate the effect of surface topography on the hydrophobicity of the resulting fibrous adsorbents. The oil adsorption capacity and oil – water separation efficiency of the proposed fibrous adsorbents were studied using 2 different types of oils; sunflower oil and machine oil.

3.3.1. Results and Discussion

Through this study, the effect of solvent system on the electrospun fiber morphology was examined (Figure 3.1). In addition, the effect of the electrospun fiber mats on oily wastewater remediation ability was investigated. The solvents were chosen with respect to their vapor pressure. THF (vapor pressure ~ 200 hPa) and DMF (vapor pressure ~ 3.5 hPa) were selected as high vapor pressure solvent and low vapor pressure solvent, respectively.

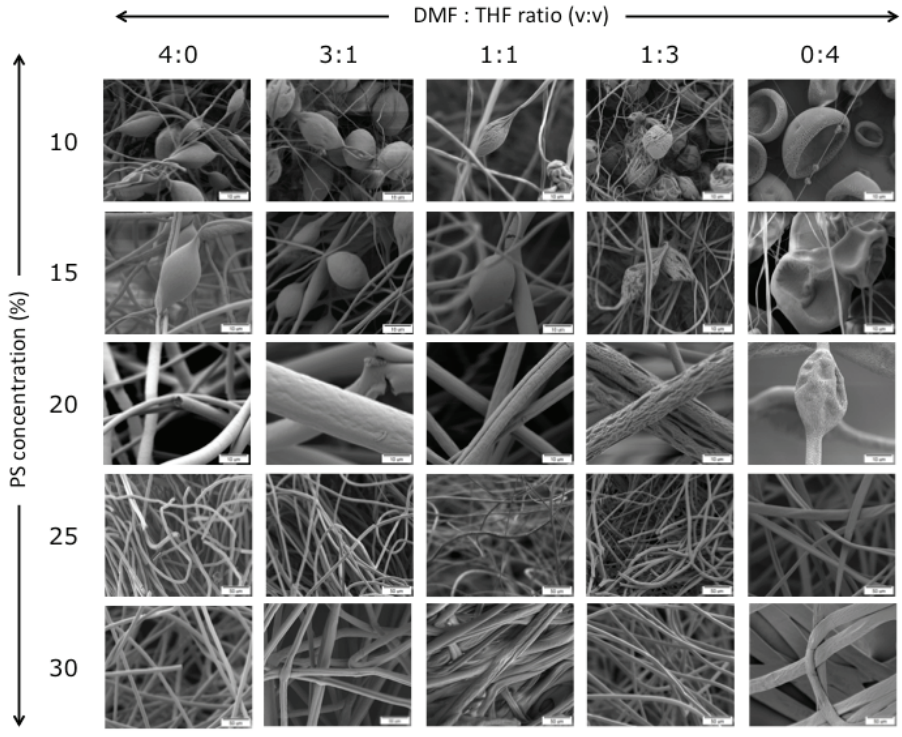

Figure 3.1. SEM micrographs of vir-PS fibers with respect to different solvent compositions and vir-PS solution concentrations (Scale bar is 10 μm)

Five different PS solution concentrations were chosen for 5 different solvent systems. The unary and binary solvent systems were prepared and three characteristic fiber morphologies (beads, bead-on-string and fiber) for both vir-PS and f-PS were obtained. In Figure 3.1, SEM micrographs of vir-PS fibers in unary DMF solvent (DMF : THF = 1:0) demonstrate the smooth surface due to the high dielectric constant and high electrical conductivity of DMF. The lower concentrations of polymer solutions, especially 10 and 15wt% ones have 'beads on string' structure that low viscosity of solution favours the formation of thinner fibers with beads (Demir et al. 2002, Isik et al. 2017, Isik et al. 2016). The bead size of these structures ranges around 10 μm and the average fiber diameter (AFD) is increased from 1.8 to 13 μm by increasing the concentration of polymer solution from 10 to 30 wt%. In binary solvent systems, the solvent ratio is the most significant key factor that determines the formation of pores or grooves texture of fibers. The porosity formation on the electrospun fibers with binary solvent systems is quite complex due to simultaneous thermally induced phase separation (TIPS) and vapour induced phase separation (VIPS) (Casper et al. 2004, Kongkhlang et al. 2008). During the electrospinning process in air environment, the evaporation of solvent outward and penetration of vapour in air occur concurrently. The rapid evaporation of solvent from Taylor cone consumes the heat of vaporization by cooling the surface and leads the formation of thermodynamically unstable jets, which results in the phase separation of polymer and solvent domains (Bognitzki et al. 2001, Ziabicki 1976). While solvent-rich domain of solution forms pores after the solvent dried out, polymer-rich domain of solution forms solidified parts (Figure 3.2) (Arnauts and Berghmans , Lin et al. 2010). Because THF is a highly volatile solvent; there is absorption of heat that cools the surface of the fibers. Thus, water vapour starts to condense on the fiber surface and create water droplets, which leave water imprints behind after the evaporation of water and this process is also called as breath figure formation (Lu and Xia 2013). Hereby, 3 different binary solvent systems with different volumetric compositions were investigated (DMF: THF = 3:1, 1:1, 1:3). The small portion of THF addition (3:1 ratio) into the solvent system does not have an observable affect that electrospun fibers have nearly smooth surface as in unary DMF system. However, the addition of THF promotes the thin fiber formation such that AFD is smaller than the one obtained by unary DMF system. AFD ranges between 0.6 to 12 μm and the bead size is nearly 11 μm, which almost same in the unary DMF system.

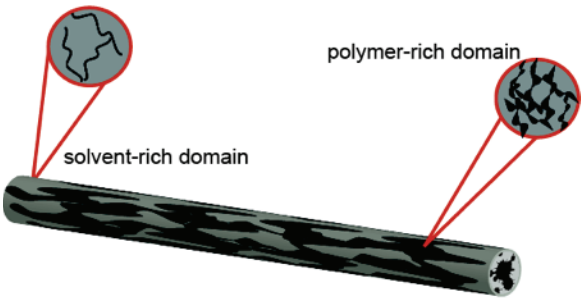

Figure 3.2. Schematic representation of phase separation that solvent-rich domain consists of a small amount of polymer and polymer-rich domain consists of small portion of solvent

When DMF: THF ratio was equal or higher than 1:1, all the resultant fibers come out with grooves or large scale pores. The equivolume mixture of DMF and THF results in the formation of wrinkled surface due to the buckling of cylindrical polymer shell under compressive radial stress, which arises from removal of solvent from the core of jet or a lateral contraction effect from the axial tensile stress that arises from the continuous stretching of jet (Pai, Boyce, and Rutledge 2009). The bead size of the bead on string structure is around 10 µm and AFD ranges between 2.1 to 15 µm.

The increment in the high vapour pressure solvent amount, THF, increases the solidification and evaporation rate of solvent system that size and shape of the pores are related with these rates. Whereas faster rates preserve the initial phase separation and form small pores, lower rates lead to the formation of further phase separation due to the stretching of electrospun fibers or beads under electric field and form large scale and shallow pores (Lin et al. 2010). It should be pointed out that all fibers, which were fabricated from 1:3 DMF to THF ratio, have elongated and large voids on their surface. The difference between the evaporation rates of DMF and THF is essential on the formation of texture on the vir-PS fibers. The highly volatile solvent can easily forms glassy skin and voids due to the phase separation and fast evaporation rate. Meanwhile, low volatile solvent still remain in the jet that makes the polymer core wet and stretchable. The voids are elongated under electrical field due to the stretchable core and forms large and shallow voids (Liu, Huang, and Jin 2015, Huang et al. 2011, Liu, Huang, and Jin 2014). Moreover, the AFD ranges between 0.4 to 8 µm and average bead size is around 11 µm.

Furthermore, the unary THF system led to formation of a ribbon-like structure with densely packed nanoscale surface pores, (nearly 90 nm), which were uniformly

distributed on the beads and fibers most probably due to TIPS. Although most electrospun fibers are in cylindrical morphology, highly volatile solvents, (like THF and DCM) show ribbon-like PS fibers due to the rapid drying following by collapse of jet (Liu, Huang, and Jin 2015). The 'beads on string' structure of electrospun fibers was observed for 10, 15 and 20 wt% polymer concentrations, except for the 10 wt% unary THF system (DMF: THF = 0:1). This unary solvent– polymer concentration combination of electrospun samples was resulted in the formation of ~ 20 µm beads with collapsed morphology. Also, there are numerous small pores on the surface of the beads. In unary solvent systems, generally VIPS takes place that polymer and unary solvent are exposed to a vapour atmosphere, which consist of water vapour. The vapour behaves like a non-solvent and permeates into the solution by leading to the phase separation (Lu et al. 2017). Thus, the nanopores on the beads for 10 wt% unary THF system could be attributed to the VIPS. The AFD of these ribbon-like structures changes between 1.2 to 26 µm. Moreover, the increase in DMF ratio for 10 and 15 wt% vir-PS solutions resulted in the formation of beads with different morphology that elliptical bead took collapsed bead's place. This transformation of bead morphology with respect to the DMF amount could be attributed to the higher conductivity and dielectric constant (Lin et al. 2010, Uyar and Besenbacher 2008, Eda, Liu, and Shivkumar 2007). When the polymer solution concentration reaches up to a sufficient degree, beads are completely disappeared and uniform fibers could be fabricated.

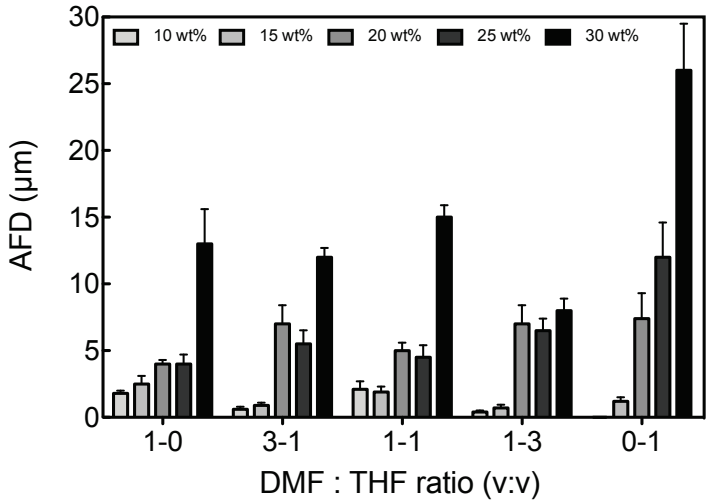

Figure 3.3. AFD of vir-PS fibers with respect to various solvent compositions and PS concentrations

Because the increment in the polymer solution concentration favours the enhancement of viscosity and sufficient chain entanglement, the electrospinning jet could be stabilized (Zheng et al. 2006). In this study, the increment in the polymer solution concentration above 15 wt% results in the disappearance of bead on string structure due to the beforementioned reason. The AFD variation of PS fibers with respect to solvent compositions and PS concentrations were given in Figure 3.3.

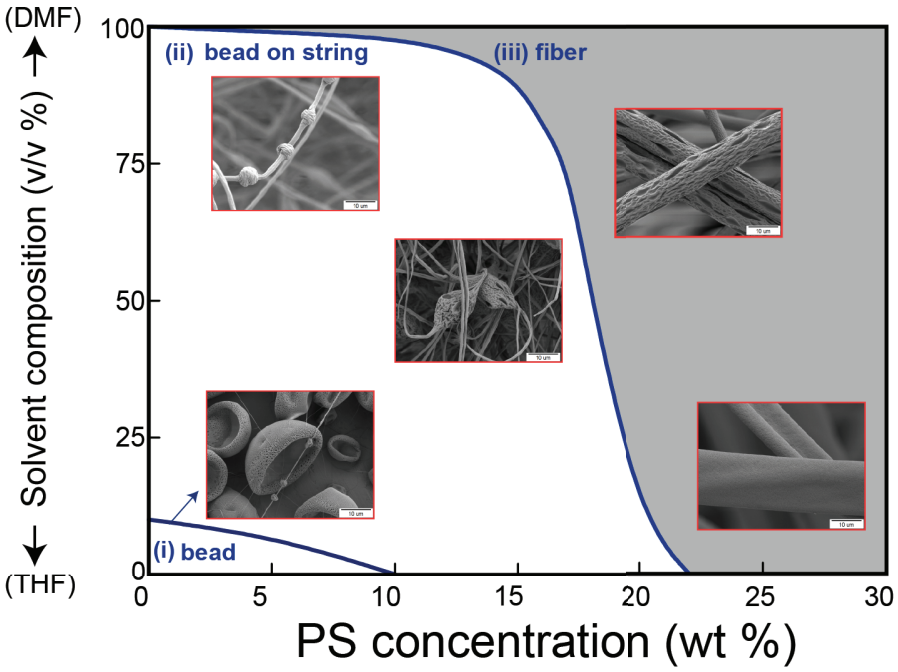

Figure 3.4. Dependence of vir – PS fiber morphology on DMF: THF composition versus PS concentration

Figure 3.4 shows the dependence of PS fiber morphology with respect to solvent composition and PS concentration. As mentioned before, bead formation on the vir-PS fibers were seen frequently and these fibers in all solvent compositions up to 20 wt% demonstrate bead on string morphology. Otherwise, the surface texture of vir-PS fibers seems similar in terms of grooves, voids and pores.

Adsorption capacity is one of the most important key factors for the applications of oil adsorbents. Table 3.1 and Figure 3.6 demonstrate the effect of fiber morphology and surface properties on oil adsorption capacities of vir-PS fibers. The results show that fibers fabricated from neat DMF or neat THF have the lowest oil adsorption capacity due to the presence of beady morphology at low PS concentrations and thick

fiber diameter at high PS concentrations. The fibers fabricated from equivolume DMF to THF ratio have low amount of beads at low concentrations. As an example, the oil adsorption capacity of 10 wt% PS solution is around 91 g/g and decreases to 41 g/g for 30 wt% PS concentration due to the increase in AFD.

Table 3.1. Properties and oil adsorption capacities of vir-PS fibers

vir-PS wt%	DMF	THF	Fiber morphology	Properties	g_{oil} / g_{fiber}
10	1	0	bead on string	thin fibers	22
	3	1	bead on string	thin fibers	24
	1	1	bead on string	intermediate fibers	91
	1	3	bead on string	intermediate fibers with macropores	17
	0	1	bead	porous beads	-
15	1	0	bead on string	intermediate fibers	32
	3	1	bead on string	intermediate fibers	44
	1	1	bead on string	intermediate fibers	66
	1	3	bead on string	intermediate fibers with macropores	15
	0	1	bead on string	thin fibers	-
20	1	0	fiber	thick fibers / interior porosity	44
	3	1	fiber	thick fibers / interior porosity	98
	1	1	fiber	thick fibers with grooves	57
	1	3	fiber	thick fibers with macropores	84
	0	1	bead on string	thick / belt shape fibers with nanopores	-
25	1	0	fiber	thick fibers / interior porosity	24
	3	1	fiber	thick fibers / interior porosity	94
	1	1	fiber	thick fibers with grooves	46
	1	3	fiber	thick fibers / interior porosity	34
	0	1	fiber	Thick / belt shape fibers with nanopores	22
30	1	0	fiber	thick fibers / interior porosity	11
	3	1	fiber	thick fibers	79
	1	1	fiber	thick fibers	41
	1	3	fiber	thick fibers with grooves	32
	0	1	fiber	thick / belt shape fibers with grooves	12

For the investigation of hydrophobicity / hydrophilicity of vir-PS fibers, water contact angle (WCA) of the fibers were determined. Figure 3.5 shows the contact angle of vir-PS fibers from various concentrations in equivolume DMF:THF solvent. According to the Cassie-Baxter model, this roughness creates cavities on the surfaces

and allows the trapping of air between surface and water droplet resulting in the inhibition of wetting the surface.

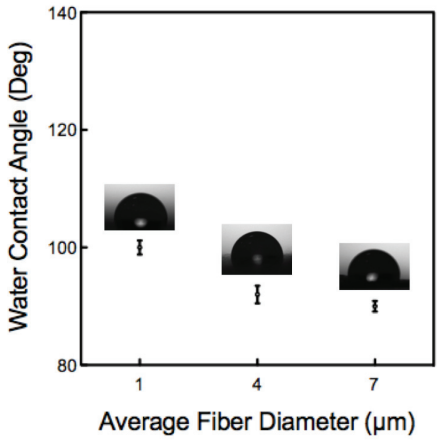

Figure 3.5. WCA of vir-PS fibers from various compositions

The surface porosity of PS fibers in 1:3 DMF to THF ratio does not have a favorable effect on oil adsorption capacity at low PS concentrations, 10 and 15wt%, due to their intense bead on string morphology. However, at 20wt% PS, where no bead morphology were observed, the oil adsorption capacity of vir-PS fibers reached up to 84 g/g and then decrease to 32 g/g at high PS concentration. The oil adsorption capacity of vir-PS fibers reached its peak at 3: 1 DMF to THF ratio although these fibers have nearly smooth surface as in unary DMF solvent. However, addition of small portion THF into the solution decreases the AFD of adsorbents and results in the enhancement of BET surface area (Figure 3.3). Moreover in Figure 3.6b and c, fibers fabricated from 3:1 solvent ratio have for more intrinsic porosity than 1:3 ones. Also, fibers fabricated from 1:3 DMF to THF ratio have glassy skin formation with a smooth surface. For vir-PS fiber adsorbents, the highest oil adsorption capacity was recorded as 98 g/g, which means that 1 g of adsorbent could adsorb 98 times its own weight. It is suggested that the oil was absorbed by physical trapping on the fiber surface and filling the voids in the nanofibrous mats. The capillary force mediate the oil molecules to diffuse into interior pores of the nanofibers (Bandegi and Moghbeli 2018). Thus, the fibers having interior porosity could have better oil adsorption capacity than the fibers with surface porosity.

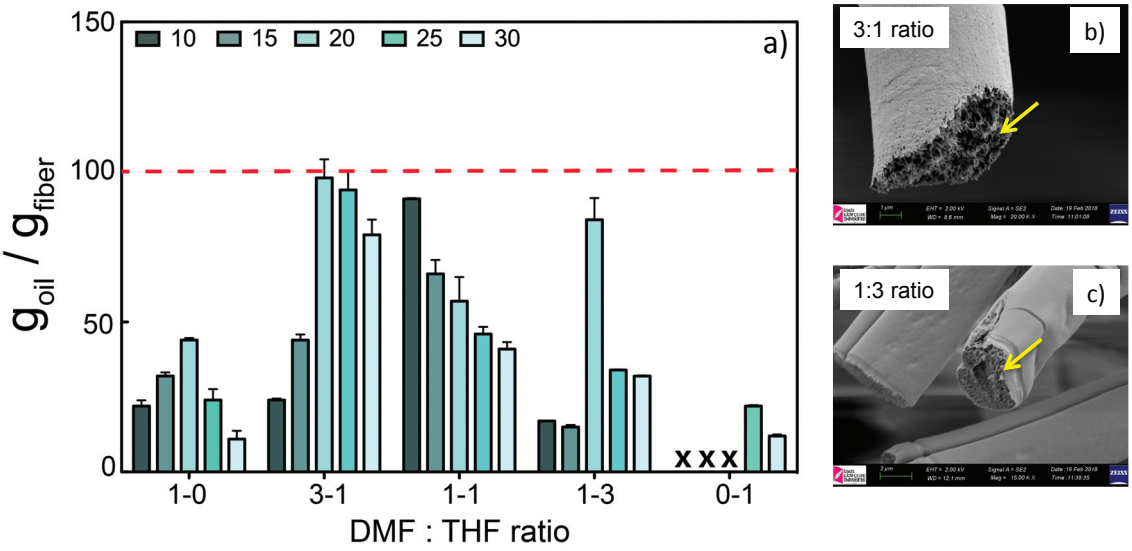

Figure 3.6. (a) Oil adsorption performance of vir-PS electrospun fibers with respect to solvent composition and initial PS concentration, SEM micrographs that show intrinsic porosity of vir-PS fibers fabricated from (b) 3:1 and (c) 1:3 DMF to THF ratio.

The oil separation efficiency of fibers was also investigated in different concentrations of oily waters. Figure 3.7 shows the comparison of oil separation efficiency of vir-PS and f-PS fibers.

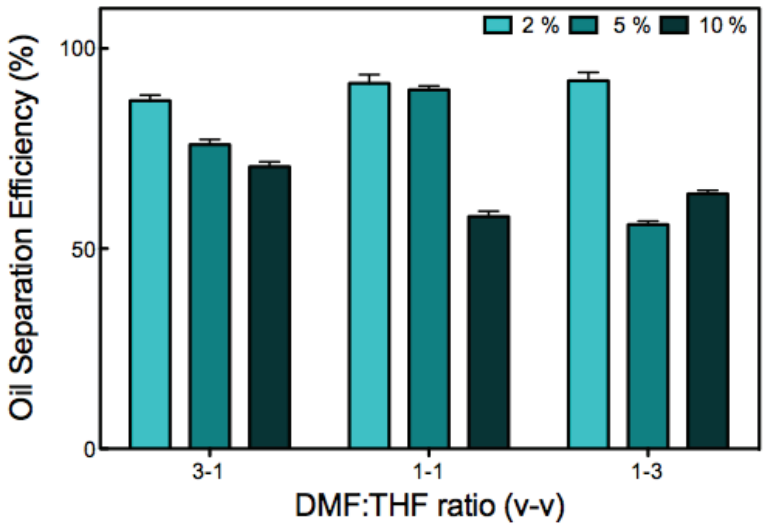

Figure 3.7. Oil separation efficiency of vir-PS fibers from oil contaminated water mixtures with respect to sunflower oil concentration.

At low oil concentrations (2%, v/v), all of the fibers show more than 90% of separation efficiency independent of the PS source and PS concentration. However, the

increment the oil amount in the oil-water mixture makes a significant difference on the separation efficiency of fibers and the separation efficiency of other fibers decreases after 5% of oil contamination. f-PS fibers with highest oil adsorption capacity, where the DMF:THF ratio was 3:1 (v:v), have also the highest separation efficiency, 94%, and they clean nearly all of the oil from the oil contaminated water up to 10% of oil concentration.

3.4. Recycling of Expanded Polystyrene by Electrospinning: Instead of Landfill Remediate Oily Wastewaters

Barely using fresh material components as starting material can lead to secondary pollution. When the requirement of large amount of adsorbent materials is taken into account, the cost of raw materials becomes crucial. Therefore, it is urgently necessary to develop novel adsorbents with low cost and high oil adsorption capacity that simplifies the oil spill clean-up procedures. Since the beginning of the polymer production from petrochemical sources, the production and consumption of plastics have developed to a great extent. Expanded polystyrene (EPS) is a widely used commodity polymer for insulation and packing materials. However, the disposal of EPS poses a serious problem due to taking up large space in landfills and being non-biodegradable. Because environmental consideration gives rise to major problems, landfill or incineration of EPS are not appropriate approaches for the waste management. If EPS can be recycled into electrospun fibers after its single usage, volume reduction of more than 100 times can be achieved and produced fibers could be used as adsorbents. Lee *et al.* prepared electrospun PS nanofibers onto stainless steel mesh for the removal of oil spills (Lee et al. 2013). Other studies also elucidate the utilization of PS fibers for oily wastewater remediation (Lin et al. 2012, Chen and Tung 2017) but there are limited number of researches for the fabrication of PS fibers from waste Styrofoam (expanded PS, EPS) (Shin 2006, Shin, Chase, and Reneker 2005, Shin and Chase 2006).

The objective of this work is both recycling EPS wastes into fibrous materials by electrospinning and fabricating oil adsorbents to reduce the catastrophic effects of oily wastewaters on aquatic ecosystems. After dissolving EPS waste in organic solvents in different PS concentrations and solvent systems, the oil adsorption and oil / water

separation efficiencies of fibrous materials were evaluated. The oil adsorption capacity and oil – water separation efficiency of the proposed fibrous adsorbents were studied using 2 different types of oils; sunflower oil and machine oil. Our results show that the adsorption capacity of the EPS fibers obtained from waste reaches up to 120 g/g for sunflower oil. The proposed fibrous materials are promising both for the recycling of EPS wastes and remediation of oily wastewaters.

3.4.1. Results and Discussion

Waste-EPS (f-PS) was dissolved in DMF and / or THF at various concentrations and subjected to electrospinning at 1.0 kV cm^{-1}. Various morphologies of individual fibers (porous polymer cups, wrinkled beads-on-string, smooth fibers, wrinkled fibers and porous ribbon-shaped fibers) were achieved. It is well known that the viscosity of solution increases as the concentration of polymer solution and *Mw* of polymer chains increase due to the chain entanglement (Shenoy et al. 2005). For that purpose, virgin PS (vir-PS) and foam waste PS (f-PS) samples were characterized based on their molecular weight (*Mw*) that *Mw* of vir-PS sample was found 322 kDa that deviates 8 % from the data given by the producer, while f-PS was found 40 kDa. Along with the neat DMF (4:0) or THF (0:4), their mixtures (DMF: THF = 3:1, 1:1, and 1:3, 0:1) were employed in this study. Table 3.2 shows physical properties of all f-PS solutions and their corresponding fibers as well as their surface and interior morphology. Figure 3.8 presents SEM micrographs of all PS fibers fabricated from the neat and binary solvent systems. The majority of the solutions yield electrospun fibers of various morphology. The first column of the SEM images given in Fig. 3.8 shows the electrospun fibers obtained from neat DMF, (*DMF : THF = 4:0)* at different f-PS concentrations. The fibers favor 0.4 μm AFD with a smooth surface at 10 wt%. When the concentration increases to 30 wt%, AFD increases up to 5 μm. It is well established that increasing the concentration, i.e. viscosity of the solution, increases the AFD (Zheng et al. 2006, Isik and Demir 2018). At high concentration, the entanglements of the chains enhance the formation of stable jet with higher mass transfer. Since DMF has high electrical conductivity, the electrospun jet is exposed to high electrical force and bead-free uniform fibers were obtained at low f-PS concentrations. On the other hand, the usage of neat THF as solvent (depicted to the rightest image on the first row) leads to the

formation of collapsed beads with a uniform surface porosity. It is well established that the utilization of binary solvent systems promotes the porosity formation through the fiber structure due the difference between evaporation rates of THF and DMF. Note that the vapour pressures of solvents are ~ 200 hPa and ~ 3.5 hPa, respectively.

Table 3.2. The characteristics of PS solutions and the resulting electrospun PS fibers

f-PS wt%	DMF	THF	Viscosity (mPa · s)	Properties	Fiber diameter (µm)
10	4	0	24	thin fiber	0.4 ± 0.1
	3	1	52	thin fibers	0.5 ± 0.1
	1	1	44	medium thickness fibers	2.0 ± 0.6
	1	3	34	medium fibers with macropores	1.5 ± 0.1
	0	4	28	porous polymer cups	-
15	4	0	95	medium thickness fibers	1.0 ± 0.2
	3	1	171	medium thickness fibers	1.9 ± 0.6
	1	1	130	medium thickness fibers with grooves	2.5 ± 0.4
	1	3	140	medium thickness fibers with grooves and macro-pores	2.0 ± 0.3
	0	4	88	porous polymer cups	-
20	4	0	580	medium thickness fibers	1.8 ± 0.3
	3	1	681	thick fibers / interior porosity	4.0 ± 0.4
	1	1	554	thick fibers / interior porosity	3.5 ± 0.6
	1	3	311	thick fibers with grooves and macro-pores	2.2 ± 0.7
	0	4	279	thick/belt shape fibers with nanopores	3.5 ± 0.5
25	4	0	1400	thick fibers	4.0 ± 0.7
	3	1	2630	thick fibers	4.0 ± 0.8
	1	1	1862	thick fibers with grooves	3.0 ± 0.9
	1	3	756	thick fibers with macro-pores	3.5 ± 0.9
	0	4	507	thick / belt shape fibers with nanopores	14.0 ± 2.6
30	4	0	2319	thick fibers	5.0 ± 0.6
	3	1	5867	thick fibers	8.0 ± 0.7
	1	1	2517	thick fibers with grooves	5.0 ± 0.9
	1	3	2750	thick fibers with grooves and macro-pores	5.0 ± 0.9
	0	4	2120	thick / belt shape fibers with nanopores	16.0 ± 3.5

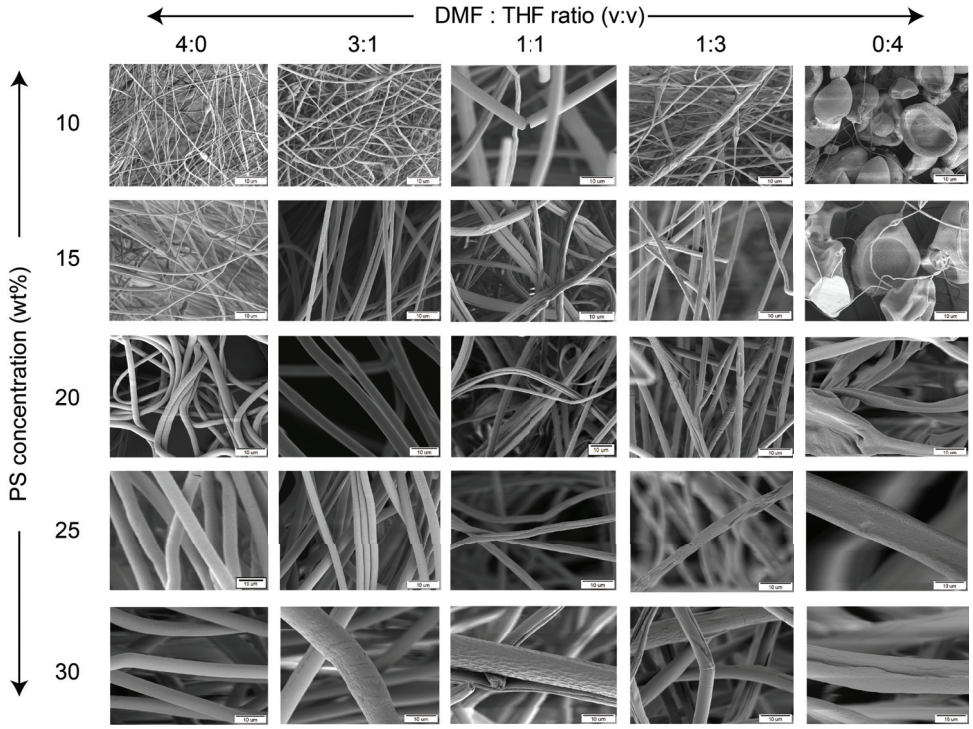

Figure 3.8. SEM micrographs of f-PS fibers with respect to different solvent compositions and f-PS solution concentrations (Scale bar is 10 μm)

The first row of the SEM micrograph set presented in Fig. 3.8 shows the fibers obtained from various compositions of the co-solvents DMF and THF. Neat DMF provides straight fibers with uniform AFD without beads. However, the addition of small portion THF *(DMF : THF = 3:1)* into the solvent system does not have remarkable effect on the surface texture that electrospun fibers have nearly smooth surface as observed in fibers obtained from neat DMF. The equivolume mixture of DMF and THF *(DMF : THF = 1:1)* results in the formation of wrinkled surface texture especially at high PS concentrations. Since the presence of THF in solvent system increases the vapor pressure and accelerates the solvent evaporation, the occurrence of surface texture occurs most probably due to the buckling of cylindrical polymer shell under compressive radial or a lateral contraction from the axial tensile stresses (Pai, Boyce, and Rutledge 2009).. The rise in the amount of high vapor pressure solvent, THF, increases the solidification and evaporation rate of solvent system. While faster rates preserve the initial phase separation and form small pores, lower rates lead to the formation of further phase separation due to the stretching of electrospun fibers or beads under elongation force and form large scale shallow pores (Lin et al. 2010). The fibers

fabricated from 1:3 solvent *(DMF : THF = 1:3),* have elongated and large voids on their surface. The development of this structure may arise from the rapid removal of solvent from the core of jet and the continuous stretching of jet, respectively. The highly volatile solvent can rapidly forms glassy skin and voids due to the phase separation and fast evaporation rate. Meanwhile, low volatile solvent still remains in the jet that makes the polymer core wet and stretchable. The voids are elongated under electrical field due to the stretchable core and forms large and shallow voids (Liu, Huang, and Jin 2015, Huang et al. 2011, Liu, Huang, and Jin 2014).

Furthermore, the neat THF system *(DMF: THF = 0:4)* causes to the formation of a ribbon-like morphology with densely packed nanoscale surface pores (nearly 90 nm) uniformly distributed on the beads and fibers. Although most electrospun fibers are in cylindrical morphology, highly volatile solvents, (like THF and DCM) show ribbon-like morphology due to the rapid drying following by collapse of jet and this morphology results in the large AFD varying between 3.5 to 16 μm (Liu, Huang, and Jin 2015). The neat THF system led to the fabrication of porous polymer cups with ~ 20 μm size at low f-PS concentrations (10 to 20 wt%) due to the low viscosity of f-PS solutions. Generally, bead or bead-on-string formation is observed when the polymer solution is fairly diluted because of the both insufficient viscosity and electrical conductivity of THF. The formation of pores may attribute to the both phase separations (VIPS and TIPS) along with breath figure formation mechanism. Previously, Lu *et al.* proposed that VIPS plays a pivotal role in the formation of this structure that internal and external porous PS yarns were obtained by conducting electrospinning at high relative humidity (Lu and Xia 2013).

Fiber diameter is a function of solution properties so that AFD is examined as a function co-solvents composition (Demir et al. 2002, Isik et al. 2017, Isik et al. 2016). A rise in the AFD was observed at all f-PS concentrations when the portion of THF increases in DMF. AFD is 1.0 ± 0.2 μm when neat DMF is used for spinning process of 15 wt% f-PS solution. The addition of THF increases the diameter 1.9 ± 0.6 μm (DMF:THF=3:1). The reason of increasing AFD could be the increase in viscosity upon incorporation of THF. The viscosity of DMF increases from 95 to 171 mPa·s (Table 3.5). It is well established that viscosity is the dominant parameter in diameter of electrospun fibers. The overall evaluation of all solutions suggests two important results. First, DMF solutions have higher viscosity than THF solutions. Not surprising,

DMF (0.92 mPa.s at 25 °C) itself has higher viscosity than THF (0.48 mPa.s at 25 °C). Second, the mixture of co-solvents shows higher viscosity than the one of the polymer solution prepared by neat solvents either DMF or THF. The further increase of the amount of THF in DMF may reduce the viscosity of the mixture at all f-PS concentrations. Thus, low viscosity of solution favours the formation of thinner fibers with beads especially at 10 and 15 wt% f-PS concentrations.

Conductivity of precursor solution is another important parameter in electrospinning. Since the process takes place under high electrical field, the stretching of the spinning jet rigorously occurs for conductive solvents (Angammana and Jayaram 2011, Uyar and Besenbacher 2008). Dielectric constants of DMF and THF are 38.25 and 7.52, respectively. Because of the lower electrical conductivity of THF, the addition of this cosolvent in the mixture inhibits the stretching of jet and results in larger AFD. As an example, a significant increase was observed from 1.8 to 4.0 μm when 20 wt% of f-PS electrospun from 4:0 and 3:1 (DMF:THF), respectively (Table 3.4). The effect of the addition of THF on the AFD could be observed more explicitly in equivolume DMF:THF solvent system such that the lowest AFD was measured as 2 μm at 10 wt% f-PS concentration. When the portion of THF exceeds DMF (DMF: THF = 1:3), beads on string with ~8 μm size is achieved.

Based on the overall data presented in Fig. 3.8, a map of various fiber surface textures as a function of the solvent composition and polymer solution concentration can be achieved. Figure 3.9 shows the mapping, in other words phase diagram of f-PS fiber morphology with respect to both parameters. The boundaries were constructed by estimation using the SEM micrographs. Polymer cups with surface porosity were observed from the 10 and 15 wt% f-PS concentrations in neat THF. On the other hand, the f-PS fibers fabricated from low portion of DMF (THF rich systems) at low PS concentrations demonstrate wrinkled beads-on-string morphology. In addition to the elliptical-like beads, collapsed ones were also obtained at low f-PS concentrations depending on the vapour pressure of the solvent mixture. While, DMF as low vapour pressure solvent systems form elliptical bead morphology, high vapour pressure solvent system shows collapsed beads. This phenomenon can be attributed to the formation of instable fluid jet at low polymer concentration (Lin et al. 2010, Uyar and Besenbacher 2008). The grey region of the scheme illustrates the fibrous region that fibers were fabricated with various morphological characteristics. From top to down, in other words

from high to low DMF ratio, smooth fibers give their place to wrinkled and porous fibers due to the before-mentioned phase separation mechanisms.

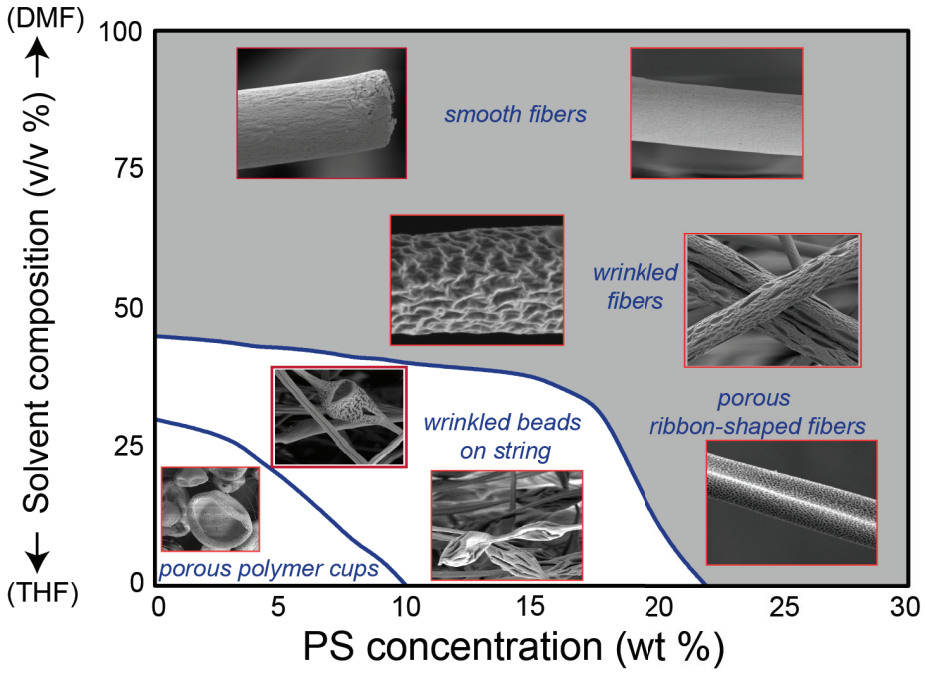

Figure 3.9. Dependence of surface texture on DMF:THF composition versus f-PS solution concentration (solid lines were estimated by using the SEM micrographs in Figure 3.8.)

Figure 3.10 shows the thin sheaths and porous cores of 20 wt% f-PS fibers electrospun from the solvent compositions. The fibers fabricated from neat DMF or 3:1 solvent composition (DMF:THF) consist of interior porosity and fibrils aligned along the fiber axis most probably due to the longitudinal strain rate of jet during the electrospinning (Lin et al. 2010). Water molecules are inevitably present in the solution system. One source could be the organic solvents that are hygroscopic, i.e. absorb certain amount of water molecules. Another source could be humidity from the air, which is nearly 52% in the spinning environment. The water molecules play active role for the generation of interior porosity. DMF is trapped inside the electrospinning jet. Cooling of the jet upon solvent evaporation forms a glassy skin around the fibers such that the solvent molecules are unable to escape from the electrospinning jet. Water and DMF undergo a liquid-liquid phase separation where DMF is solvent; however, water is non-solvent. The removal of the water molecules leaves behind pores.

The increase of THF portion disappears the presence of interior porosity (Fig. 3.10d and 3.10e). However, the addition of THF to the electrospinning solution causes the formation of surface texture (porosity). The fibers fabricated from neat THF solvent do not have interior porosity. Since THF has a much higher vapour pressure than water, the jet−air interface was always saturated by THF even under high humidity, which effectively hindered the formation of a sheath as well as internal pores by preventing the water vapor from penetrating into the jet and inducing phase separation. Consistent with the literature, low vapor pressure of DMF plays a significant role in the generation of internal porosity, while THF plays a critical role on the surface texture of PS fibers with pores by discouraging the formation of interior pores.

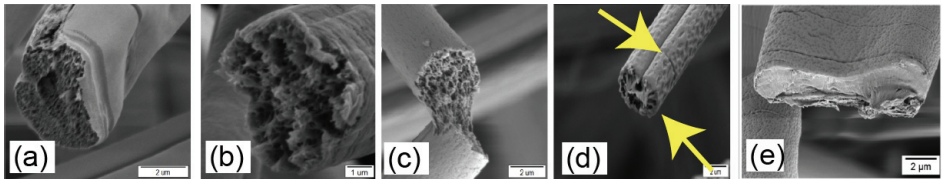

Figure 3.10. Cross-sectional SEM micrographs of the fibers fabricated from 20 wt% f-PS solutions with various solvent compositions of DMF:THF ratio **(a)** 1-0, **(b)** 3-1, **(c)** 1-1, **(d)** 1-3, and **(e)** 0-1

There is a competitive penetration and diffusion of two liquids and vapour (DMF, THF and water) has some primary effects, which are formation of thin but strong sheath due to the interface precipitation (VIPS and TIPS), internal phase separation due to the penetration of water vapour (VIPS), and gathering of condensed water on the surface due to the evaporative cooling (breath figure formation) (Lu and Xia 2013, Srinivasarao et al. 2001). Electrospinning is a non-equilibrium process because the structure formation occurs in a very short period of time, on the order of 0.1 sec (Greiner and Wendorff 2007). The stage at which the phenomenon of phase separation occurs is a true question. Considering high elongation rate and high speed of electrospun jet (≈40 m/s), the penetration of water vapour is hard under these circumstances so that VIPS and TIPS should occur before the transportation of jet trough the collector presumably on the Taylor cone. The rapid evaporation of solvent from Taylor cone consumes the heat of vaporization by cooling the surface and leads the formation of thermodynamically unstable jets. The separation of phases as well as

the breath figure formation may take place at this stage, where Taylor cone forms on the surface of a stationary solution droplet (Bognitzki et al. 2001, Ziabicki 1976).

For the investigation of hydrophobic / hydrophilic character of the fabricated fibrous materials, water contact angle (WCA) of the f-PS fiber mats fabricated from the various solvent compositions at 20 wt% polymer concentration was measured. Figure 3.11a demonstrates the dependence of WCA of the fibers with respect to the DMF:THF ratio along with foam itself and cast film of the pristine foam. The pristine foam presents WCA of 60°. The f-PS solution was cast on a glass slide and its WCA was also measured for comparison. WCA of the cast film is 90, i.e. lies between the pristine foam and the fibrous electrospun mats. Because all fibrous mats independent of the solvent compositions depict WCA >100° indicating that the fiber mats are hydrophobic. The hydrophobicity of the f-PS fiber mats may predominantly originate from the rough surface of the electrospun fibers. According to the Cassie-Baxter model, this roughness creates cavities on the surface and allows the trapping of air between surface and water droplet resulting in the inhibition of wetting the surface (Isik et al. 2017, Gao et al. 2014, Kim, Kim, and Kim 2013). The fibers fabricated from 1:3 DMF to THF ratio demonstrated the highest WCA among all mats because more rough surfaces with cavities and surface texture show more hydrophobic behaviour most probably due to the increment in the trapped air in cavities (Patankar 2009). On the other hand, smooth fibers with neat DMF solvent show the lowest WCA among the all-fibrous mats.

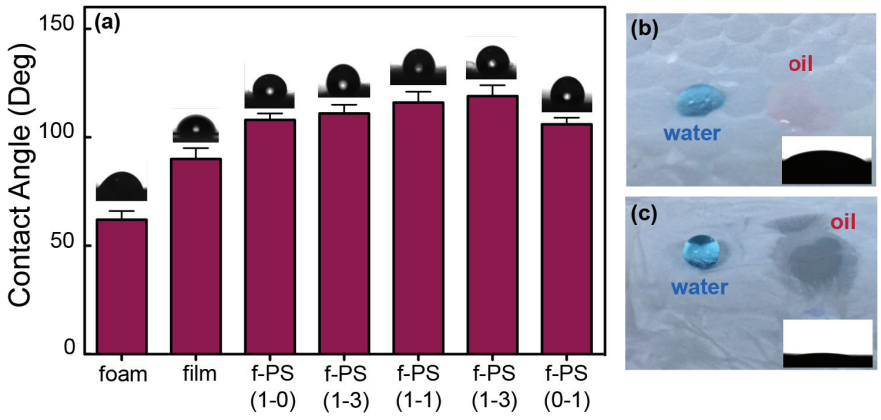

Figure 3.11. (a) Water contact angle comparison of the f-PS adsorbents fabricated from different solvent combinations with 20wt% solution concentration, photographic images of water and oil droplets on (b) pristine foam and (c) f-PS fiber. (The numbers in parenthesis indicate the solvent composition, DMF-THF ratio.)

The neat THF system resulted in the lowest WCA among the all-fibrous mats presumably due to the ribbon-like cross section of the resulting fibers, which have fewer cavities than the circular ones. In conjunction with the hydrophobicity, the fibers show further oleophilicity. This hydrophobic / oleophilic nature of the PS fibers is a requirement for oil-water separation. The photographs in Figure 3.11(b-c) show the wettability of water and oil droplets on the pristine foam and electrospun f-PS fiber mats, respectively. It is obviously seen that red stained vegetable oil quickly wets the surface of the f-PS fibers while the same amount of oil droplet stays on the pristine foam without being adsorbed. In addition, blue stained water droplet stays on the f-PS fiber surface in nearly round shape whilst the blue droplet spreads on the surface of the pristine foam. These results suggest that the f-PS fibers could be served as promising oil adsorbent. For further understanding of f-PS fibers' hydrophobic nature, their WCA hysteresis with respect to time has been observed in 60 sec (Figure 3.12). It is observed that the water droplets were not penetrated through the f-PS surfaces and remains nearly unchanged during this time period.

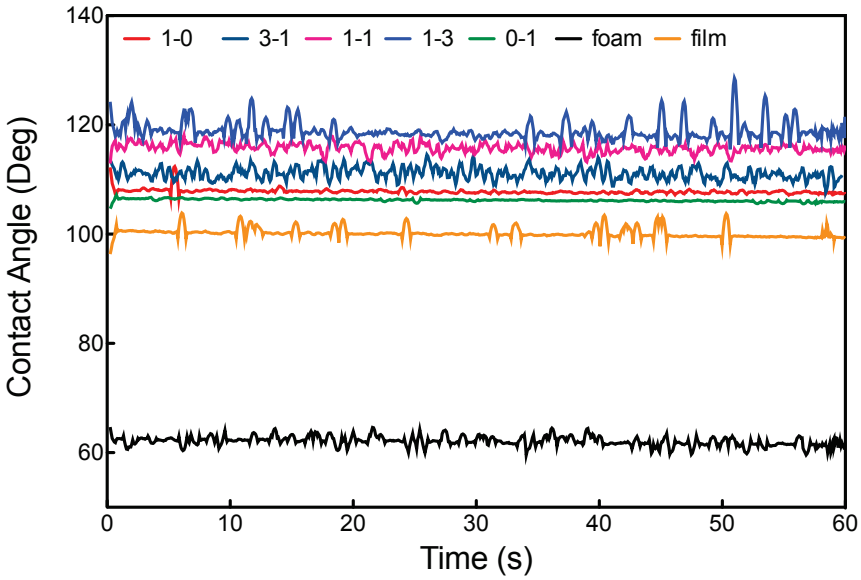

Figure 3.12. WCA hysteresis of f-PS fibers and their comparison with foam

Adsorption capacity is one of the most important key factors for the application of oil adsorbents. The required contact time for the oil adsorption was determined 60 sec, which is the optimum time for the highest oil adsorption and the shortest time

(Figure 3.13a). For each f-PS fiber, the oil adsorption capacity increases with adsorption time until the fibers reach saturation.

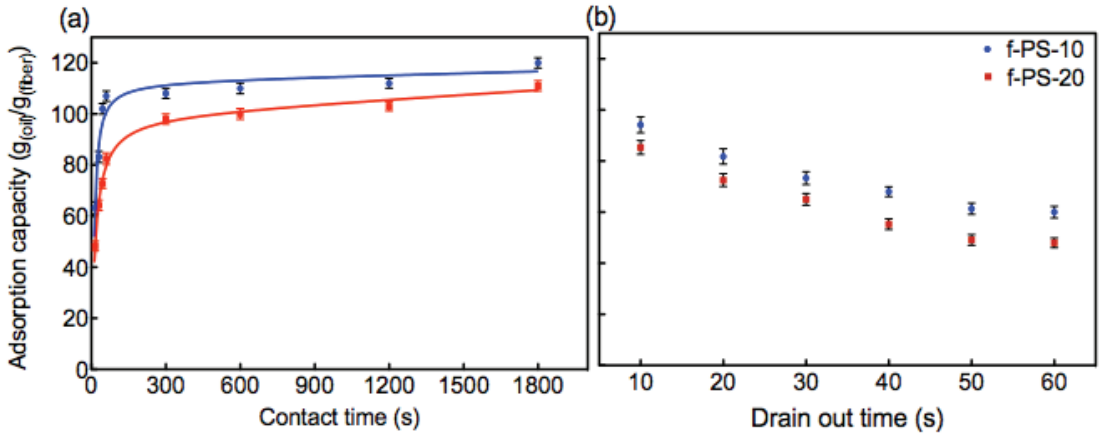

Figure 3.13. Oil adsorption variation of electrospun f-PS fibers with respect to (a) contact time and (b) drain out time

Plots of $ln(q_e-q_t)$ versus $ln(q_e)-k_1 \cdot t$ were described in Figure 3.14 and adsorption constant (K) in Table 3.3 were obtained from the slope of pseudo order plots. The *K* value decreased with raising the polymer solution concentration from 10 to 20 wt%. The fibers were taken in another vessel before measuring their weights and the excess oil on the fibers, which is not adsorbed by the fibrous material, was drained out.

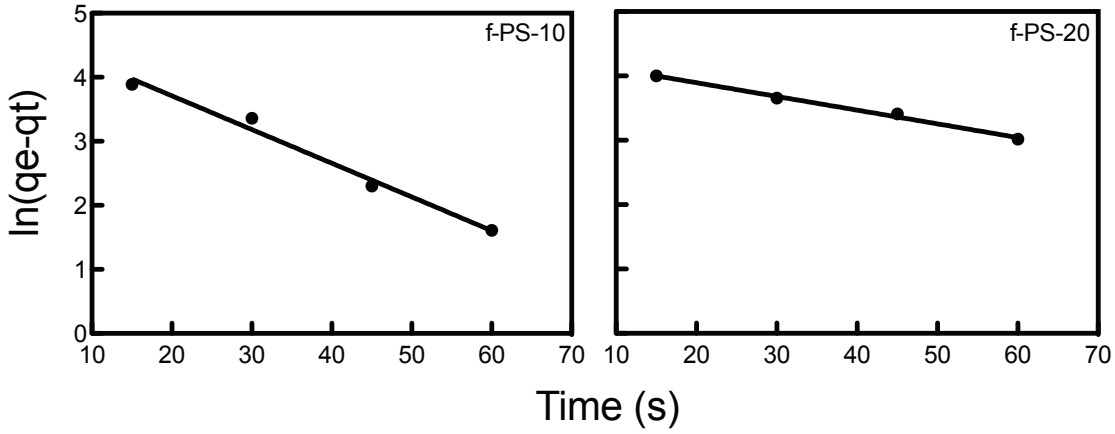

Figure 3.14. Pseudo first order plots of f-PS-10 and f-PS-20 adsorbents

Table 3.3. Analytically calculated Pseudo first order constants for oil adsorption on PS fibers

Adsorbent type	K (s^{-1})	R^2
f-PS-10	0,05262	0,9852
f-PS-20	0,0213	0,9935

The required drain out time of fibers before performing gravimetric analysis was determined as 30 sec because the weight of the adsorbed oil remains almost unchanged dramatically after 30 sec (Figure 3.13b). The removal efficiency of oil from the aqueous mixtures was examined by preparing different concentrations of oil polluted water mixtures 2, 5, and 10% (v/v) in 20 mL water by adding vegetable or engine oil droplets. An amount of 25 mg of fiber was immersed in oily water and mixed for 60 sec. Then, the difference between initial and final weight of fiber were measured with an analytical balance. The results are reported as percentage oil separation efficiency with their standard deviations. The oil adsorption capacity and oil water separation efficiency were examined for pristine foam and a commercial adsorbent, which was supplied by Municipality of İzmir, for the comparison of as-prepared fibers with the existing products.

Figure 3.15 demonstrates the oil adsorption capacity of the f-PS fibers with various surface textures. Whilst neat THF results in the polymer cups or wrinkled beads on string at low PS concentrations, the oil adsorption capacity of these samples could not be measured because the fiber mat do not have enough mechanical integrity. The increase in the f-PS concentration, accordingly AFD, results a decrease in oil adsorption capacity. For instance, the oil adsorption capacity of f-PS fibers fabricated from 10 wt% of PS concentration in equivolume DMF and THF solvent system is around 109 g/g; and the capacity decreases to 60 g/g for the fibers obtained from 30 wt% f-PS concentration due to having less specific surface area as AFD increases. The thicker the fiber is, the lower the surface area is. The fabricated f-PS fibers were expected to be a promising candidate for the adsorption of oil due to their hydrophobic and oleophilic nature. The van der Waals forces between fibers and oil may play a significant role in oil adsorption (Wu, An, et al. 2017, Deschamps et al. 2003). Moreover, sieving of the molecular aggregates of oil that is inevitably occurs at high oil concentration in water could be another mechanism of oil separation. The aggregates enter the gaps between

interconnected fibers due to the oleophilic property of adsorbent; then, moves through the surface and fills the voids / pores / grooves on the surface by capillary forces (Wu, An, et al. 2017).

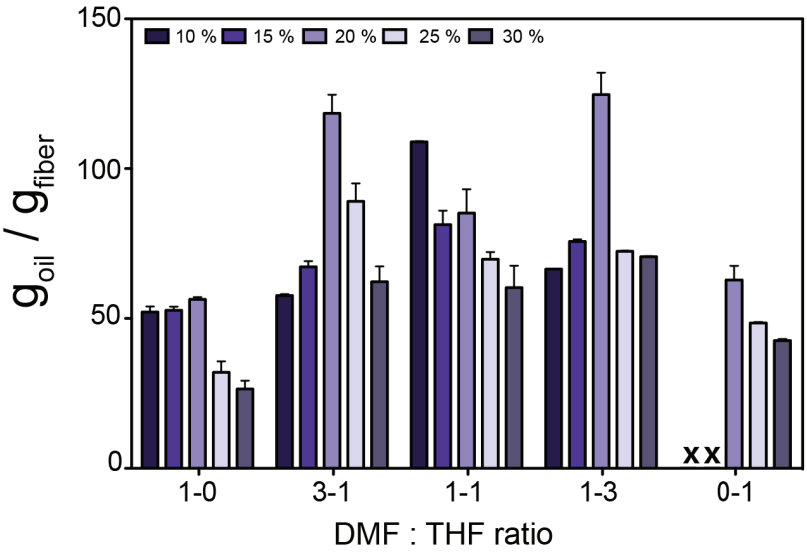

Figure 3.15. Vegetable oil adsorption capacity of f-PS electrospun fibers with respect to solvent composition and initial PS concentration. The letters '**xx**' refer to the absence of data points in the dataset probably due to the polymer cup formation and beads on string instead of fibers.

When neat THF or DMF solvents were used for the fabrication of f-PS fibers, low oil adsorption capacities have been observed that can be attributed to the enclosed cross-section and less interior and / or surface porosity of these fibers (Figure 3.10a and 3.10e). On the other hand, f-PS fibers fabricated from binary solvent systems result in better oil adsorption capacity than neat DMF or THF ones. The porous structure of f-PS fibers commonly contributes to higher specific surface area of the f-PS fibers (Figure 3.10b-d). The oil adsorption capacity of f-PS fibers fabricated from 3:1 DMF :THF solvent composition reached up to 118 g/g due to their interior porosity although these fibers have nearly smooth surface as in neat DMF solvent (Figure 3.10b). At low f-PS concentrations, the surface texture coming from 1:3 solvent composition (DMF: THF) does not have a significant effect on oil adsorption capacity due to the bead on string morphology. However, at 20wt% PS concentration, the capacity reaches to its highest value although the fibers have higher AFD. The combination of both interior porosity and surface texture enhanced the permeability by contributing to a high oil adsorption

(Figure 3.10d). The highest oil adsorption capacity was recorded as 124 g/g indicating that 1 g of adsorbent could adsorb 124 times its own weight. Physical trapping on the fiber surface and filling the voids on the fibers to reduce the surface free energy of the fibers. The voids between individual fibers and porous structure play a significant role on oil adsorption (Wu, An, et al. 2017, Deschamps et al. 2003, Chen and Tung 2017). Pores increase the specific surface area, which is helpful for the adhesion and adsorption of oil on the fiber surface. From the thermodynamic point of view, the oleophilicity of f-PS fibers plays a pivotal role for oil adsorption at first stage, because the oleophilic nature of adsorbent serves a minimum energy barrier for oil to spread on the surface and finally diffuse into the fibrous adsorbent (Wu et al. 2012, Gao et al. 2018). Thus, the fibers having both interior porosity and surface texture are promising candidates for the fabrication of oil adsorbents and they demonstrated better oil adsorption performance than the fibers having smooth surfaces. Normally the fibers are needed to be thin to have large surface area. On the other hand, the fibers should have mechanical integrity and resistance under the harsh conditions of adsorption. Large AFD provides mechanical resistance particularly under continuous flow. The results were compared with the oil adsorption capacity of pristine foam and commercial adsorbent (Figure 3.16). The pristine foam and commercial adsorbent show much lower oil adsorption capacity than the prepared f-PS adsorbents due to their low surface area and non-porous structure.

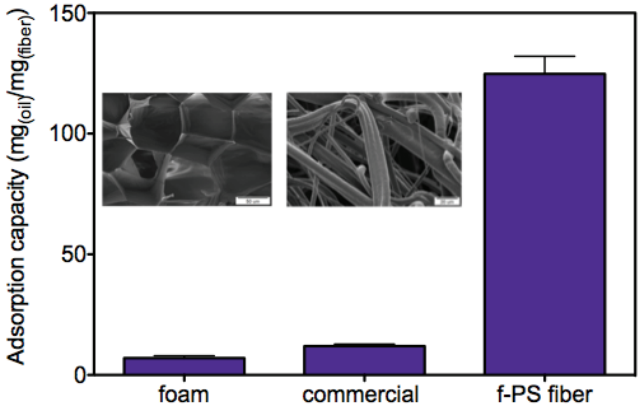

Figure 3.16. Comparison of the vegetable oil adsorption capacity of pristine foam, commercial adsorbent and f-PS fibers fabricated from 1:3 (DMF:THF) solvent system. Insets show the SEM micrographs of pristine foam and commercial adsorbent.

Synthetic oily wastewater mixtures were prepared by changing the oil concentration in water from 2 to 10 % (w/w) and oil separation efficiency of f-PS fibers were studied. Figure 3.17 shows the process to capture of oil from water successfully by using the f-PS fibers. When a piece of the f-PS adsorbent brought into contact with oil-polluted mixture, the fiber floated on the water surface and adsorbed both red coloured vegetable and engine oil selectively within a few seconds. After treatment with the f-PS adsorbent, the previously polluted water turned transparent and clean. Moreover, the fibrous adsorbents exhibited buoyancy that they were able to stay on the surface even after oil adsorption. Hereby, f-PS adsorbent stays compact after capturing the oil from water by conserving their mechanical integrity. This property of the f-PS mats is also important for the removal of adsorbents after oil-spill clean-up.

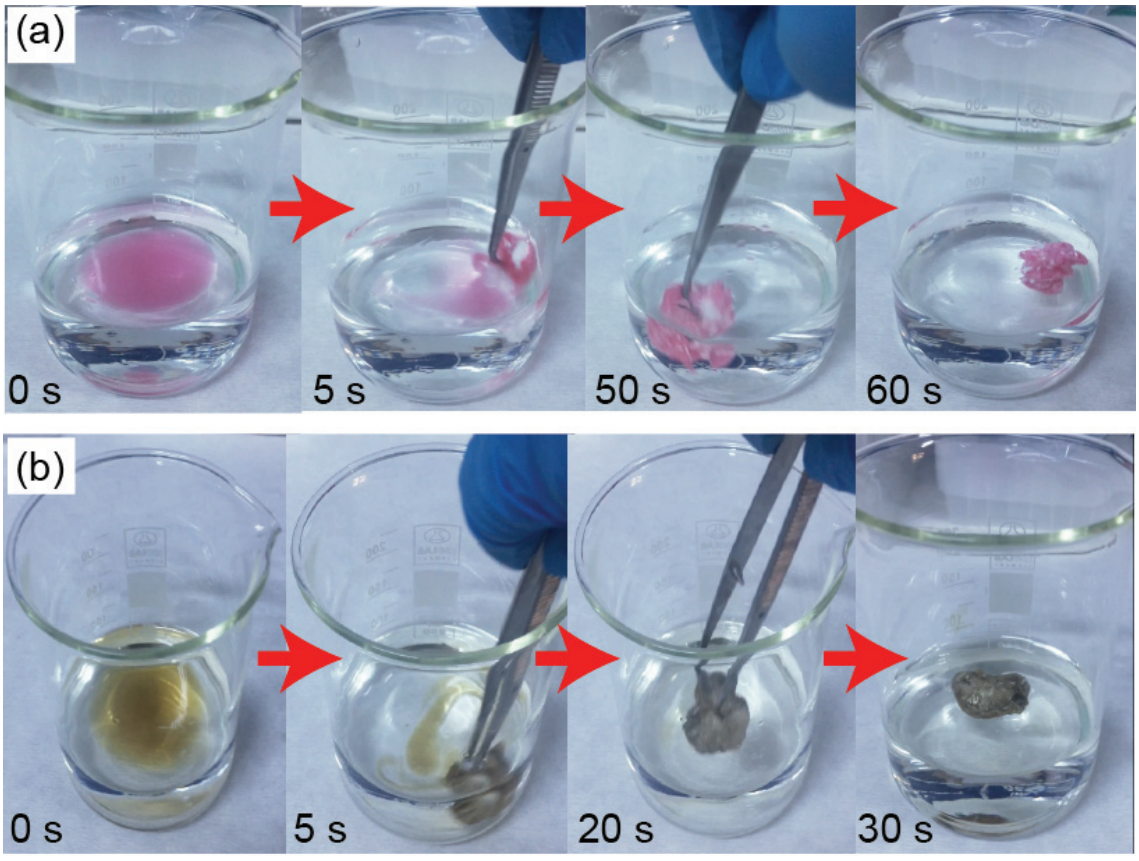

Figure 3.17. The adsorption processes of (a) vegetable oil and (b) engine oil using the as-prepared f-PS adsorbent with 5% oil-polluted water

Figure 3.18a shows the comparison of oil separation efficiency of the proposed f-PS fibers fabricated from 20wt% concentration from binary solvent systems. The oil separation efficiency of the fibers were examined by changing the vegetable oil

concentration from 2 to 10 v/v% in oil polluted water. All the fibers showed more than 98% of separation efficiency independent of the f-PS surface texture in 2% oil-polluted water. Increasing the oil concentration to 5 % reduces this ability to 75 % for the f-PS fabricated from 1:3 DMF to THF ratio. When the oil concentration reaches up to 10 %, the fibers fabricated from 3:1 DMF to THF ratio shows the separation efficiency around 94%.

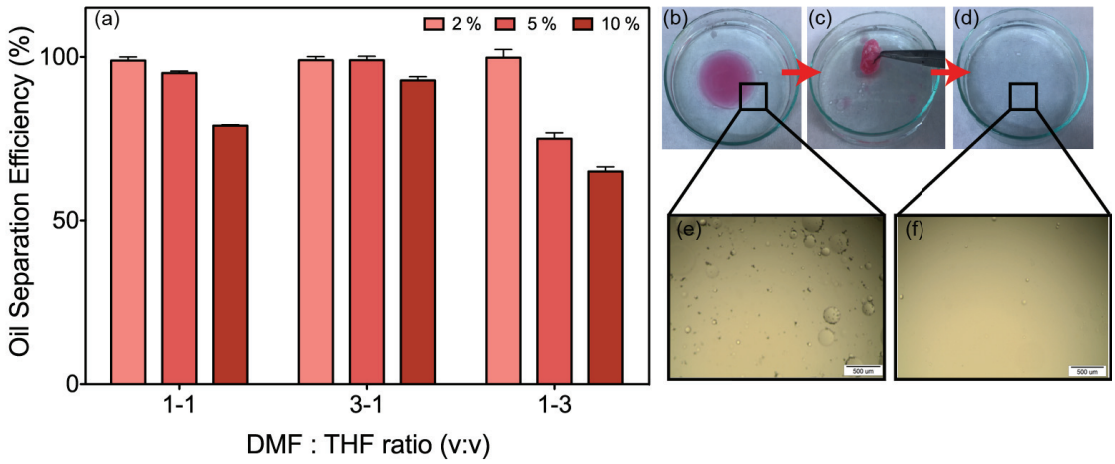

Figure 3.18. (a) Oil separation efficiency of electrospun fibers using vegetable oil, photographs of oil-water mixture (b-c) before adsorption, (d) after adsorption, optical micrographs of mixture (e) before adsorption, and (f) after adsorption of 5 % oil polluted water

The efficiency of f-PS fibers goes down 79 and 65 % for 1:1 and 1:3 DMF to THF ratio, respectively. Thus, the performance of the oil separation is mainly governed by the morphology of the individual fibers and electrospun mats. The fibers prepared from 20wt% concentration in DMF:THF (1:3) mixture offers the best oil sorption. Figure 3.18(b-f) shows the photographic and optical microscopy images of oil droplets before and after the treatment with f-PS fibers. The oil droplets were diminished after the treatment and only little amount of small droplets were remained in the water. These droplets might arise from the remaining volume of the oil droplets after separation. The disappearance of large amount of the droplets may suggest that the electrospun fibers of f-PS wastes are effective for the removal of oil from water. In order to investigate the practical application of oil separation efficiency of f-PS fibers, we prepared an engine oil / water mixture by using waste engine oil and compared our results with the real oil-water mixture sample from a big Shipyard in Izmir (one of the biggest in Europe).

Figure 3.19 shows the comparison of oil separation efficiency of pristine foam, commercial adsorbent and f-PS fibers fabricated from 20 wt% PS solution in 1:3 (DMF:THF) solvent system. Considering the growing number of oil-spill accidents and variable oil compositions, the adsorbents should be used to collect multiple types of oil. Therefore, the separation efficiency of adsorbents was also investigated for the engine oil / water mixture (10 %, v/v) and f-PS adsorbents show 82 % separation efficiency, while the pristine foam and commercial adsorbent have 16 and 44 % efficiency under same circumstances, respectively.

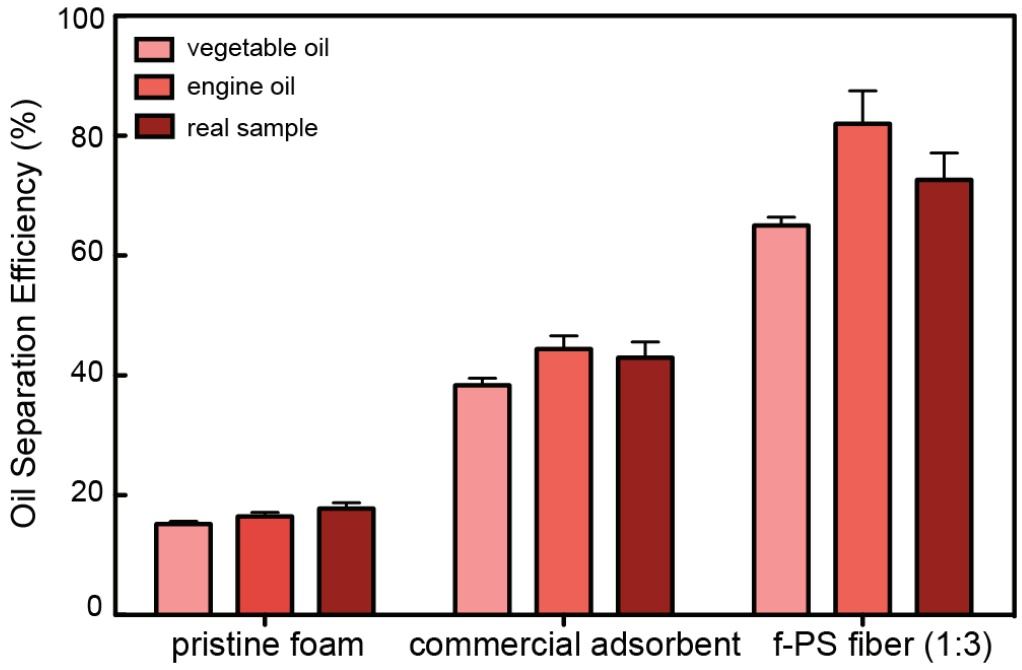

Figure 3.19. Oil separation efficiency comparison of pristine foam, commercial adsorbent and proposed f-PS fiber (1:3) by using vegetable oil, engine oil, and real oily wastewater sample

The oil content in the real sample was ~ 10 % engine oil by volume. The separation efficiency of f-PS adsorbent was found 73 %, which is much higher than the performance of the pristine foam or commercial adsorbent (18 and 43 %, respectively), thanks the electrospinning of waste EPS. Hereby, the proposed f-PS adsorbents are up-and-coming candidates for the remediation of oil-spills in comparison with the commercial adsorbent. In Table 3.4, the sorption capacity of the electrospun fibers from previously reported in literature is given.

Table 3.4. Comparison of oil adsorption capacities of polymeric electrospun fibers

Electrospun material	AFD/ µm	Oil type	Adsorption capacity (g/g)	Ref.
Polyvinylidene fluoride	0,055	Soybean oil	14	(Jiang et al. 2015)
Polyvinylidene fluoride / Polystyrene	2	Vegetable oil	46	(Jiang et al. 2015)
Polyvinylidene fluoride / Polystyrene / Fe_3O_4	2	Soybean oil	35	(Jiang et al. 2015)
Polysulfone	1	Engine oil	39	(Cojocaru et al. 2017)
Polyimide	3	Engine oil	76	(Tian et al. 2017)
Polystyrene	3	Vegetable oil / engine oil	97 / 114	(Lee et al. 2013)
Polystyrene / Fe_3O_4	1	Soybean oil	70	(Jiang et al. 2015)
Polystyrene from foam waste	4	Vegetable oil / engine oil	124 / 95	This study

Generally, the neat polymer fibers fabricated without using any other additives such as magnetic nanoparticles, carbon nanotubes, etc. show lower oil adsorption capacities than the f-PS fibers obtained from waste. This short comparison of oil adsorption capacities through the literature strongly suggests that the PS fibers fabricated from waste products with both surface and interior porosity can be a low-cost alternative to the oil separation from water systems.

3.5.Conclusion

vir-PS and EPS wastes were readily processed by electrospinning from the solvent mixture of THF and DMF. Freestanding and highly flexible fiber mats were achieved and used as adsorbent materials for oil water separation. A detailed phase diagram is proposed for the determination of fiber morphology (diameter, shape, surface and interior texture) as a function of the co-solvent composition and polymer concentration of the precursor electrospinning solution. Not surprisingly, low polymer concentration solutions lead to bead-like; on the other hand, high concentrations provide straight and thick fibers. While THF rich solvent mixtures cause the formation of

surface porosity due to the breath figure formation mechanism, the DMF rich ones facilities the formation of pores both on the surface of the fibers and on interior pores in their cross-section due to the contribution of VIPS and TIPS mechanisms. This variation of surface morphology remarkably influences the hydrophobicity /oleophilicity of the fiber mats, i.e sorption capacity against oily wastewaters. Cassie–Baxter model postulates that droplets hang on the rough surfaces and allow air trapping between the surface and the droplet (Kim, Kim, and Kim 2013). When the WCA of flat surfaces (drop casting or smooth surface ones) and rough electrospun fibers were compared, the porous fibers have much greater value than the drop casting or smooth ones due to the deposition of porous fibers and trapped air between their interfibrillar spaces and pores.

Note that the f-PS fibers show better oil adsorption and separation performance compared to vir-PS or pristine foam does. The vegetable oil adsorption capacity of f-PS reaches up to 124 g/g and they have nearly 93% oil separation efficiency for highly oil-polluted mixtures (10% oil by volume). For low oil concentrations, they could clean nearly the whole vegetable oil from the water with 98% efficiency. It must also be said that the f-PS mat depicts 10 times higher adsorption capacity than the commercial ones when tried in real oily water samples taken from the Izmir Shipyard at 10% of oil in water. Finally, this work may provide a versatile avenue for the fabrication of adsorbents, which are excellently suited for recycling of wastes other than EPS and efficient separation of various oil polluted waters.

CHAPTER 4

REMOVAL OF URANIUM IONS FROM AQUEOUS SYSTEMS VIA AMIDOXIMATED PIM-1 FIBERS

This study reports a novel adsorbent material for the for the removal of U(VI) ions from aqueous systems under continuous flow. Fibrous membranes were electrospun from Polymers of intrinsic microporosity (PIM-1), which are one of the most promising polymer candidates for adsorption applications due to their high surface area and diversified functional groups. Bead-free and uniform amidoxime functionalized PIM-1 (AF-PIM-FM) fibrous membranes were fabricated with 1.69±0.34 μm average fiber diameter by *Prof. Uyar's Group* in Bilkent Unviersity. For comparison, neat PIM-1 fibrous membranes (PIM-FM) were also prepared as control group. All samples were characterized by using SEM, FT-IR, ^{1}H-NMR, XPS, BET, TGA and DSC analyses. The results showed that the enhanced porosity of the AF-PIM-FM samples were maintained after amidoxime functionalization. Firstly, powder and fibrous membrane form of amidoxime PIM-1 adsorbents were compared by using batch adsorption process. Then, the experiments were continued with column adsorption to make the membranes more feasible for real applications. AF-PIM-FM adsorbents enhanced the uranium adsorption capacity up to 20 times when compared with neat adsorbents. Several parameters were studied by changing pH, initial concentration and regeneration of adsorbents were also investigated. AF-PIM-FM adsorbents were used for five adsorption-desorption cycles without any structural deformation.

4.1. Introduction

Nuclear industry has been growing attention due to the increasing demand for energy and providing high energy density. Uranium is one of the principal elements in nuclear cycles and the reserves in terrestrial ores leak away in less than 100 years with the current consumption rates (Piechowicz et al. 2016, Wang, Yuan, et al. 2016). The oceans are limitless sources for uranium recovery that they reserve nearly 99% of uranium inventory on earth. On the other hand, huge amounts of uranium are released

into the biosphere and threat the environmental safety. According to the reports of World Health Organization (WHO), the concentration of uranium in drinking water should not exceed 15 ppb and the tolerable daily intake is 0.6 μg/kg of body weight (Zhang et al. 2016). Therefore, efficient and selective recovery of uranium from aqueous systems - oceans or other water sources – is highly desirable for both sustainability of nuclear source and reduction of environmental damages. There are several methods for the removal of U(VI) ions from aqueous sources such as solvent extraction (Ruhela et al. 2015), co-precipitation (Luo et al. 2009), electrodeposition ion exchange (Ladeira and Morais 2005), membrane filtration (Shen and Schäfer 2014, Favre-Reguillon et al. 2003), biosorption (Aytas, Turkozu, and Gok 2011), and adsorption (Li et al. 2018, Wiechert et al. 2018). Among these various processes, adsorption is one of the most efficient and versatile options due to its cost-effectiveness and simplicity. Different adsorbent materials have been used for U(VI) removal including metal oxides (Camtakan, Erenturk, and Yusan 2012), activated carbon (Mishra et al. 2015), silica (Zhao et al. 2015) and polymers (Brown et al. 2016, Wu, Pu, et al. 2017). Nevertheless, there is a still challenge to develop new adsorbent materials with better adsorption performances. Amidoxime is most widely used functional group in the studies about uranium removal from aqueous systems due to its chelating ability and selectivity (Chen et al. 2017). Various adsorbents have been functionalized with amidoxime groups in the literature such as polymer fibers (Horzum et al. 2012), ceramic sorbents (Horzum et al. 2012) , magnetic microspheres (Zhao et al. 2014) and hydrogels (Wang, Li, et al. 2016) but amidoxime functionalized polymers are found more applicable (Yue et al. 2013). The major issue for these amidoxime modified polymers is the slow adsorption kinetics due to the low surface area of adsorbents that hinders the effective transportation of U(VI) ions throughout the material (Chen et al. 2017).

Because of the high surface area by means of unusual chemical structure (Budd et al. 2004, Budd et al. 2005) and high stability under harsh conditions (Budd, McKeown, and Fritsch 2005, McKeown and Budd 2006), polymers of intrinsic microporosity (PIM-1) has gained significant interest in adsorption and separation applications. Moreover, these novel polymers could be modified with several functional groups to selectively capture targeted species thanks to the nitrile group in the backbone and they could provide an opportunity diversification. Throughout the literature, some successful modifications of PIM-1 have been reported (Satilmis and Budd 2014,

Satilmis, Alnajrani, and Budd 2015, Satilmis and Budd 2017). Recently, for the removal of uranium ions, non-invasive functionalization of PIM-1 by hydroxylamine to amidoxime have reported by Patel *et al*. (Sihn et al. 2016) that this novel adsorbent shows both high uranium affinity and fast sorption kinetics. However, the utilization of adsorbents in powder form limits their applicability in filtration. PIM adsorbents can be prepared in fibrous form by the help of electrospinning due to their hood processability. Thus their practical usage could be enhanced in filtration applications (Budd et al. 2004, Bonso, Kalaw, and Ferraris 2014). There are some reports about electrospinning of modified or neat PIM-1 through literature (Satilmis and Uyar 2018a, b, Satilmis, Budd, and Uyar 2017) but the uranium removal application of these amidoxime modified PIM-1 fibers under continuous flow have not been considered yet.

In this part of thesis, PIM-1 with uranyl chelating amidoxime groups and fabricated fibrous membranes by electrospinning. The main objectives of this study were to functionalize PIM-1 fibrous mats with amidoxime group, to investigate the fiber morphology and to compare the adsorption capacity of neat and amidoxime PIM-1 fibers against U(VI). Moreover, the effect of adsorption method (shaking or stirring), initial concentration, and pH were investigated using a continuous flow method. At the end of the study, the regeneration of fibrous membranes through several successive adsorption / desorption cycles was demonstrated.

4.2. Experimental

Through this study, we only performed the part, which includes the uranyl sorption study of as-fabricated fibers. The synthesis of neat and amodixime functionalized PIM-1 polymers and fabrication of fibrous adsorbents were achieved at Bilkent University by Prof. Uyar's group.

Electrospinning of PIM-1 and amidoxime PIM-1 was achieved as reported by our collaborator's group earlier. (Satilmis and Uyar 2018b) The characterization of fibrous mats were carried out by Uyar's group and reported in literature. (Satilmis et al.) Uranium (VI) aqueous solutions was prepared by dissolving uranylacetate dihydrate ($UO_2(CH_3COO)_2 \cdot 2H_2O$; Merck) into sodium acetate buffer solution (pH ~ 5.2, Fluka). In order to show the applicability of amidoxime functionalized PIM-1 fibrous adsorbent in the continuous removal of Uranyl ions from aqueous solutions, column sorption

studies were carried out. A homemade column system involving plastic syringe with an internal diameter of 9.0 mm was employed through the experiments. Both PIM-1 and amidoximated PIM-1 fibers were cut into round shape with nearly 9.0 mm diameter, and 10.0 mg of each adsorbent was filled in plastic syringes. The photographic representation of the experimental setup is illustrated in Figure 4.1. In a typical adsorption experiment, 10.0 mg of adsorbent was placed in syringe and U(VI) solution flowed through the syringe column at a flow rate of 0.15 mL min^{-1} by using an infusion pump (New Era NE300 Infusion Pump, Farmingdale, NY, USA). The samples of effluent were collected at 3 mL volume fractions at various initial concentrations and pH values.

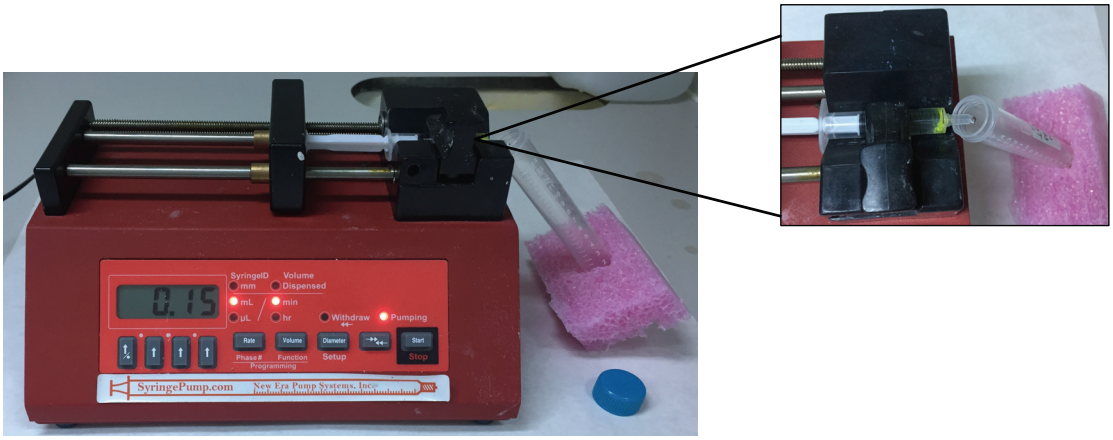

Figure 4.1. The photographic representation of experimental set-up

The effect of initial concentration on the U(VI) adsorption capacity of fibers was conducted at 50 ppb, 100 ppb, 500 ppb, 1 ppm, 5 ppm, 10 ppm, 20 ppm, and 50 ppm concentrations. In each measurement, pH was adjusted to 5.2 and 3.0 mL of U(VI) solution was used. The experiments investigating the effect of pH were performed by adjusting the pH of U(VI) solution to 4.0, 5.2, and 8.0 using sodium acetate-acetic acid, sodium acetate, and Tris-EDTA buffer solutions, respectively. The concentration of U(VI) solution was 5 ppm and 3.0 mL of solution was used. Desorption study of proposed fibrous adsorbents was carried out using sodium bicarbonate ($NaHCO_3$, Sigma Aldrich) as desorption agent. The U(VI) ion loaded adsorbent was treated with 20.0 mL of 1M $NaHCO_3$ and consecutive sorption-desorption cycles were performed after washing the adsorbents with deionized water after each cycle to study the reusability of proposed fibrous adsorbents. The speciation analysis of uranium-

containing ions at various pH values was performed using Visual MINTEQ software. (Figure 4.2)

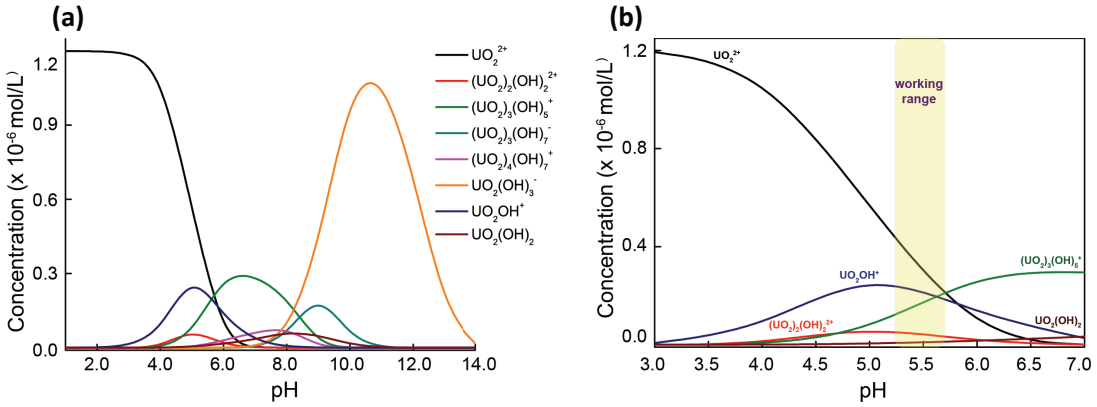

Figure 4.2. Speciation diagram of U(VI) between a pH range (a) 2.0 to 14.0 and (b) 3.0 to 7.0

Finally, the eluted solutions were analysed by ICP-MS. The concentration of uranium (VI) ions was determined using Inductively Coupled Plasma – Mass Spectrometer (ICP-MS) (Agilent 7500ce Series, Japan). The ICP-MS operation parameters are given in Table 4.1. The main stock solutions (10 ppm, 1 ppm, 100 ppb, and 10 ppb) were prepared by dilution of 1000 ppm U(VI) stock solution. Then, standard solutions of 0.05, 0.1, 0.2, 0.5, 1.0, 2.0, 5.0, 10.0, 20.0, 50.0, 100.0, 200.0, 500.0, 750.0, and 1000.0 ppb concentrations were prepared by appropriate dilution of main stock solutions to the required volume.

Table 4.1. ICP-MS operation parameters

Operation Parameters	**Value**
RF power	1550 W
RF matching	1.78 V
Make up gas flow rate	0.15 L/min
Argon carrier gas flow rate	0.95 L/min
Chamber temperature	2°C
Sample depth	8 mm
Nebulizer	Concentric
Nebulizer pump	0.1 rps
Tune setting (m/z)	7/89/205
Isotopes monitored (m/z)	^{238}U

Terbium internal standard solution was added in all samples and standard solutions at same concentration level through all ICP-MS analysis to improve the precision of quantitative analysis. Moreover, all samples and standard solutions were acidified by addition of concentrated HNO_3 to produce 1.0 % (v/v) acid in the final solution. The uranium ion adsorption capacity of fibers (μg U · g^{-1} dry adsorbent) was calculated using the following equation:

$$Q = \frac{(C_i - C_f)V}{W} \quad (4)$$

where Q is the adsorption capacity of fiber (μg · g^{-1}), C_i is the initial concentration of U(VI) (ppb), C_f is the final concentration of effluent U(VI) (ppb), V is the volume of the solution passed through the fiber, and W is the weight of the fiber. The percentage of uranium adsorption was calculated using the following equation:

$$\%\, Sorption = \frac{C_i - C_f}{C_i} \times 100 \quad (5)$$

4.3. Results and Discussion

The characterization of fabricated PIM-1 and amidoxime PIM-1 fibers were carried out by Uyar's group. The results of contact angle, FTIR, NMR, XPS, TGA, DSC and BET analysis were given in a literature article of Satilmis *et al.* (Satilmis et al.). Figure 4.3 demonstrates the SEM micrographs and fiber diameter distributions of PIM-1 and amidoxime functionalized PIM-1 fibers. Both fibers possess smooth surfaces and they are suitable for continuous adsorption application due to their self-standing form. PIM-1 and amidoxime functionalized PIM-1 fibers have 2.38 ± 0.42 and 1.37 ± 0.44 μm average fiber diameter, respectively. Figure 4.4 shows the structures of neat and amidoxime functionalized PIM-1 fibers, and their speculative binding mechanism to uranyl ions. Through the literature, there is only one study about the uranium removal application of PIM-1 powders and Patel *et al.* showed that the fastest and highest adsorption was only achieved in batch adsorption systems (Sihn et al. 2016). Firstly, we tested the uranium ion removal efficiency of amidoxime functionalized PIM-1 powder as control sample (AF-PIM-PWD) and amidoxime functionalized PIM-1 fibrous

membrane (AF-PIM-FM) in a batch adsorption system by using magnetic stirrer then compared our results with the reported results by Patel *et al.* (Sihn et al. 2016).

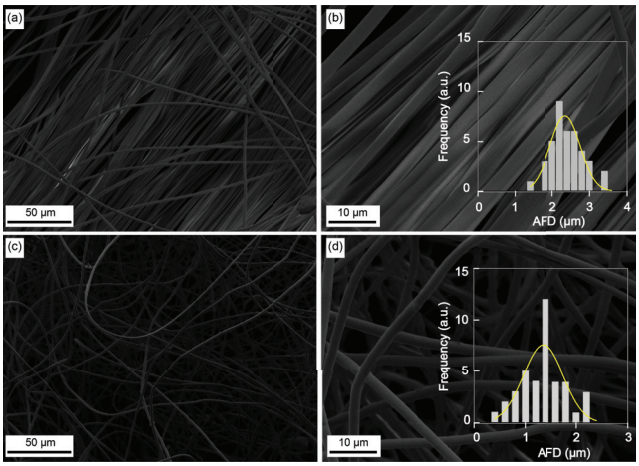

Figure 4.3. SEM micrographs of (a-b) PIM-FM and (c-d) AF-PIM-FM fibers (insets show the fiber diameter distributions)

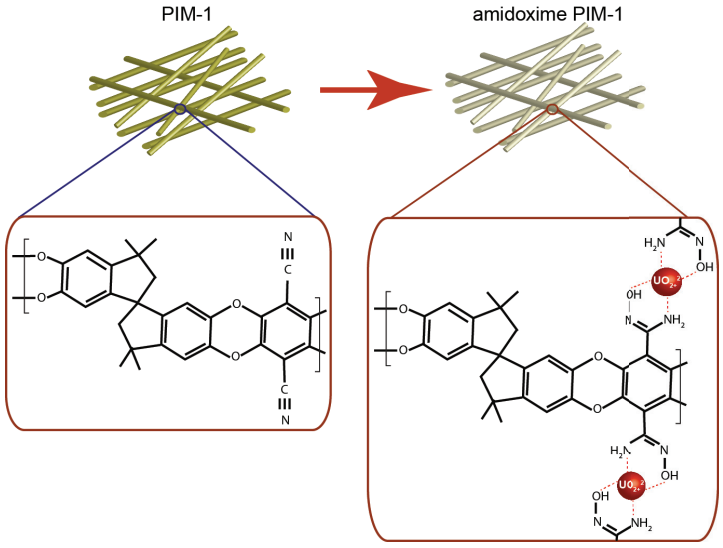

Figure 4.4. Structure of fibrous membranes before and after functionalization and their speculative binding mechanism to uranyl ions

After 24 h of batch adsorption with 5 ppm concentration of uranyl solution, AF-PIM-PWD samples adsorbed 4.04 mg g^{-1} Uranium(VI) (Figure 4.5). This result is in coherence with the reported data in literature (Sihn et al. 2016). The effect of shaking and stirring methods on uranium adsorption capacity was compared for AF-PIM-PWD. When the magnetic stirrer was used instead of a shaker, nearly 10 % more uranium ions

was adsorbed by AF-PIM-PWD at the end of 20 min. The adsorption capacity of fibrous samples was carried out by using a shaker instead of magnetic stirrer, because stirrer could damage the fibers physically. The 'adsorption capacity' term refers to the measured adsorption capacity of electrospun fibers at given conditions, not their equilibrium maximum adsorption capacities. However, the fibrous form of the PIM-1 samples adsorbs fewer amounts of uranyl ions than the powders forms although all the experimental conditions were the same. The reduction in uranyl adsorption capacity is based on the reduction in the surface area of the fibrous form of PIM-1 samples (Satilmis and Uyar 2018b). Although the reduced surface area of AF-PIM-FM samples, they could adsorb nearly 50% of uranyl ions in the system. Because the practical usage of powders is limited in sorption applications due to the additional processes required for the removal of sorbent powders from the system, self-standing fibrous membranes are more appropriate for the continuous column adsorption system. Thus, we continued to the further studies by using fibrous membranes fabricated from pristine and amidoxime functionalized PIM-1 samples.

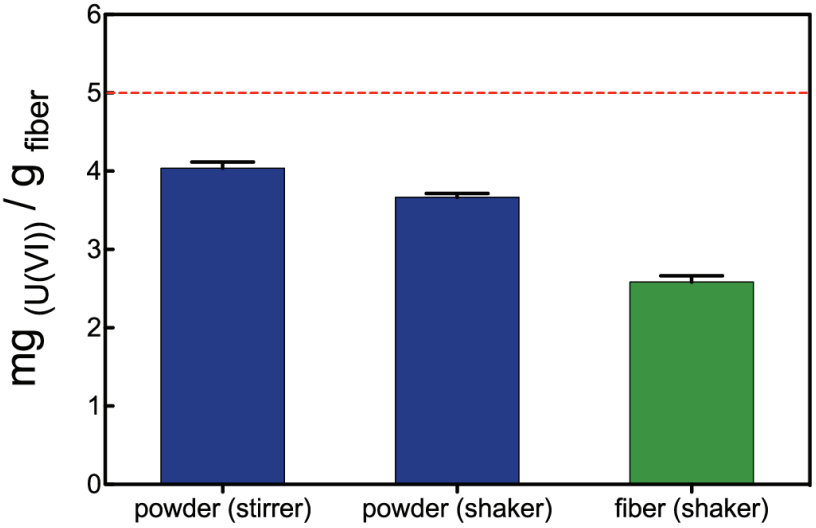

Figure 4.5. Batch adsorption study of amidoxime functionalized PIM-1 powder (blue) and membrane (green) using stirrer and shaker. Red dashed lines show the initial uranyl solution concentration.

As we mentioned in Figure 4.2, uranium ions are found in several forms at different pH values. Thus, pH of the solution is critical for the understanding of adsorption behaviour of uranium ions. Three different pH values were chosen for the

study (pH 4, 5.5 and 8) at 5 ppm concentration for both pristine and amidoxime functionalized PIM-1 fibers. The results showed that amidoxime functionalized fibers demonstrated a significant uranyl adsorption capacity than the pristine ones (Figure 4.6). The highest adsorption capacity was achieved by AF-PIM-FM at pH 4 with 590 μg g^{-1} uranyl, which is 20 times higher than the PIM-FM ones (30 μg g^{-1}). The adsorption capacity of fibrous membranes was reduced slightly at higher pH values, at pH 5.5 and 8, due to the steric effect of other ions present in the solution.

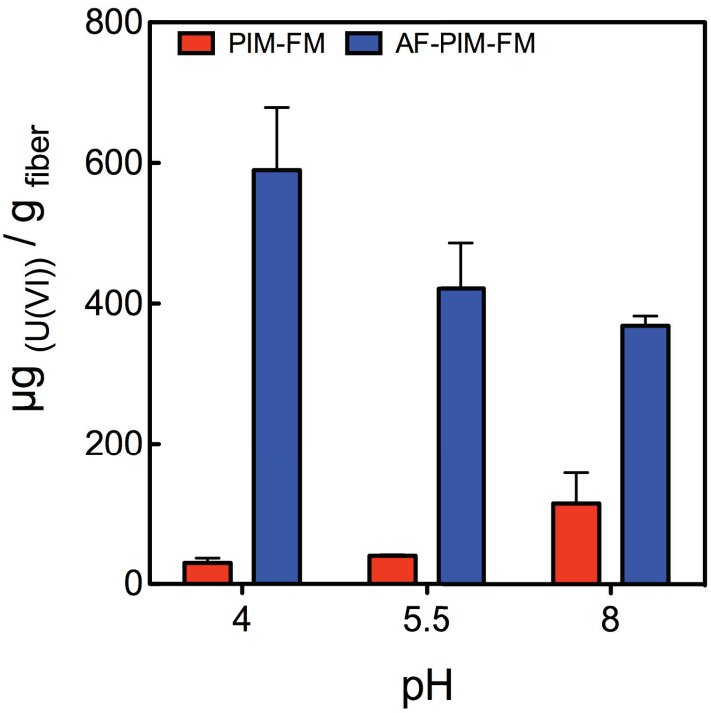

Figure 4.6. Column adsorption study of U(VI) as a function of pH

Then, the adsorption ability of PIM-FM and AF-PIM-FM was also investigated in terms of the initial concentration of uranyl ions. We kept the amount of adsorbent (20 mg) and pH constant (at pH 5.5) through the experiments and concentration range was changed from 50 ppb to 50 ppm. Figure 4.7 shows the effect of initial concentration on the adsorption capacity of fibrous membranes. The uranyl adsorption of both PIM-FM and AF-PIM-FM samples increased with increasing initial concentration. Even at 50 ppm uranyl concentration, the fibers did not achieve a plateau. AF-PIM-FM has 1697 μg g^{-1} U(VI) ion adsorption capacity at 50 ppm concentration and it is nine times higher than PIM-FM one.

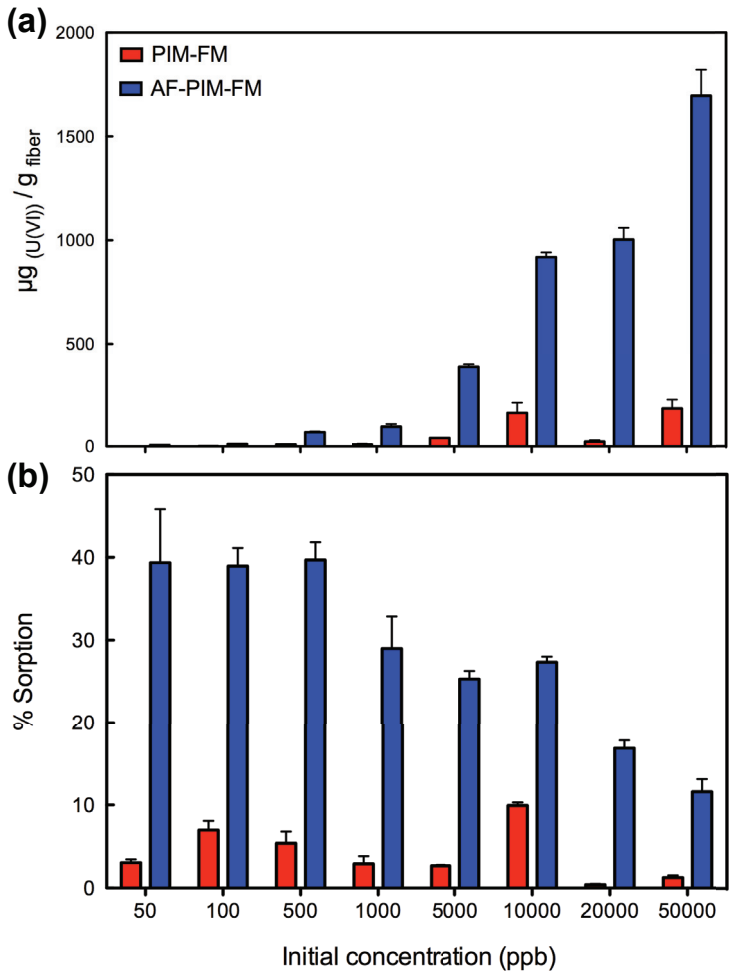

Figure 4.7. Column adsorption study of U(VI) as a function of initial concentration in terms of (a) µg U(VI) / g fiber and (b) % sorption

When the percentage sorption results were considered, the increased concentration reduces the percentage sorption that at low concentration AF-PIM-FM has nearly 40 % sorption capacity while this value decreases to 12 % at 50 ppm concentration.

The repetitive usability of PIM-FM and AF-PIM-FM fibers was tested by exposing the fibrous samples for 15 successive trials with 3 mL portions of 5 ppm fresh U(VI) solutions at pH 5.5. Figure 4.8 shows the AF-PIM-FM fibers are more effective for the removal of uranyl ions even after 15 uses. More uranyl ions removed from the system at initial trials and the percentage sorption decreased from nearly 30 to 12%. This result indicates the applicability of AF-PIM-FM sorbents for consecutive uses and reusability is an important parameter for the utilization of adsorbent materials in real-life problems.

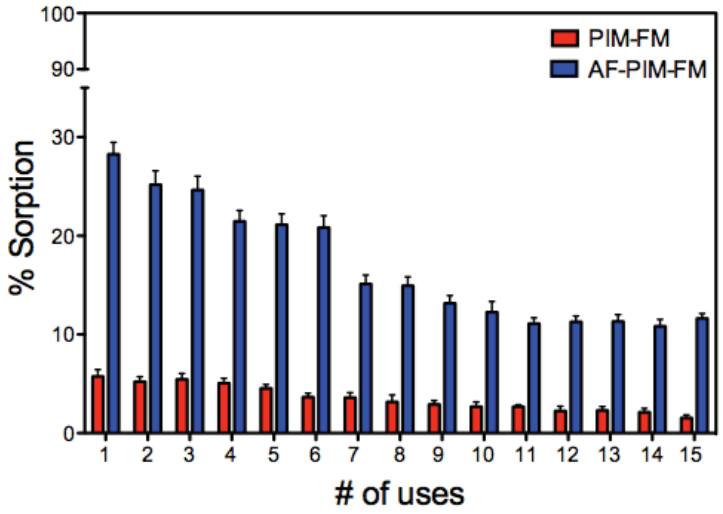

Figure 4.8. Variation of percentage sorption of uranyl ions with the number of repetitive uses of the same fibrous sorbent at 5 ppm U(VI) concentration

Firstly, the attention was given on desorption of uranium ions from AM-PIM-FM and desorption efficiency of fibers was investigated by using two different concentrations of sodium bicarbonate solutions as a function of volume. Figure 4.9 shows that desorption efficiency enhanced with the increase in the volume of sodium bicarbonate solution. Moreover, concentration of desorption reagent has a slight effect on desorption efficiency that desorption efficiency is higher when 1 M of $NaHCO_3$ solution was used as desorbing agent.

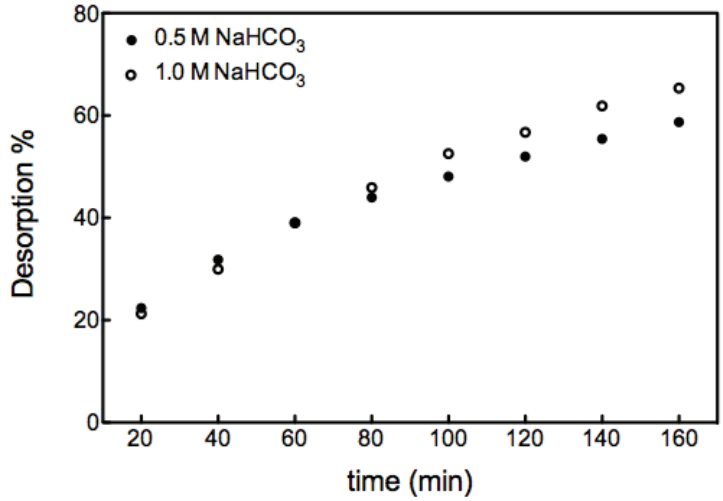

Figure 4.9. Percentage uranyl desorption as a function of time for PIM-FM and AF-PIM-FM

Figure 4.10 shows the regeneration performance of fibrous membranes, which were used for five consecutive adsorption – desorption trials. For each trial, fibrous sorbents were exposed firstly to 3 mL of fresh U(VI) solution (5 ppm concentration at pH 5.5) and then 20 mL of 1 M sodium bicarbonate ($NaHCO_3$) solution was passed through the fibers as desorption reagent. It can be easily seen that desorption is slower than the adsorption due to the strong interaction between amidoxime groups and uranyl ions.

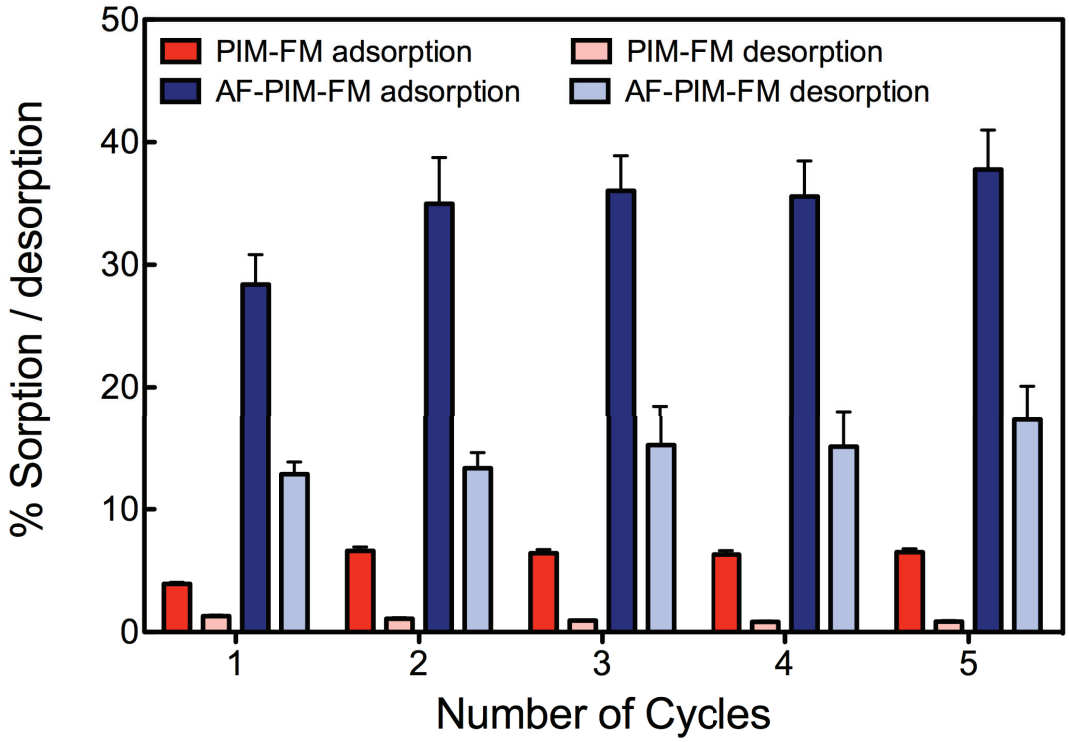

Figure 4.10. Consecutive sorption / desorption cycles of fibrous membranes for 5 ppm U(VI) solution using 1 M $NaHCO_3$ as the desorbing agent

On the other hand, the sorption percentages of second and subsequent cycles are always greater than the first cycle. After five cycles, the sorption efficiency of fibers increased from nearly 28 to 38%. The reason might be the potential interactions of carbonate ions with dioxouranium $(UO_2)^{2+}$ ions. Although the fibrous samples were washed with distilled water after desorption, some of the carbonate ions could stick on or through the fiber. Then, the amount of adsorbed uranyl ions may be increased after desorption due to the presence of carbonate moieties.

4.4. Conclusion

The utilization of amidoxime functionalized PIM fibers was achieved for the removal of uranyl ions from the aqueous systems under continuous flow. Functionalization of fibers with amidoxime groups improved the adsorption performance up to 20 times when compared with pristine PIM-1 ones although the reduced surface area of amidoxime functionalized ones. The AF-PIM-FM achieved 1697 μg g^{-1} U(VI) adsorption capacity at 50 ppm concentration. Moreover, regeneration of fibrous membranes was achieved by using sodium bicarbonate solution as reducing agent. AF-PIM-FM was used 5 times without having any damage on its fibrous structure. These fibers are promising candidates for the environmental remediation applications.

CHAPTER 5

HYDROPHILIC TO HYDROPHOBIC CONVERSION OF PHOTOCHEMICALLY PREPARED METHACRYLATE-BASED POLYMERS WITH VARIOUS CHAIN ARCHITECTURES

Linear poly(hydroxyethyl methacrylate-co-methyl methacrylate) P(HEMA-co-MMA) and poly(dimehylaminoethyl methacrylate-co-methyl methacrylate) P(DMAEMA-co-MMA) and their corresponding hyperbranched copolymers were synthesized by conventional photoinitiated free radical polymerization and self-condensing vinyl polymerization (SCVP) using *Type I* and *Type II* photoinitiators, respectively. Then, the polymers were processed by electrospraying in *N, N*-dimethylformamide. The surface of the resulting electrospray coatings was examined by SEM, XPS, and WCA then compared with those prepared by drop casting. Regardless of the structural nature of the polymers, electrospraying allows the preparation of rough surface that shows more hydrophobic behavior. Electrospray coatings with linear and hyperbranched copolymers exhibited WCA as ~150° and ~130°, respectively, indicating that branching reduces the WCA (Figure 5.1).

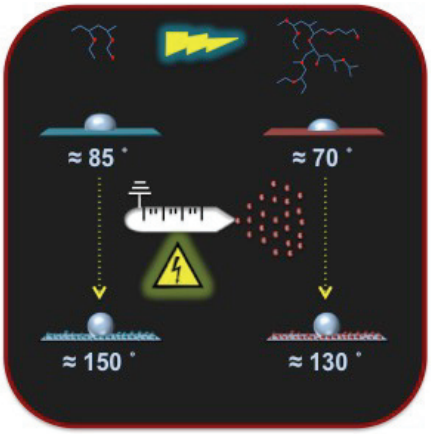

Figure 5.1. Schematic representation of the purpose of the study

5.1. Introduction

Water repellency is a crucial feature for the potential applications such as anti-contamination and self-cleaning technologies (Blossey 2003, Furstner et al. 2005, Lafuma and Quere 2003, Liu and Jiang 2012). Nature designs unique and unusual Lotus leaves, which shows superhydrophobicity and self-cleaning feature due to having hierarchical micro- and nano-structure on leaf surface that minimizes the droplet's adhesion. The wetting capability of a solid surface can be utilized by measuring the contact angle of the liquid on that surface and it is widely known that superhydrophobic surfaces show substantially high water contact angle (WCA, close to or higher than 150˚) (Yao, Song, and Jiang 2011, Zhang et al. 2008). Tailoring the chemical composition and the surface roughness (Quere 2008) allow to control the wettability of surfaces. So far, many methods have been developed to fabricate rough surfaces such as etching, (Liu et al. 2013) deposition,(Kajikawa 2008) sol-gel,(Basu et al. 2010) electrospraying(Wang et al. 2018, Kim, Lee, and Kim 2012), and lithography (Shiu et al. 2004). Electrospraying has been recognized as a powerful approach to obtain high surface roughness. It is a well-established process based on the application of high electrical voltage to a polymer solution. The process relies on the flowing out of a liquid from the capillary nozzle and then forming a fine jet following by atomization of liquid into fine droplets (Bock, Dargaville, and Woodruff 2012). A grounded conductive substrate is employed to collect the coating material. The viscosity of the sample solution (both concentration and molecular weight) is the dominant parameter for the morphology of the resulting coating. Low solution viscosity yields electrospraying that causes the formation of spheres of different size on the collector. On the other hand, at high viscosity (high concentration and / or high molecular weight) the process shifts to electrospinning regime. The continuous micron / sub-micrometer fibers are obtained due to severe entanglement of polymer chains (Demir et al. 2002).

It has been apparently showed that hydrophobic behaviour of the electrospraying / electrospinning surface results from the high surface roughness such that changing the surface topography can minimize the interfacial energy between solid and liquid. Notably, the presence of fluorine atoms or fluorine containing groups is considered to be prerequisite that renders the hydrophobicity of the surfaces by reducing the surface tension. For instance, Zheng *et al.* produced polymer surfaces with high WCA by

electrospraying of polystyrene (Zheng et al. 2006). Polyvinyl butyral nanofibrous mats exhibit hydrophobic and superoleophilic properties and high separation efficiency for oil-water mixtures (Song and Xu 2016). Guo *et al.* also synthesized poly(methyl methacrylate)-*b*-poly (dodecafluoroheptyl methacrylate) diblock copolymer and established superhydrophobic surfaces with lotus effect by electrospraying of this copolymer (Guo, Tang, and Gong 2012).

Hyperbranched polymers represent inherent characteristics compared to their linear analogs due to the peculiar properties such as higher solubility, reduced solution viscosity (Hawker and Frechet 1992, Wooley, Frechet, and Hawker 1994) and increased level of terminal functionality (Sunder, Mulhaupt, and Frey 2000, Sunder et al. 2000). In recent years, many approaches have been developed for the synthesis of such complex architectures (Inoue 2000, Jikei and Kakimoto 2001, Voit and Lederer 2009). Among them, self-condensing vinyl polymerization (SCVP) is the most widely used technique due to the operational simplicity and synthetic versatility to form highly branched structures with desired functional groups (Ambade and Kumar 2000). It has also been modified to a wide variety of controlled polymerization systems via inimer structure variations (Gaynor, Edelman, and Matyjaszewski 1996, Wang et al. 2003, Hawker et al. 1995, Liu et al. 2009). In the recent reports from the authors' laboratory, novel photochemical methods have been introduced for the preparation of hyperbranched polymers. Depending on the structure of the inimer, either photo-induced bromine abstraction by $Mn_2(CO)_{10}$ (Bektas, Ciftci, and Yagci 2013) or the reaction of photochemically generated radical with double and triple bonds at different rates, were successfully employed (Ciftci et al. 2012). In this connection, it should be pointed out that the organomanganese compound used in the process can also be applied for the fabrication of various macromolecular structures through a similar halide abstraction process (Ciftci, Kork, et al. 2015, Ciftci et al. 2013, Ciftci, Norsic, et al. 2015, Ciftci et al. 2016, Ciftci, Tasdelen, and Yagci 2016).

In this work, we employed poly(methyl methacrylate) (PMMA)–based copolymers consisting of two types of comonomer segments, hydroxyethyl methacrylate (HEMA) and dimethylamino ethyl methacrylate (DMAEMA) < 10 mol %. The effect of chain topology (linear and hyperbranched) for different levels of branching and chemistry of comonomer on water contact angle of the electrosprayed coating is examined. We have shown that chain architecture and structural differences have strong influence on the surface chemistry, morphology, and therefore wettability.

5.2. Experimental

In this study, the synthesis of linear and hyperbranched polymers was carried out by Yagci's group. The polymerization and polymer characterization details can be found in the literature (Isık et al. 2017, Aydogan, Ciftci, and Yagci 2016). The synthesized copolymers were dissolved separately in 1 mL of DMF with 15 w/v % concentration and stirred for 12 h until homogeneous solutions were achieved. Then, each solution was transferred into the 2 mL plastic syringe with stainless steel needle (18 gauges) and the needle was connected horizontally to a high voltage supply under 12 kV. (Gamma High Voltage Research Ormond Beach, FL, US). By using a microinfusion pump, (New Era NE300 Infusion Pump, Farmingdale, NY, USA) the flow rate was fixed as 2 mL h^{-1} and tip to collector distance was set as 15 cm. (The potential difference was 0.8 kV cm^{-1}.) Electrospray beads were obtained on the grounded aluminium foil collector. The morphology of samples was examined using Scanning Electron Microscope (SEM, FEI Quanta250 FEG, Oregon, USA) and X-ray Photoelectron Spectrometer (XPS, Thermo Scientific K-Alpha Surface Analysis, Massachusetts, USA). Contact angle measurements were achieved with Contact Angle Meter. (Attension Lite, Biolin Scientific, Stockholm, Sweden) The average size of the beads were estimated by statistically from SEM micrographs using ImageJ software (Schneider 2012).

For the drop casting, the glass slides were covered with aluminium foil to attain flat surfaces. Then, synthesized copolymers were dissolved in 200 µL DMF with 3 w/v % concentration and casted on flat aluminium foils as check samples. The coatings were air- dried for 24 h prior to characterizations.

5.3. Results and Discussion

The molecular weight of the polymers and their structural confirmation by ^{1}H NMR and FTIR analysis were given in the published article (Isık et al. 2017). The polymers with different branching densities and molecular weights were dissolved in DMF with a concentration of 15 w/v % and subjected to electrospraying at 0.8 kV · cm^{-1}. Usually, beads are formed when the polymer solution is fairly diluted due the insufficient viscosity (Zheng et al. 2006). The SEM micrographs of the drop casting and

electrospray coating surfaces of the linear and hyperbranched P(HEMA-*co*-MMA) copolymers are given in Figure 5.2. The surfaces prepared by drop casting of Lin-PH1 and Hyp-PH1 copolymers appear flat and show hydrophilic behaviour with a water contact angle (WCA) of 87˚ and 72˚, respectively (Figure 5.2a-b).

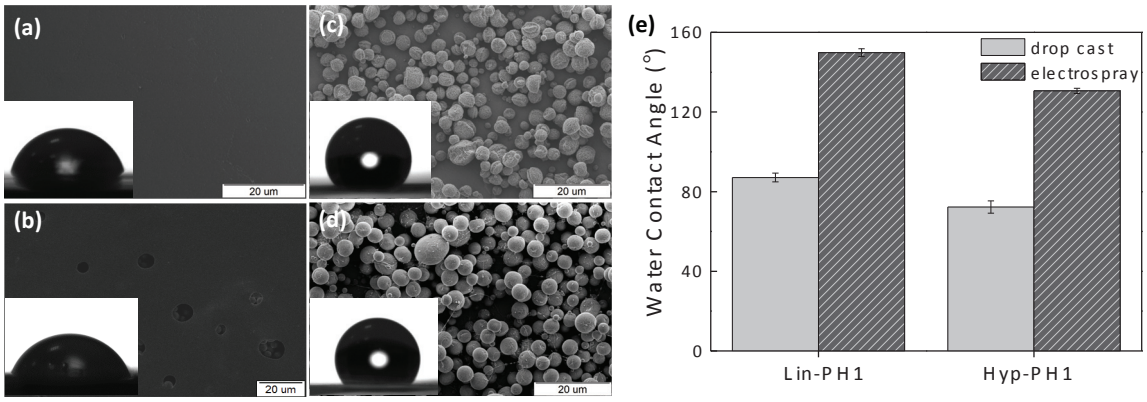

Figure 5.2. SEM micrographs of copolymers (a) Lin-PH1 drop cast, (b) Hyp-PH1 drop cast, (c) Lin-PH1 electrospray, and (d) Hyp-PH1 electrospray samples. Insets show profiles of water droplets with their water contact angles. (e) Water contact angle comparison of Lin-PH1 and Hyp-PH1 samples

The electrospraying process changes the morphology of both Lin-PH1 and Hyp-PH1 surfaces from flat to rough by disintegration of polymer solution in to porous spherical beads. This rough surface increases the WCA up to 150˚ and 131˚ meaning that the surface shows almost superhydrophobic behaviour (Figure 5.2c - d). The size of beads is heterogeneous in diameter (Figure 5.3). Therefore, the electrospray coating shows broader distribution in roughness amplitude and develops a macroscopic level of roughness. For the heterogeneous patterned surface and the presence of cavities, more air is trapped underneath the film to support water droplets and therefore corresponds to a more hydrophobic surface as compared to film casting surface. It is well known that the water contact angle of air is assumed 180° and trapped air has a significant importance on the hydrophobicity. Electrospraying improves the surface hydrophobicity by increasing the surface roughness and the resulting polymer microspheres decrease the contact area between solid and water while the contact area between the air and water is enhanced (Gao et al. 2014). The insets in Figure 5.2 shows the optical photographs of water droplets on the surfaces prepared by drop casting and electrospray

coating. The behavior of this type non-ideal surface is generally explained in terms of either Wenzel model or Cassie–Baxter model.

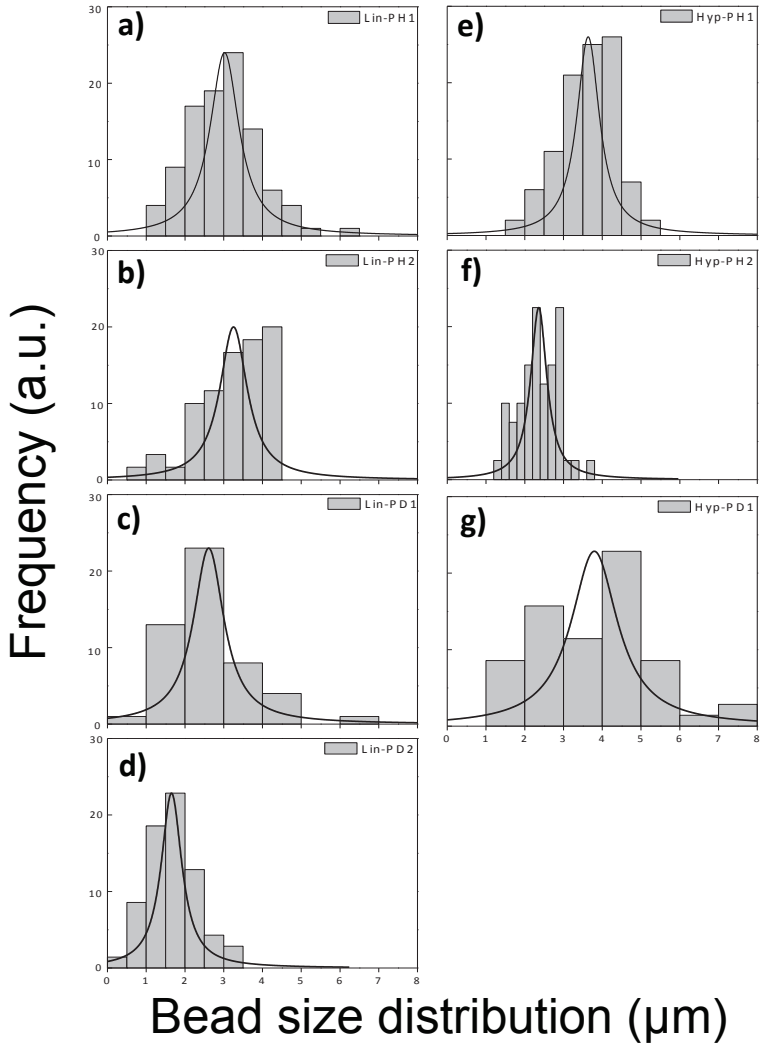

Figure 5.3. Bead size distributions of (a) Lin-PH1, (b) Lin-PH2, (c) Lin-PD1, (d) Lin-PD2, (e) Hyp-PH1, (f) Hyp-PH2, and (g) Hyp-PD2 electrospray samples

Basically, Cassie–Baxter model postulates that droplets hang on the rough surfaces and allow air trapping between the surface and the droplet (Kim, Kim, and Kim 2013). When the WCA of flat surfaces (namely drop casting ones) and rough electrospray coatings were compared, our proposed electrospray coatings have much greater value than the drop casting ones (up to 60°) due to the deposition of irregular microspheres and trapped air between them. This outcome demonstrates that electrospray coatings better fits to Cassie-Baxter model. A similar comparison was

applied between film casting and electrospray coating of Lin-PD2 and Hyp-PD1 copolymers in Figure 5.4.

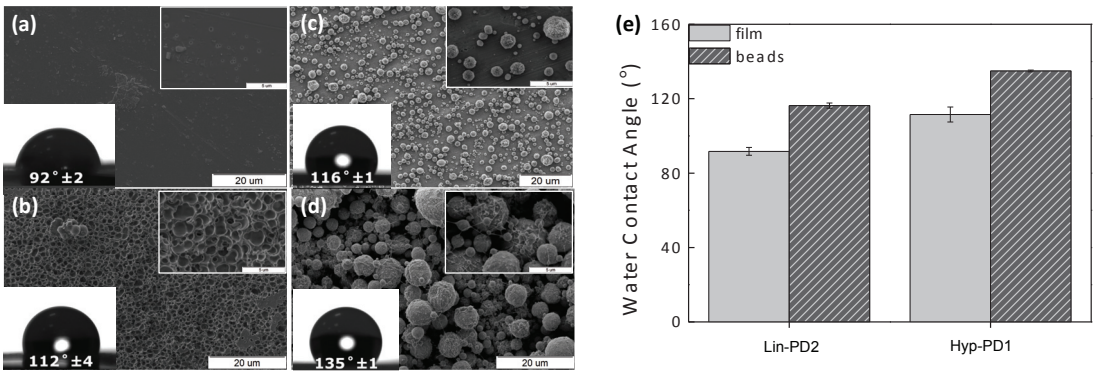

Figure 5.4. SEM micrographs of co-polymers **(a)** Lin-PD2 drop cast, **(b)** Hyp-PD1 drop cast, **(c)** Lin-PD2 electrospray, and **(d)** Hyp-PD1 electrospray samples. Insets show profiles of water droplets with their water contact angles. **(e)** Water contact angle comparison of Lin-PD2 and Hyp-PD1 samples

Contrasting to Lin-PH1 and Hyp-PH1, these polymers show already hydrophobic behavior when they were drop casted. The electrospray process increases the WCA of hydrophobic surfaces from 92˚ to 116° and from 112˚ to 135° for both linear and hyperbranched copolymers, respectively (Figure 5.4). While Lin-PD2 drop cast film has a flat surface, Hyp-PD1 film consists of bubble-like morphology that results in higher WCA for hyperbranched sample.

Figure 5.5 demonstrates SEM micrographs of the electrospray coatings from linear and hyperbranched copolymers. The coatings prepared from hyperbranched samples show lower WCA than those prepared from the linear chains. WCA of linear samples are 146° and 150° whereas the one of hyperbranched samples are 130° and 107°. The size of beads are 3.0±0.3 μm and 3.3±0.6 μm for Lin-PH1 and Lin-PH2, and 3.6±0.7 μm and 2.4±0.4 μm for Hyp-PH1 and Hyp-PH2 samples, respectively (Figure 5.3). Note that in addition to beady structure, fiber formation is observed in some regions of Fig. 5.5d.

The surface morphology of the all electrosprayed samples looks similar at first glance. So that, the surface composition of the samples was examined by XPS to get insight about the surface chemistry of the linear and hyperbranched surfaces along with drop casting films.

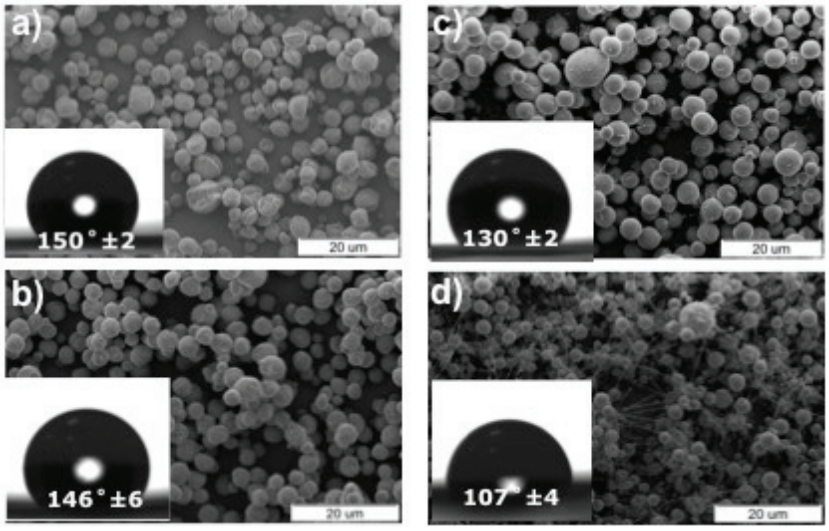

Figure 5.5. SEM micrographs and WCA profiles of **(a)** Lin-PH1, (**b)** Lin-PH2, **(c)** Hyp-PH1 and **(d)** Hyp-PH2 copolymers

The survey XPS spectra of C(1s) and O(1s) regions for the drop cast and electrospray coatings of P(HEMA-co-MMA) copolymers plotted as the emitted electrons versus binding energy (Figure 5.6). The insets show the spectra of C(1s) and O(1s) that separated into sub-Gaussian curve fitted signals corresponding to the C and O bonding states. The C(1s) signals with binding energies between 280 – 290 eV can be assigned to C-O-C, O-C=O, C-C and C-H groups. In the same manner, the O(1s) signals with binding energies around 530 eV can be assigned to C-O-C and O-C=O regions of the spectra. The surface compositions of linear and hyperbranched samples varies in terms of the C\O ratio. It is well established that C-rich surfaces show hydrophobic, while O-rich ones yield hydrophilic behavior (Gutierrezrodriguez and Aplan 1984). The atomic percentages of carbon and oxygen on the surfaces of the copolymers are summarized in Table 5.1. The electrospray samples of all copolymers have lower C\O ratio than the drop cast samples. Notably, increased oxygen amount on their surfaces results an increase in the WCA value. Linear copolymers show higher C\O ratio than hyperbranched ones when the samples were prepared by drop casting. In other words, the oxygen percentage on the surface of hyperbranched ones is greater than their linear ones. Thus, the water contact angle of the drop casting hyperbranched surfaces is lower than the linear ones due to the hydrophilicity of oxygen (Gutierrezrodriguez and Aplan 1984, Tan et al. 2010) (Figure 5.2e).

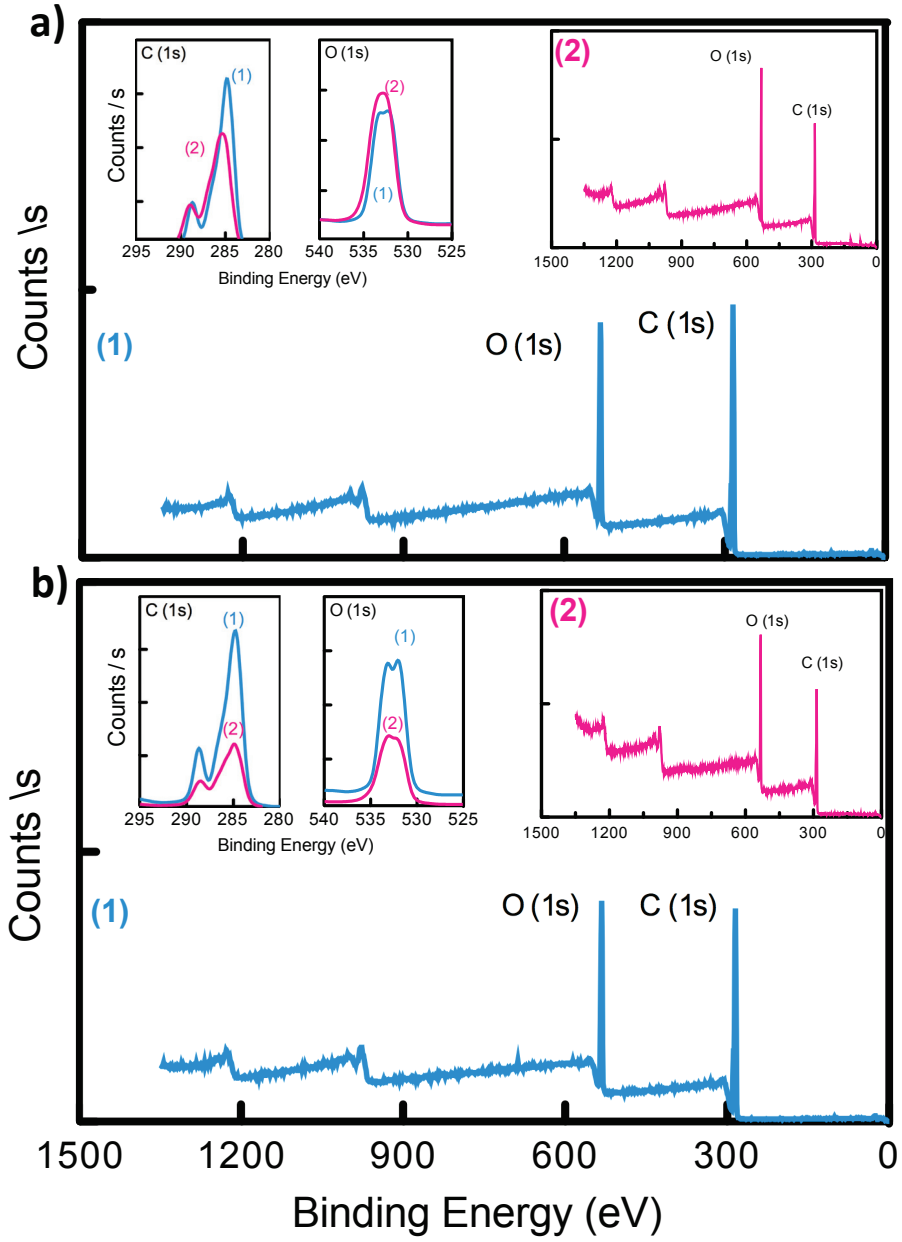

Figure 5.6. XPS spectra of **(a)** Lin-PH1 and **(b)** Hyp-PH1 copolymers. Insets show (1) drop cast and (2) electrospray samples.

Drop casting is an equilibrium process so that linear chains direct the nonpolar alkyl rich groups to the surface. The lower C\O ratio in the drop casting hyperbranched surfaces is most probably due to the limited chain mobility of copolymer that carbon atom may not rise up due to its larger radius than oxygen atom.

Table 5.1. Surface chemical compositions of linear and hyperbranched copolymers calculated from C(1s) and O(1s) XPS spectra

Sample name	Drop casting			Electrospray		
	C(1s) %	O(1s) %	C/O	C(1s) %	O(1s) %	C/O
Lin-PH1	76.1	23.9	3.2	68.6	31.4	2.2
Hyp-PH1	74.6	25.4	2.9	69.6	30.4	2.3
Lin-PD2	73.8	25.1	2.9	66.3	32.7	2.1
Hyp-PD1	72.8	26.4	2.8	70.1	29.1	2.4

On the other hand, when electrospraying is applied, the C/O ratio is higher in the hyperbranched surfaces than the linear ones. Although electrosprayed hyperbranched samples are rich in terms of carbon atoms and expected to be more hydrophobic compared to linear analogs, they show less hydrophobicity compared to the coatings prepared by linear chains. Note that linear ones provide larger bead size compared to the hyperbranched ones (Figure 5.3). The average bead size decreases from 3.2±0.6 to 3.0±0.6 μm for the linear and hyperbranched copolymers, respectively. This result confirms the idea that surface roughness is a prerequisite for superhydrophobicity and the surface roughness of the electrospray coatings dominates the chemistry of the surfaces in wettability.

The wettability of a polymeric surface is absolutely produced by the nature of monomers. In drop casting films, WCA of DMAEMA -co-MMA is higher than the one of HEMA-co-MMA (not surprisingly) because it has more alkyl groups and high carbon atom content (Figure 5.2e and Figure 5.4e). In such an equilibrium process, the chains have enough time and energy for directing the nonpolar alkyl groups of chains to the drop-air interface. Since air is composed of nonpolar gas molecules for instance O_2, N_2, and CO_2, it has nonpolar nature. A nonpolar-nonpolar hydrophobic interaction takes place between droplet surface and surrounding air molecules. On the other hand, the result is opposite for the coatings prepared by electrospraying. WCA of coating prepared by electrospraying of HEMA is higher than those prepared by DMAEMA. In contrast to drop casting, electrospraying is a non-equilibrium process and the structure formation rapidly occurs in the order of seconds.(Demir, Ozen, and Ozcelik 2009) DMAEMA has bigger bulky pendant group compared to HEMA and HEMA has higher

mobility and tendency for the surface segregation of nonpolar segments, nominately alkyl groups (Yi et al. 2014).

The polymer solution concentration has a significant importance on the morphology of the electrospray samples (Festag et al. 1998). The water contact angle measurements indicate that different morphologies of substrates correspond to different contact angles (Figure 5.7) and it is consistent with the literature (Li, Wang, et al. 2014, Zheng et al. 2006). While the drop casting surface with flat surface has 85° WCA and bead-on-fiber sample has 110°, the electrospray sample with fully beads show 140° WCA. The more rough surfaces with cavities show more hydrophobic behavior due to the trapping air in these cavities in accordance with Cassie-Baxter model (Patankar 2009). The presence of fibers obviously decreases the roughness magnitude, implicitly the WCA, and creates a nano-tailored surface while beads enhance the roughness at the micrometer level.

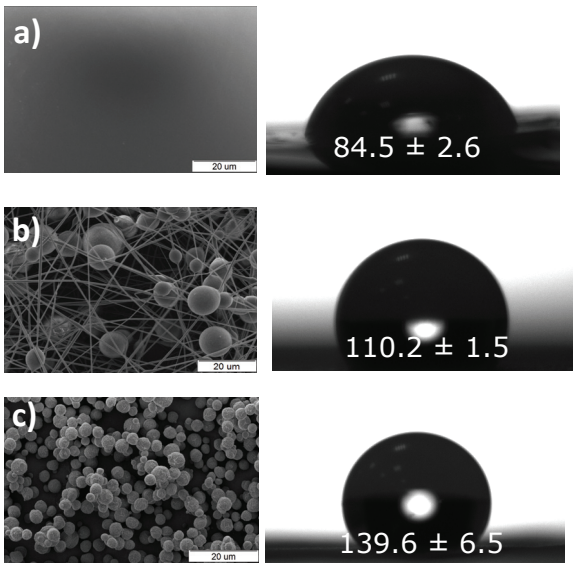

Figure 5.7. SEM micrographs and water contact angle profiles of Lin-PH2 coatings prepared by **(a)** drop casting, **(b)** 45 w/v% and **(c)** 15 w/v% electrospraying

5.4. Conclusion

In summary, the synthesized methacrylate based linear and hyperbranched copolymers were subjected to drop casting or electrospray coating from DMF solution. Independent of the structure and chain architecture of the polymers, electrospray coatings exhibit hydrophobic behavior and higher WCA than the surfaces prepared by

drop casting. Moreover, the coatings prepared by electrospraying of linear chains present higher WCA than their hyperbranched analogs. We show that the fluorine-free polymeric systems can also exhibit hydrophobic behavior via electrospraying. Although having comparable beady structure, HEMA was found to be more convenient co-monomer for PMMA in preparation of hydrophobic polyacrylate coatings. It gives better response to electrical field due to its polar nature and linear morphology. DMAEMA, on the other hand, has larger pendant group that may prevent the chain mobility. XPS results suggest that electrical field applied during the process may favor the surface segregation of alkyl groups that can increase the WCA of the coatings. Branching chain architecture restricts the mobility of chains and prevents the surface segregation; thus, decreases the WCA of the coating.

CHAPTER 6

EVALUATION AND OVERALL CONCLUDING REMARKS

Electrospinning is a versatile method for the production of functional fibrous materials from various types of polymers. The resulting materials have several significant characteristics from large surface area to high porosity and unique physical characteristics to flexibility. Moreover, the design flexibility of electrospun fibers by chemical or physical functionalization makes them suitable candidates in water filtration and remediation applications. This thesis has illuminated the fabrication, characterization and potential adsorbent applications of electrospun fibers of both virgin and recycled polymers of waste products.

As a recycling approach, electrospinning could be used by minimizing the utilization of primary raw sources and manufacturing the secondary products from waste materials. In the first part, polystyrene wastes have been recycled for the remediation of medical- and oily-wastewaters. Firstly, electrospun fibers from CD-cover wastes (CD-PS) and expanded polystyrene wastes (EPS) were fabricated and their adsorption capacity towards protein-rich medical wastes were investigated. The model analyte-adsorbent system for medical waste remediation was demonstrated by using BSA, MYO and TRY proteins and electrospun fibers demonstrated a significant adsorption capacity in the following order: BSA > MYO > TRY. Due to the presence of $CaCO_3$ moieties in CD-cover wastes, the electrostatic interaction between Ca^{2+} negatively charged BSA molecules were enhanced their protein adsorption affinity.

Secondly, EPS wastes were processed by electrospinning and the surface morphology of resulting fibrous materials was diversified by changing the solvent composition of polymer solution. Then, freestanding fibrous mats were utilized as adsorbent material for the remediation of oily wastewaters. The diversified surface morphology remarkably influenced the hydrophobicity and oleophilicity of fibers that results in different oil adsorption capacities. The results were compared with the pristine foam, virgin PS fibers, which were fabricated in the same manner, and a

commercial adsorbent. Moreover, the performance of the adsorbent materials was evaluated by using a real sample taken from the İzmir Shipyard.

For further studies, other commodity plastic wastes (i.e. PET, PVC, PP, HDPE, LDPE) can be recycled by electrospinning for their applications in wastewater remediation. Instead of solution electrospinning, melt electrospinning method could be utilized for fabrication of fibrous materials to get rid of organic solvent usage.

The morphology of electrospun PS fibers strongly depends on the spinning environment. Particularly, humidity has significant influence on the surface and interior porosity of fibers. For instance, Rabolt *et al.* claimed that surface features, pores become evident when electrospinning is proceed in atmosphere with more than 30% relative humidity and the number, shape, and distribution of pores increase by increasing humidity (Casper et al. 2004). Such that, seasonal variations, particularly in İzmir, have strong influence on the interior and surface texture of fibers.

Not only the macromolecules like proteins and dyes but also the removal of uranyl ions from the aqueous systems was studied through this thesis. *Uyar's Group* fabricated electrospun fibers from Polymers of Intrinsic Microporosity (PIM-1) and functionalized these fibers with amidoxime groups. Then, we investigated the uranyl ion adsorption capacity of the amidoxime functionalized PIM-1 fibers that amidoxime functionalization improved their adsorption performance up to 20 times when compared with neat PIM-1 fibers. Besides, fibrous membranes preserved their integrity up to 5 adsorption / desorption cycles without losing their adsorption capacity.

Finally, we highlighted the ability of electrospinning / spraying technique for the generation of hydrophobic surfaces. The synthesized linear and hyperbranched co-polymers by *Yagci's Group* were subjected to drop casting or electrospray coating from their solutions. The resulting beady coatings after electrospraying process showed remarkable hydrophobic behaviour and linear co-polymers presented different water contact angle than the branched ones due to the restricted mobility of chains. We demonstrated that fluorine-free polymers could also show hydrophobic behaviour via electrospraying.

REFERENCES

Al-Qadhi, M., N. Merah, A. Matin, N. Abu-Dheir, M. Khaled, and K. Youcef-Toumi. 2015. "Preparation of superhydrophobic and self-cleaning polysulfone non-wovens by electrospinning: influence of process parameters on morphology and hydrophobicity." *Journal of Polymer Research* 22 (11). doi: 10.1007/s10965-015-0844-x.

Aluigi, A., C. Vineis, C. Tonin, C. Tonetti, A. Varesano, and G. Mazzuchetti. 2009. "Wool Keratin-Based Nanofibres for Active Filtration of Air and Water." *Journal of Biobased Materials and Bioenergy* 3 (3):311-319. doi: 10.1166/jbmb.2009.1039.

Ambade, A. V., and A. Kumar. 2000. "Controlling the degree of branching in vinyl polymerization." *Progress in Polymer Science* 25 (8):1141-1170. doi: 10.1016/S0079-6700(00)00023-X.

Angammana, C. J., and S. H. Jayaram. 2011. "Analysis of the Effects of Solution Conductivity on Electrospinning Process and Fiber Morphology." *Ieee Transactions on Industry Applications* 47 (3):1109-1117. doi: 10.1109/tia.2011.2127431.

Anton, Formhals. 1929. Process and apparatus for preparing artificial threads. Richard Schreiber Gastell

Arnauts, Jan, and H Berghmans. "Amorphous Thermoreversible Gels of Solutions of Atactic Polystyrene." In *Physical Networks Polymers and Gels*, edited by W Burchard and B Ross-Murphy. London and New York: Elsevier Applied Science.

Aydogan, C., M. Ciftci, and Y. Yagci. 2016. "Hyperbranched Polymers by Type II Photoinitiated Self-Condensing Vinyl Polymerization." *Macromolecular Rapid Communications* 37 (7):650-654. doi: 10.1002/marc.201500721.

Aytas, S., D. A. Turkozu, and C. Gok. 2011. "Biosorption of uranium(VI) by bi-functionalized low cost biocomposite adsorbent." *Desalination* 280 (1-3):354-362. doi: 10.1016/j.desal.2011.07.023.

Bandegi, A., and M. R. Moghbeli. 2018. "Effect of solvent quality and humidity on the porous formation and oil absorbency of SAN electrospun nanofibers." *Journal of Applied Polymer Science* 135 (1). doi: 10.1002/app.45586.

Basu, B. J., V. Hariprakash, S. T. Aruna, R. V. Lakshmi, J. Manasa, and B. S. Shruthi. 2010. "Effect of microstructure and surface roughness on the wettability of superhydrophobic sol-gel nanocomposite coatings." *Journal of Sol-Gel Science and Technology* 56 (3):278-286. doi: 10.1007/s10971-010-2304-8.

Bektas, S., M. Ciftci, and Y. Yagci. 2013. "Hyperbranched Polymers by Visible Light Induced Self-Condensing Vinyl Polymerization and Their Modifications." *Macromolecules* 46 (17):6751-6757. doi: 10.1021/ma401534w.

Berber, E., N. Horzum, B. Hazer, and M. M. Demir. 2016. "Solution Electrospinning of Polypropylene-based Fibers and Their Application in Catalysis." *Fibers and Polymers* 17 (5):760-768. doi: 10.1007/s12221-016-6183-7.

Bhardwaj, N., and S. C. Kundu. 2010. "Electrospinning: A fascinating fiber fabrication technique." *Biotechnology Advances* 28 (3):325-347. doi: 10.1016/j.biotechadv.2010.01.004.

Blossey, R. 2003. "Self-cleaning surfaces - virtual realities." *Nature Materials* 2 (5):301-306. doi: 10.1038/nmat856.

Bock, N., T. R. Dargaville, and M. A. Woodruff. 2012. "Electrospraying of polymers with therapeutic molecules: State of the art." *Progress in Polymer Science* 37 (11):1510-1551. doi: 10.1016/j.progpolymsci.2012.03.002.

Bognitzki, M., W. Czado, T. Frese, A. Schaper, M. Hellwig, M. Steinhart, A. Greiner, and J. H. Wendorff. 2001. "Nanostructured fibers via electrospinning." *Advanced Materials* 13 (1):70-+. doi: 10.1002/1521-4095(200101)13:1<70::aid-adma70>3.0.co;2-h.

Bonso, Jeliza S., Grace D. Kalaw, and John P. Ferraris. 2014. "High surface area carbon nanofibers derived from electrospun PIM-1 for energy storage applications." *Journal of Materials Chemistry A* 2 (2):418-424. doi: 10.1039/C3TA13779A.

Boyaci, E., N. Horzum, A. Cagir, M. M. Demir, and A. E. Eroglu. 2013. "Electrospun amino-functionalized PDMS as a novel SPME sorbent for the speciation of inorganic and organometallic arsenic species." *Rsc Advances* 3 (44):22261-22268. doi: 10.1039/c3ra43622e.

Brown, S., S. Chatterjee, M. J. Li, Y. F. Yue, C. Tsouris, C. J. Janke, T. Saito, and S. Dai. 2016. "Uranium Adsorbent Fibers Prepared by Atom-Transfer Radical Polymerization from Chlorinated Polypropylene and Polyethylene Trunk Fibers." *Industrial & Engineering Chemistry Research* 55 (15):4130-4138. doi: 10.1021/acs.iecr.5b03667.

Budd, Peter M., Bader S. Ghanem, Saad Makhseed, Neil B. McKeown, Kadhum J. Msayib, and Carin E. Tattershall. 2004. "Polymers of intrinsic microporosity (PIMs): robust, solution-processable, organic nanoporous materials." *Chemical Communications* (2):230-231.

Budd, Peter M., Neil B. McKeown, and Detlev Fritsch. 2005. "Free volume and intrinsic microporosity in polymers." *Journal of Materials Chemistry* 15 (20):1977-1986. doi: 10.1039/B417402J.

Budd, Peter M., Kadhum J. Msayib, Carin E. Tattershall, Bader S. Ghanem, Kevin J. Reynolds, Neil B. McKeown, and Detlev Fritsch. 2005. "Gas separation membranes from polymers of intrinsic microporosity." *Journal of Membrane Science* 251 (1–2):263-269. doi: 10.1016/j.memsci.2005.01.009.

Camtakan, Z., S. Erenturk, and S. Yusan. 2012. "Magnesium oxide nanoparticles: Preparation, characterization, and uranium sorption properties." *Environmental Progress & Sustainable Energy* 31 (4):536-543. doi: 10.1002/ep.10575.

Casper, C. L., J. S. Stephens, N. G. Tassi, D. B. Chase, and J. F. Rabolt. 2004. "Controlling surface morphology of electrospun polystyrene fibers: Effect of humidity and molecular weight in the electrospinning process." *Macromolecules* 37 (2):573-578. doi: 10.1021/ma0351975.

Celik, A., G. Koc, E. Erdogan, T. Shahwan, A. Baba, and M. M. Demir. 2017. "Use of electrospun fiber mats for the remediation of hypersaline geothermal brine." *Desalination and Water Treatment* 62:94-100. doi: 10.5004/dwt.2017.20151.

Chan, C. M., J. S. Wu, J. X. Li, and Y. K. Cheung. 2002. "Polypropylene/calcium carbonate nanocomposites." *Polymer* 43 (10):2981-2992. doi: 10.1016/s0032-3861(02)00120-9.

Chaudhary, J. P., S. K. Nataraj, A. Gogda, and R. Meena. 2014. "Bio-based superhydrophilic foam membranes for sustainable oil-water separation." *Green Chemistry* 16 (10):4552-4558. doi: 10.1039/c4gc01070a.

Chaukura, N., W. Gwenzi, T. Bunhu, D. T. Ruziwa, and I. Pumure. 2016. "Potential uses and value-added products derived from waste polystyrene in developing countries: A review." *Resources Conservation and Recycling* 107:157-165. doi: 10.1016/j.resconrec.2015.10.031.

Chaukura, N., B. B. Mamba, and S. B. Mishra. 2017. "Conversion of post consumer waste polystyrene into a high value adsorbent and its sorptive properties for Congo Red removal from aqueous solution." *Journal of Environmental Management* 193:280-289. doi: 10.1016/j.jenvman.2017.02.023.

Chen, L., Z. L. Bai, L. Zhu, L. J. Zhang, Y. W. Cai, Y. X. Li, W. Liu, Y. L. Wang, L. H. Chen, D. W. Juan, J. Q. Wang, Z. F. Chai, and S. Wang. 2017. "Ultrafast and Efficient Extraction of Uranium from Seawater Using an Amidoxime Appended Metal-Organic Framework." *Acs Applied Materials & Interfaces* 9 (38):32446-32451. doi: 10.1021/acsami.7b12396.

Chen, P. Y., and S. H. Tung. 2017. "One-Step Electrospinning To Produce Nonsolvent-Induced Macroporous Fibers with Ultrahigh Oil Adsorption Capability." *Macromolecules* 50 (6):2528-2534. doi: 10.1021/acs.macromo1.6b02696.

Chu, Z. L., Y. J. Feng, and S. Seeger. 2015. "Oil/Water Separation with Selective Superantiwetting/Superwetting Surface Materials." *Angewandte Chemie-International Edition* 54 (8):2328-2338. doi: 10.1002/anie.201405785.

Ciftci, Mustafa, Mustafa Arslan, Michael Buchmeiser, and Yusuf Yagci. 2016. "Polyethylene-g-Polystyrene Copolymers by Combination of ROMP, Mn2(CO)10-Assisted TEMPO Substitution and NMRP." *ACS Macro Letters* 5 (8):946-949. doi: 10.1021/acsmacrolett.6b00460.

Ciftci, Mustafa, Pınar Batat, A. Levent Demirel, Guangjuan Xu, Michael Buchmeiser, and Yusuf Yagci. 2013. "Visible Light-Induced Grafting from Polyolefins." *Macromolecules* 46 (16):6395-6401. doi: 10.1021/ma401431h.

Ciftci, Mustafa, Muhammet U. Kahveci, Yusuf Yagci, Xavier Allonas, Christian Ley, and Haja Tar. 2012. "A simple route to synthesis of branched and cross-linked polymers with clickable moieties by photopolymerization." *Chemical Communications* 48 (82):10252-10254. doi: 10.1039/c2cc35607d.

Ciftci, Mustafa, Senem Kork, Guangjuan Xu, Michael R. Buchmeiser, and Yusuf Yagci. 2015. "Polyethylene-g-poly(cyclohexene oxide) by Mechanistic Transformation from ROMP to Visible Light-Induced Free Radical Promoted Cationic Polymerization." *Macromolecules* 48 (6):1658-1663. doi: 10.1021/acs.macromol.5b00086.

Ciftci, Mustafa, Sébastien Norsic, Christophe Boisson, Franck D'Agosto, and Yusuf Yagci. 2015. "Synthesis of Block Copolymers Based on Polyethylene by Thermally Induced Controlled Radical Polymerization Using Mn2(CO)10." *Macromolecular Chemistry and Physics* 216 (9):958-963. doi: 10.1002/macp.201500016.

Ciftci, Mustafa, Mehmet Atilla Tasdelen, and Yusuf Yagci. 2016. "Macromolecular design and application using Mn2(CO)10-based visible light photoinitiating systems." *Polymer International* 65 (9):1001-1014. doi: 10.1002/pi.5111.

Cojocaru, C., P. P. Dorneanu, A. Airinei, N. Olaru, P. Samoila, and A. Rotaru. 2017. "Design and evaluation of electrospun polysulfone fibers and polysulfone/NiFe204 nanostructured composite as sorbents for oil spill cleanup." *Journal of the Taiwan Institute of Chemical Engineers* 70:267-281. doi: 10.1016/j.jtice.2016.11.005.

Demir, M. M. 2010. "Investigation on glassy skin formation of porous polystyrene fibers electrospun from DMF." *Express Polymer Letters* 4 (1):2-8. doi: 10.3144/expresspolymlett.2010.2.

Demir, M. M., B. Ozen, and S. Ozcelik. 2009. "Formation of Pseudoisocyanine J-Aggregates in Poly(vinyl alcohol) Fibers by Electrospinning." *Journal of Physical Chemistry B* 113 (34):11568-11573. doi: 10.1021/jp902380n.

Demir, M. M., and G. Wegner. 2012. "Challenges in the Preparation of Optical Polymer Composites With Nanosized Pigment Particles: A Review on Recent Efforts." *Macromolecular Materials and Engineering* 297 (9):838-863. doi: 10.1002/mame.201200089.

Demir, M. M., I. Yilgor, E. Yilgor, and B. Erman. 2002. "Electrospinning of polyurethane fibers." *Polymer* 43 (11):3303-3309. doi: 10.1016/s0032-3861(02)00136-2.

Demirkurt, M., Y. A. Olcer, M. M. Demir, and A. E. Eroglu. 2018. "Electrospun polystyrene fibers knitted around imprinted acrylate microspheres as sorbent for paraben derivatives." *Analytica Chimica Acta* 1014:1-9. doi: 10.1016/j.aca.2018.02.016.

Deschamps, G., H. Caruel, M. E. Borredon, C. Bonnin, and C. Vignoles. 2003. "Oil removal from water by selective sorption on hydrophobic cotton fibers. 1. Study of sorption properties and comparison with other cotton fiber-based sorbents." *Environmental Science & Technology* 37 (5):1013-1015. doi: 10.1021/es020061s.

Eda, G., J. Liu, and S. Shivkumar. 2007. "Solvent effects on jet evolution during electrospinning of semi-dilute polystyrene solutions." *European Polymer Journal* 43 (4):1154-1167. doi: 10.1016/j.eurpolymj.2007.01.003.

Esmaeili, E., F. Deymeh, and S. A. Rounaghi. 2017. "Synthesis and characterization of the electrospun fibers prepared from waste polymeric materials." *International Journal of Nano Dimension* 8 (2):171-181. doi: 10.22034/ijnd.2017.25087.

Favre-Reguillon, Alain, Gerard Lebuzit, Jacques Foos, Alain Guy, Micheline Draye, and Marc Lemaire. 2003. "Selective Concentration of Uranium from Seawater

by Nanofiltration." *Industrial & Engineering Chemistry Research* 42 (23):5900-5904. doi: 10.1021/ie030157a.

Feng, L., Z. Y. Zhang, Z. H. Mai, Y. M. Ma, B. Q. Liu, L. Jiang, and D. B. Zhu. 2004. "A super-hydrophobic and super-oleophilic coating mesh film for the separation of oil and water." *Angewandte Chemie-International Edition* 43 (15):2012-2014. doi: 10.1002/anie.200353381.

Festag, R., S. D. Alexandratos, D. C. Joy, B. Wunderlich, B. Annis, and K. D. Cook. 1998. "Effects of molecular entanglements during electrospray of high molecular weight polymers." *Journal of the American Society for Mass Spectrometry* 9 (4):299-304. doi: 10.1016/s1044-0305(98)00004-x.

Fornes, T. D., P. J. Yoon, H. Keskkula, and D. R. Paul. 2001. "Nylon 6 nanocomposites: the effect of matrix molecular weight." *Polymer* 42 (25):9929-9940. doi: 10.1016/s0032-3861(01)00552-3.

Furstner, R., W. Barthlott, C. Neinhuis, and P. Walzel. 2005. "Wetting and self-cleaning properties of artificial superhydrophobic surfaces." *Langmuir* 21 (3):956-961. doi: 10.1021/la0401011.

Gao, J. F., W. Li, J. S. P. Wong, M. J. Hu, and R. K. Y. Li. 2014. "Controllable morphology and wettability of polymer microspheres prepared by nonsolvent assisted electrospraying." *Polymer* 55 (12):2913-2920. doi: 10.1016/j.polymer.2014.04.033.

Gao, J. F., X. Song, X. W. Huang, L. Wang, B. Li, and H. G. Xue. 2018. "Facile preparation of polymer microspheres and fibers with a hollow core and porous shell for oil adsorption and oil/water separation." *Applied Surface Science* 439:394-404. doi: 10.1016/j.apsusc.2018.01.013.

Gaynor, S. G., S. Edelman, and K. Matyjaszewski. 1996. "Synthesis of branched and hyperbranched polystyrenes." *Macromolecules* 29 (3):1079-1081. doi: 10.1021/ma9513877.

Gopal, R., S. Kaur, Z. W. Ma, C. Chan, S. Ramakrishna, and T. Matsuura. 2006. "Electrospun nanofibrous filtration membrane." *Journal of Membrane Science* 281 (1-2):581-586. doi: 10.1016/j.memsci.2006.04.026.

Gopi, S., P. Balakrishnan, A. Pius, and S. Thomas. 2017. "Chitin nanowhisker (ChNW)-functionalized electrospun PVDF membrane for enhanced removal of Indigo carmine." *Carbohydrate Polymers* 165:115-122. doi: 10.1016/j.carbpol.2017.02.046.

Greiner, A., and J. H. Wendorff. 2007. "Electrospinning: A fascinating method for the preparation of ultrathin fibres." *Angewandte Chemie-International Edition* 46 (30):5670-5703. doi: 10.1002/anie.200604646.

Guner, T., G. Topcu, U. Savaci, A. Genc, S. Turan, E. Sari, and M. M. Demir. 2018. "Polarized emission from CsPbBr3 nanowire embedded-electrospun PU fibers." *Nanotechnology* 29 (13). doi: 10.1088/1361-6528/aaaaef.

Guo, Y. D., D. Y. Tang, and Z. L. Gong. 2012. "Superhydrophobic Films Fabricated by Electrospraying Poly(methyl methacrylate)-b-poly(dodecafluoroheptyl methacrylate) Diblock Copolymers." *Journal of Physical Chemistry C* 116 (50):26284-26294. doi: 10.1021/jp305562s.

Gupta, Amit, Carl D. Saquing, Mehdi Afshari, Alan E. Tonelli, Saad A. Khan, and Richard Kotek. 2009. - 42 (- 3):- 715.

Gupta, P., C. Elkins, T. E. Long, and G. L. Wilkes. 2005. "Electrospinning of linear homopolymers of poly(methyl methacrylate): exploring relationships between fiber formation, viscosity, molecular weight and concentration in a good solvent." *Polymer* 46 (13):4799-4810. doi: 10.1016/j.polymer.2005.04.021.

Gutierrezrodriguez, J. A., and F. F. Aplan. 1984. "The Effect of Oxygen on the Hydrophobicity and Floatability of Coal." *Colloids and Surfaces* 12 (1-2):27-51. doi: 10.1016/0166-6622(84)80087-6.

Haridas, A. K., C. S. Sharma, V. Sritharan, and T. N. Rao. 2014. "Fabrication and surface functionalization of electrospun polystyrene submicron fibers with controllable surface roughness." *Rsc Advances* 4 (24):12188-12197. doi: 10.1039/c3ra44170a.

Hawker, C. J., and J. M. J. Frechet. 1992. "Monodispersed Dendritic Polyesters with Removable Chain Ends - A Versatike Approach to Globular Macromolecules with Chemically Reversible Polarities." *Journal of the Chemical Society-Perkin Transactions 1* (19):2459-2469. doi: 10.1039/p19920002459.

Hawker, C. J., J. M. J. Frechet, R. B. Grubbs, and J. Dao. 1995. "Preparation OF Hyperbranched and Star Polymers by a Living, Self-Condensing Free-Radical Polymerization." *Journal of the American Chemical Society* 117 (43):10763-10764. doi: 10.1021/ja00148a027.

Hohman, M. M., M. Shin, G. Rutledge, and M. P. Brenner. 2001a. "Electrospinning and electrically forced jets. I. Stability theory." *Physics of Fluids* 13 (8):2201-2220. doi: 10.1063/1.1383791.

Hohman, M. M., M. Shin, G. Rutledge, and M. P. Brenner. 2001b. "Electrospinning and electrically forced jets. II. Applications." *Physics of Fluids* 13 (8):2221-2236. doi: 10.1063/1.1384013.

Hopewell, J., R. Dvorak, and E. Kosior. 2009. "Plastics recycling: challenges and opportunities." *Philosophical Transactions of the Royal Society B-Biological Sciences* 364 (1526):2115-2126. doi: 10.1098/rstb.2008.0311.

Horzum, N., E. Boyaci, A. E. Eroglu, T. Shahwan, and M. M. Demir. 2010. "Sorption Efficiency of Chitosan Nanofibers toward Metal Ions at Low Concentrations." *Biomacromolecules* 11 (12):3301-3308. doi: 10.1021/bm100755x.

Horzum, N., M. M. Demir, M. Nairat, and T. Shahwan. 2013. "Chitosan fiber-supported zero-valent iron nanoparticles as a novel sorbent for sequestration of inorganic arsenic." *Rsc Advances* 3 (21):7828-7837. doi: 10.1039/c3ra23454a.

Horzum, N., D. Mete, E. Karakus, M. Ucuncu, M. Emrullahoglu, and M. M. Demir. 2016. "Rhodamine-Immobilised Electrospun Chitosan Nanofibrous Material as a Fluorescence Turn-On Hg2+ Sensor." *Chemistryselect* 1 (5):896-900. doi: 10.1002/slct.201600027.

Horzum, N., T. Shahwan, O. Parlak, and M. M. Demir. 2012. "Synthesis of amidoximated polyacrylonitrile fibers and its application for sorption of aqueous uranyl ions under continuous flow." *Chemical Engineering Journal* 213:41-49. doi: 10.1016/j.cej.2012.09.114.

Horzum, N., D. Tascioglu, C. Ozbek, S. Okur, and M. M. Demir. 2014. "VOC sensors based on a metal oxide nanofibrous membrane/QCM system prepared by electrospinning." *New Journal of Chemistry* 38 (12):5761-5768. doi: 10.1039/c4nj00884g.

Hossain, M. S., N. N. N. Ab Rahman, V. Balakrishnan, V. R. Puvanesuaran, M. Z. I. Sarker, and M. O. Ab Kadir. 2013. "Infectious Risk Assessment of Unsafe Handling Practices and Management of Clinical Solid Waste." *International Journal of Environmental Research and Public Health* 10 (2):556-567. doi: 10.3390/ijerph10020556.

Hossain, M. S., N. A. N. Norulaini, A. A. Banana, A. R. M. Zulkhairi, A. Y. A. Naim, and A. K. M. Omar. 2016. "Modeling the supercritical carbon dioxide inactivation of Staphylococcus aureus, Escherichia coli and Bacillus subtilis in human body fluids clinical waste." *Chemical Engineering Journal* 296:173-181. doi: 10.1016/j.cej.2016.03.120.

Huang, C., Y. W. Tang, X. Liu, A. Sutti, Q. F. Ke, X. M. Mo, X. G. Wang, Y. Morsi, and T. Lin. 2011. "Electrospinning of nanofibres with parallel line surface texture for improvement of nerve cell growth." *Soft Matter* 7 (22):10812-10817. doi: 10.1039/c1sm06430d.

Huang, Z. M., Y. Z. Zhang, M. Kotaki, and S. Ramakrishna. 2003. "A review on polymer nanofibers by electrospinning and their applications in nanocomposites." *Composites Science and Technology* 63 (15):2223-2253. doi: 10.1016/s0266-3538(03)00178-7.

Incel, A., C. Varlikli, C. D. McMillen, and M. M. Demir. 2017. "Triboluminescent Electrospun Mats with Blue-Green Emission under Mechanical Force." *Journal of Physical Chemistry C* 121 (21):11709-11716. doi: 10.1021/acs.jpcc.7b02875.

Inoue, K. 2000. "Functional dendrimers, hyperbranched and star polymers." *Progress in Polymer Science* 25 (4):453-571. doi: 10.1016/s0079-6700(00)00011-3.

Isık, T. , M. M. Demir, C. Aydogan, M. Ciftci, and Y. Yagci. 2017. "Hydrophobic Coatings from Photochemically-Prepared Hydrophilic Polymethacrylates via Electrospraying " *Journal of Polymer Science A: Polymer Chemistry* 55:1338-1344.

Isık, T., and M. M. Demir. 2018. "Medical Waste Treatment via Waste Electrospinning of PS." *Fiber and Polymers* 19 (4):767 - 774.

Isik, T., and M. M. Demir. 2018. "Protein-rich Medical Waste Treatment via Waste Electrospinning." *Fibers and Polymers* 19 (4):767-774.

Isik, T., M. M. Demir, C. Aydogan, M. Ciftci, and Y. Yagci. 2017. "Hydrophobic Coatings from Photochemically Prepared Hydrophilic Polymethacrylates via Electrospraying." *Journal of Polymer Science Part a-Polymer Chemistry* 55 (8):1338-1344. doi: 10.1002/pola.28501.

Isik, T., N. Horzum, U. H. Yildiz, B. Liedberg, and M. M. Demir. 2016. "Utilization of Electrospun Polystyrene Membranes as a Preliminary Step for Rapid Diagnosis." *Macromolecular Materials and Engineering* 301 (7):827-835. doi: 10.1002/mame.201600127.

Jeannette M. Garcia, and Megan L. Robertson. 2017. "The future of plastics recycling." *Science* 358 (6365):870-872. doi: 10.1126/science.aaq0324.

Jiang, L., Z. G. Tang, R. M. Clinton, V. Breedveld, and D. W. Hess. 2017. "Two-Step Process To Create "Roll-Off" Superamphiphobic Paper Surfaces." *Acs Applied Materials & Interfaces* 9 (10):9195-9203. doi: 10.1021/acsami.7b00829.

Jiang, Z., L. D. Tijing, A. Amarjargal, C. H. Park, K. J. An, H. K. Shon, and C. S. Kim. 2015. "Removal of oil from water using magnetic bicomponent composite nanofibers fabricated by electrospinning." *Composites Part B-Engineering* 77:311-318. doi: 10.1016/j.compositesb.2015.03.067.

Jikei, M., and M. Kakimoto. 2001. "Hyperbranched polymers: a promising new class of materials." *Progress in Polymer Science* 26 (8):1233-1285. doi: 10.1016/s0079-6700(01)00018-1.

Kajikawa, Y. 2008. "Roughness evolution during chemical vapor deposition." *Materials Chemistry and Physics* 112 (2):311-318. doi: 10.1016/j.matchemphys.2008.06.008.

Kalaoglu, O. I., C. H. Unlu, and O. G. Atici. 2016. "Synthesis, characterization and electrospinning of corn cob cellulose-graft-polyacrylonitrile and their clay nanocomposites." *Carbohydrate Polymers* 147:37-44. doi: 10.1016/j.carbpol.2016.03.073.

Khin, M. M., A. S. Nair, V. J. Babu, R. Murugan, and S. Ramakrishna. 2012. "A review on nanomaterials for environmental remediation." *Energy & Environmental Science* 5 (8):8075-8109. doi: 10.1039/c2ee21818f.

Khorram, M., A. Mousavi, and N. Mehranbod. 2017. "Chromium removal using adsorptive membranes composed of electrospun plasma-treated functionalized polyethylene terephthalate (PET) with chitosan." *Journal of Environmental Chemical Engineering* 5 (3):2366-2377. doi: 10.1016/j.jece.2017.04.010.

Kim, E. K., J. Y. Kim, and S. S. Kim. 2013. "Synthesis of superhydrophobic SiO2 layers via combination of surface roughness and fluorination." *Journal of Solid State Chemistry* 197:23-28. doi: 10.1016/j.jssc.2012.08.017.

Kim, E. K., C. S. Lee, and S. S. Kim. 2012. "Superhydrophobicity of electrospray-synthesized fluorinated silica layers." *Journal of Colloid and Interface Science* 368:599-602. doi: 10.1016/j.jcis.2011.11.047.

Kiyohiko, Hagiwara. 1929. Process for manufacturing artificial silk and other filaments by applying electric current. JAPAN.

Kongkhlang, T., M. Kotaki, Y. Kousaka, T. Umemura, D. Nakaya, and S. Chirachanchai. 2008. "Electrospun polyoxymethylene: Spinning conditions and its consequent nanoporous nanofiber." *Macromolecules* 41 (13):4746-4752. doi: 10.1021/ma800731r.

Korycka, Paulina, Adam Mirek, Katarzyna Kramek-Romanowska, Marcin Grzeczkowicz, and Dorota Lewińska. 2018. "Effect of electrospinning process variables on the size of polymer fibers and bead-on-string structures established with a 23 factorial design." *Beilstein Journal of Nanotechnology* 9:2466-2478. doi: 0.3762/bjnano.9.231.

Ladeira, A. C. Q., and C. A. Morais. 2005. "Uranium recovery from industrial effluent by ion exchange—column experiments." *Minerals Engineering* 18 (13):1337-1340. doi: 10.1016/j.mineng.2005.06.012.

Lafuma, A., and D. Quere. 2003. "Superhydrophobic states." *Nature Materials* 2 (7):457-460. doi: 10.1038/nmat924.

Lalia, B. S., V. Kochkodan, R. Hashaikeh, and N. Hilal. 2013. "A review on membrane fabrication: Structure, properties and performance relationship." *Desalination* 326:77-95. doi: 10.1016/j.desal.2013.06.016.

Laxminarayan, A., K. S. McGuire, S. S. Kim, and D. R. Lloyd. 1994. "Effect of Initial Composition, Phase-Separation Temperature and Polymer Crystallization on the Formation of Microcellular Structures via Thermally-Induced Phase-Separation." *Polymer* 35 (14):3060-3068. doi: 10.1016/0032-3861(94)90420-0.

Lee, M. W., S. An, S. S. Latthe, C. Lee, S. Hong, and S. S. Yoon. 2013. "Electrospun Polystyrene Nanofiber Membrane with Superhydrophobicity and Superoleophilicity for Selective Separation of Water and Low Viscous Oil." *Acs Applied Materials & Interfaces* 5 (21):10597-10604. doi: 10.1021/am404156k.

Leong, M. F., K. S. Chian, P. S. Mhaisalkar, W. F. Ong, and B. D. Ratner. 2009. "Effect of electrospun poly(D,L-lactide) fibrous scaffold with nanoporous surface on attachment of porcine esophageal epithelial cells and protein adsorption." *Journal of Biomedical Materials Research Part A* 89A (4):1040-1048. doi: 10.1002/jbm.a.32061.

Li, K. Q., X. R. Zeng, H. Q. Li, and X. J. Lai. 2014. "Facile fabrication of a robust superhydrophobic/superoleophilic sponge for selective oil absorption from oily water." *Rsc Advances* 4 (45):23861-23868. doi: 10.1039/c4ra01227e.

Li, X., C. Wang, Y. Yang, X. F. Wang, M. F. Zhu, and B. S. Hsiao. 2014. "Dual-Biomimetic Superhydrophobic Electrospun Polystyrene Nanofibrous

Membranes for Membrane Distillation." *Acs Applied Materials & Interfaces* 6 (4):2431-2438. doi: 10.1021/am4048128.

Li, Y., L. L. He, X. F. Zhang, N. Zhang, and D. L. Tian. 2017. "External-Field-Induced Gradient Wetting for Controllable Liquid Transport: From Movement on the Surface to Penetration into the Surface." *Advanced Materials* 29 (45). doi: 10.1002/adma.201703802.

Li, Y., L. Li, and J. Q. Sun. 2010. "Bioinspired Self-Healing Superhydrophobic Coatings." *Angewandte Chemie-International Edition* 49 (35):6129-6133. doi: 10.1002/anie.201001258.

Li, Yi, Luyan Li, Tao Chen, Tao Duan, Weitang Yao, Kui Zheng, Lichun Dai, and Wenkun Zhu. 2018. "Bioassembly of fungal hypha/graphene oxide aerogel as high performance adsorbents for U(VI) removal." *Chemical Engineering Journal* 347:407-414. doi: 10.1016/j.cej.2018.04.140.

Lima, J., S. R. Sousa, A. Ferreira, and M. A. Barbosa. 2001. "Interactions between calcium, phosphate, and albumin on the surface of titanium." *Journal of Biomedical Materials Research* 55 (1):45-53. doi: 10.1002/1097-4636(200104)55:1<45::aid-jbm70>3.0.co;2-0.

Lin, J. Y., B. Ding, J. Y. Yu, and Y. Hsieh. 2010. "Direct Fabrication of Highly Nanoporous Polystyrene Fibers via Electrospinning." *Acs Applied Materials & Interfaces* 2 (2):521-528. doi: 10.1021/am900736h.

Lin, J. Y., Y. W. Shang, B. Ding, J. M. Yang, J. Y. Yu, and S. S. Al-Deyab. 2012. "Nanoporous polystyrene fibers for oil spill cleanup." *Marine Pollution Bulletin* 64 (2):347-352. doi: 10.1016/j.marpolbul.2011.11.002.

Liu, Jinyao, Wei Huang, Yongfeng Zhou, and Deyue Yan. 2009. "Synthesis of Hyperbranched Polyphosphates by Self-Condensing Ring-Opening Polymerization of HEEP without Catalyst." *Macromolecules* 42 (13):4394-4399. doi: 10.1021/ma900798h.

Liu, K. S., and L. Jiang. 2012. "Bio-Inspired Self-Cleaning Surfaces." In *Annual Review of Materials Research, Vol 42*, edited by D. R. Clarke, 231-263.

Liu, W. J., C. Huang, and X. Y. Jin. 2014. "Tailoring the grooved texture of electrospun polystyrene nanofibers by controlling the solvent system and relative humidity." *Nanoscale Research Letters* 9. doi: 10.1186/1556-276x-9-350.

Liu, W. J., C. Huang, and X. Y. Jin. 2015. "Electrospinning of Grooved Polystyrene Fibers: Effect of Solvent Systems." *Nanoscale Research Letters* 10. doi: 10.1186/s11671-015-0949-5.

Liu, W. Y., L. Y. Sun, Y. T. Luo, R. M. Wu, H. Y. Jiang, Y. Chen, G. S. Zeng, and Y. J. Liu. 2013. "Facile transition from hydrophilicity to superhydrophilicity and superhydrophobicity on aluminum alloy surface by simple acid etching and polymer coating." *Applied Surface Science* 280:193-200. doi: 10.1016/j.apsusc.2013.04.124.

Lu, P., and Y. N. Xia. 2013. "Maneuvering the Internal Porosity and Surface Morphology of Electrospun Polystyrene Yarns by Controlling the Solvent and Relative Humidity." *Langmuir* 29 (23):7070-7078. doi: 10.1021/la400747y.

Lu, W. J., Z. Z. Yuan, Y. Y. Zhao, H. Z. Zhang, H. M. Zhang, and X. F. Li. 2017. "Porous membranes in secondary battery technologies." *Chemical Society Reviews* 46 (8):2199-2236. doi: 10.1039/c6cs00823b.

Luo, Wensui, Shelly D. Kelly, Kenneth M. Kemner, David Watson, Jizhong Zhou, Philip M. Jardine, and Baohua Gu. 2009. "Sequestering Uranium and Technetium through Co-Precipitation with Aluminum in a Contaminated Acidic Environment." *Environmental Science & Technology* 43 (19):7516-7522. doi: 10.1021/es900731a.

Ma, Z. W., M. Kotaki, and S. Ramakrishna. 2005. "Electrospun cellulose nanofiber as affinity membrane." *Journal of Membrane Science* 265 (1-2):115-123. doi: 10.1016/j.memsci.2005.04.044.

MacArthur, D. E. 2017a. "Beyond plastic waste." *Science* 358 (6365):843-843. doi: 10.1126/science.aao6749.

MacArthur, Dame Ellen. 2017b. "Beyond plastic waste." *Science* 358 (6365):843. doi: 10.1126/science.aao6749.

Manna, U., and D. M. Lynn. 2015. "Synthetic Surfaces with Robust and Tunable Underwater Superoleophobicity." *Advanced Functional Materials* 25 (11):1672-1681. doi: 10.1002/adfm.201403735.

Margesin, R., and F. Schinner. 1999. "Biological decontamination of oil spills in cold environments." *Journal of Chemical Technology and Biotechnology* 74 (5):381-389.

McKeown, Neil B., and Peter M. Budd. 2006. "Polymers of intrinsic microporosity (PIMs): organic materials for membrane separations, heterogeneous catalysis and hydrogen storage." *Chemical Society Reviews* 35 (8):675-683. doi: 10.1039/B600349D.

Megelski, S., J. S. Stephens, D. B. Chase, and J. F. Rabolt. 2002. "Micro- and nanostructured surface morphology on electrospun polymer fibers." *Macromolecules* 35 (22):8456-8466. doi: 10.1021/ma020444a.

Mishra, S., J. Dwivedi, A. Kumar, and N. Sankararamakrishnana. 2015. "Studies on salophen anchored micro/meso porous activated carbon fibres for the removal and recovery of uranium." *Rsc Advances* 5 (42):33023-33036. doi: 10.1039/c5ra03168k.

Miyauchi, Y., B. Ding, and S. Shiratori. 2006. "Fabrication of a silver-ragwort-leaf-like super-hydrophobic micro/nanoporous fibrous mat surface by electrospinning." *Nanotechnology* 17 (20):5151-5156. doi: 10.1088/0957-4484/17/20/019.

Mullin, J. V., and M. A. Champ. 2003. "Introduction/overview to in situ burning of oil spills." *Spill Science & Technology Bulletin* 8 (4):323-330. doi: 10.1016/s1353-2561(03)00076-8.

Munir, Muhammad Miftahul, Ade Y. Nuryantini, Iskandar, Tri Suciati, and Khairurrijal. 2014. "Mass Production of Stacked Styrofoam Nanofibers using a Multinozzle and Drum Collector Electrospinning System." *Advanced Materials Research* 896:20-23.

Ou, R. W., J. Wei, L. Jiang, G. P. Simon, and H. T. Wang. 2016. "Robust Thermoresponsive Polymer Composite Membrane with Switchable Superhydrophilicity and Superhydrophobicity for Efficient Oil-Water Separation." *Environmental Science & Technology* 50 (2):906-914. doi: 10.1021/acs.est.5b03418.

Padaki, M., R. S. Murali, M. S. Abdullah, N. Misdan, A. Moslehyani, M. A. Kassim, N. Hilal, and A. F. Ismail. 2015. "Membrane technology enhancement in oil-water separation. A review." *Desalination* 357:197-207. doi: 10.1016/j.desal.2014.11.023.

Pai, C. L., M. C. Boyce, and G. C. Rutledge. 2009. "Morphology of Porous and Wrinkled Fibers of Polystyrene Electrospun from Dimethylformamide." *Macromolecules* 42 (6):2102-2114. doi: 10.1021/ma802529h.

Park, H., K. Lee, M. Kim, J. Lee, S. Y. Seong, and G. Ko. 2009. "Detection and hazard assessment of pathogenic microorganisms in medical wastes." *Journal of*

Environmental Science and Health Part a-Toxic/Hazardous Substances & Environmental Engineering 44 (10):995-1003. doi: 10.1080/10934520902996898.

Patankar, N. A. 2009. "Hydrophobicity of Surfaces with Cavities: Making Hydrophobic Substrates from Hydrophilic Materials?" *Journal of Adhesion Science and Technology* 23 (3):413-433. doi: 10.1163/156856108x370073.

Piechowicz, M., C. W. Abney, X. Zhou, N. C. Thacker, Z. Li, and W. B. Lin. 2016. "Design, Synthesis, and Characterization of a Bifunctional Chelator with Ultrahigh Capacity for Uranium Uptake from Seawater Simulant." *Industrial & Engineering Chemistry Research* 55 (15):4170-4178. doi: 10.1021/acs.iecr.5b03304.

Pruss, A., E. Giroult, and P. Rushbrook. 1999. Safe Management of Wastes from Healthcare Activities. World Health Organization, Geneva,.

Qing, Y. Q., C. N. Yang, Z. Y. Yu, Z. F. Zhang, Q. L. Hu, and C. S. Liu. 2016. "Large-Area Fabrication of Superhydrophobic Zinc Surface with Reversible Wettability Switching and Anticorrosion." *Journal of the Electrochemical Society* 163 (8):D385-D391. doi: 10.1149/2.0571608jes.

Quere, D. 2008. "Wetting and roughness." In *Annual Review of Materials Research*, 71-99.

Rayleigh, Lord. 1882. "On the Equilibrium of Liquid Conducting Masses Charged with Electricity." *Philosophical Magazine* 14 (87):184-186. doi: 10.1080/14786448208628425.

Reneker, D. H., and I. Chun. 1996. "Nanometre diameter fibres of polymer, produced by electrospinning." *Nanotechnology* 7 (3):216-223. doi: 10.1088/0957-4484/7/3/009.

Ruhela, R., N. Iyer, M. Yadav, A. K. Singh, R. C. Hubli, and J. K. Chakravartty. 2015. "N,N,N-Trimethyl benzyl ammonium bis-(2-ethylhexyl)-phosphonate grafted polymer - a solid supported ionic liquid for the separation of uranium from aqueous processing streams." *Green Chemistry* 17 (2):827-830. doi: 10.1039/c4gc02020k.

Rutala, W. A., and D. J. Weber. 2010. "Guideline for Disinfection and Sterilization of Prion-Contaminated Medical Instruments." *Infection Control and Hospital Epidemiology* 31 (2):107-117. doi: 10.1086/650197.

S.K., Chinta, Landage S.M. , and Yadav Krati. 2013. "Application of Chicken Feathers inTechnical Textiles." *International Journal of Innovative Research in Science, Engineering and Technology* 2 (4):1158.

Santhosh, C., V. Velmurugan, G. Jacob, S. K. Jeong, A. N. Grace, and A. Bhatnagar. 2016. "Role of nanomaterials in water treatment applications: A review." *Chemical Engineering Journal* 306:1116-1137. doi: 10.1016/j.cej.2016.08.053.

Satilmis, B., T. Isık, M. M. Demir, and T. Uyar. "Amidoxime functionalized Polymers of Intrinsic Microporosity (PIM-1) electrospun ultrafine fibers for rapid removal of uranyl ions from water - revised-." *Applied Surface Science*.

Satilmis, Bekir, Mohammed N. Alnajrani, and Peter M. Budd. 2015. "Hydroxyalkylaminoalkylamide PIMs: Selective Adsorption by Ethanolamine- and Diethanolamine-Modified PIM-1." *Macromolecules* 48 (16):5663-5669. doi: 10.1021/acs.macromol.5b01196.

Satilmis, Bekir, and Peter M. Budd. 2014. "Base-catalysed hydrolysis of PIM-1: amide versus carboxylate formation." *RSC Advances* 4 (94):52189-52198. doi: 10.1039/C4RA09907A.

Satilmis, Bekir, and Peter M. Budd. 2017. "Selective dye adsorption by chemically-modified and thermally-treated polymers of intrinsic microporosity." *Journal of Colloid and Interface Science* 492:81-91. doi: 10.1016/j.jcis.2016.12.048.

Satilmis, Bekir, Peter M. Budd, and Tamer Uyar. 2017. "Systematic hydrolysis of PIM-1 and electrospinning of hydrolyzed PIM-1 ultrafine fibers for an efficient removal of dye from water." *Reactive and Functional Polymers* 121 (Supplement C):67-75. doi: 10.1016/j.reactfunctpolym.2017.10.019.

Satilmis, Bekir, and Tamer Uyar. 2018a. "Amine modified electrospun PIM-1 ultrafine fibers for an efficient removal of methyl orange from an aqueous system." *Applied Surface Science* 453:220-229. doi: 10.1016/j.apsusc.2018.05.069.

Satilmis, Bekir, and Tamer Uyar. 2018b. "Removal of aniline from air and water by polymers of intrinsic microporosity (PIM-1) electrospun ultrafine fibers." *Journal of Colloid and Interface Science* 516:317-324. doi: 10.1016/j.jcis.2018.01.069.

NIH Image to ImageJ: 25 years of image analysis 1x. Nature methods.

Shannon, M. A., P. W. Bohn, M. Elimelech, J. G. Georgiadis, B. J. Marinas, and A. M. Mayes. 2008. "Science and technology for water purification in the coming decades." *Nature* 452 (7185):301-310. doi: 10.1038/nature06599.

Shen, Junjie, and Andrea Schäfer. 2014. "Removal of fluoride and uranium by nanofiltration and reverse osmosis: A review." *Chemosphere* 117:679-691. doi: 10.1016/j.chemosphere.2014.09.090.

Shenoy, S. L., W. D. Bates, H. L. Frisch, and G. E. Wnek. 2005. "Role of chain entanglements on fiber formation during electrospinning of polymer solutions: good solvent, non-specific polymer-polymer interaction limit." *Polymer* 46 (10):3372-3384. doi: 10.1016/j.polymer.2005.03.011.

Shin, C. 2005. "A new recycling method for expanded polystyrene." *Packaging Technology and Science* 18 (6):331-335. doi: 10.1002/pts.707.

Shin, C. 2006. "Filtration application from recycled expanded polystyrene." *Journal of Colloid and Interface Science* 302 (1):267-271. doi: 10.1016/j.jcis.2006.05.058.

Shin, C., and G. G. Chase. 2006. "Separation of liquid drops from air by glass fiber filters augmented with polystyrene nanofibers." *Journal of Dispersion Science and Technology* 27 (1):5-9. doi: 10.1081/dis-200066616.

Shin, C., G. G. Chase, and D. H. Reneker. 2005. "Recycled expanded polystyrene nanofibers applied in filter media." *Colloids and Surfaces a-Physicochemical and Engineering Aspects* 262 (1-3):211-215. doi: 10.1016/j.colsurfa.2005.04.034.

Shin, C. Y., and G. G. Chase. 2005. "Nanofibers from recycle waste expanded polystyrene using natural solvent." *Polymer Bulletin* 55 (3):209-215. doi: 10.1007/s00289-005-0421-2.

Shin, Y. M., M. M. Hohman, M. P. Brenner, and G. C. Rutledge. 2001a. "Electrospinning: A whipping fluid jet generates submicron polymer fibers." *Applied Physics Letters* 78 (8):1149-1151. doi: 10.1063/1.1345798.

Shin, Y. M., M. M. Hohman, M. P. Brenner, and G. C. Rutledge. 2001b. "Experimental characterization of electrospinning: the electrically forced jet and instabilities." *Polymer* 42 (25):9955-9967. doi: 10.1016/s0032-3861(01)00540-7.

Shiu, J. Y., C. W. Kuo, P. L. Chen, and C. Y. Mou. 2004. "Fabrication of tunable superhydrophobic surfaces by nanosphere lithography." *Chemistry of Materials* 16 (4):561-564. doi: 10.1021/cm034696h.

Sihn, Y. H., J. Byun, H. A. Patel, W. Lee, and C. T. Yavuz. 2016. "Rapid extraction of uranium ions from seawater using novel porous polymeric adsorbents." *RSC Advances* 6 (51):45968-45976. doi: 10.1039/C6RA06807C.

Simm, W., K. Gosling, R. Bonart, and G. B. von Falkai. 1972.

Song, B. T., and C. Xu. 2016. "Highly Hydrophobic and Superoleophilic Nanofibrous Mats with Controllable Pore Sizes for Efficient Oil/Water Separation." *Langmuir* 32 (39):9960-9966. doi: 10.1021/acs.langmuir.6b02500.

Song, J. L., Y. Lu, J. Luo, S. Huang, L. Wang, W. J. Xu, and I. P. Parkin. 2015. "Barrel-Shaped Oil Skimmer Designed for Collection of Oil from Spills." *Advanced Materials Interfaces* 2 (15). doi: 10.1002/admi.201500350.

Srinivasarao, M., D. Collings, A. Philips, and S. Patel. 2001. "Three-dimensionally ordered array of air bubbles in a polymer film." *Science* 292 (5514):79-83. doi: 10.1126/science.1057887.

Strain, I. N., Q. Wu, A. M. Pourrahimi, M. S. Hedenqvist, R. T. Olsson, and R. L. Andersson. 2015. "Electrospinning of recycled PET to generate tough mesomorphic fibre membranes for smoke filtration." *Journal of Materials Chemistry A* 3 (4):1632-1640. doi: 10.1039/c4ta06191h.

Sunder, A., R. Mulhaupt, and H. Frey. 2000. "Hyperbranched polyether-polyols based on polyglycerol: Polarity design by block copolymerization with propylene oxide." *Macromolecules* 33 (2):309-314. doi: 10.1021/ma991191x.

Sunder, A., R. Mulhaupt, R. Haag, and H. Frey. 2000. "Hyperbranched polyether polyols: A modular approach to complex polymer architectures." *Advanced Materials* 12 (3):235-+. doi: 10.1002/(sici)1521-4095(200002)12:3<235::aid-adma235>3.3.co;2-p.

Tan, S. H., N. T. Nguyen, Y. C. Chua, and T. G. Kang. 2010. "Oxygen plasma treatment for reducing hydrophobicity of a sealed polydimethylsiloxane microchannel." *Biomicrofluidics* 4 (3). doi: 10.1063/1.3466882.

Tan, Z., Y. Liang, H. Chen, and D. J. Wang. 2013. "Synthesis of Hexadecyl Methacrylate/Methyl Methacrylate Copolymer by High Internal Phase Emulsion Template and its High Oil-Absorbing Properties." *Separation Science and Technology* 48 (15):2338-2344. doi: 10.1080/01496395.2013.799212.

Teo, Wee-Eong. 2018. "Electrospun Recycled Materials." ElectrospinTech, accessed 21.09.2018. http://electrospintech.com/recycledmaterials.html - .W6Sm9C-B0dV.

Tian, L. D., C. Y. Zhang, X. W. He, Y. Q. Guo, M. T. Qiao, J. W. Gu, and Q. Y. Zhang. 2017. "Novel reusable porous polyimide fibers for hot-oil adsorption." *Journal of Hazardous Materials* 340:67-76. doi: 10.1016/j.jhazmat.2017.06.063.

Uyar, T., and F. Besenbacher. 2008. "Electrospinning of uniform polystyrene fibers: The effect of solvent conductivity." *Polymer* 49 (24):5336-5343. doi: 10.1016/j.polymer.2008.09.025.

vandeWitte, P., P. J. Dijkstra, J. W. A. vandenBerg, and J. Feijen. 1996. "Phase separation processes in polymer solutions in relation to membrane formation." *Journal of Membrane Science* 117 (1-2):1-31. doi: 10.1016/0376-7388(96)00088-9.

Voit, Brigitte I., and Albena Lederer. 2009. "Hyperbranched and Highly Branched Polymer Architectures-Synthetic Strategies and Major Characterization Aspects." *Chemical Reviews* 109 (11):5924-5973. doi: 10.1021/cr900068q.

Wang, B., W. W. Chen, L. T. Zhang, Z. Z. Li, C. T. Liu, J. B. Chen, and C. Y. Shen. 2017. "Hydrophobic polycarbonate monolith with mesoporous nest-like structure: an effective oil sorbent." *Materials Letters* 188:201-204. doi: 10.1016/j.matlet.2016.11.015.

Wang, B., W. X. Liang, Z. G. Guo, and W. M. Liu. 2015. "Biomimetic super-lyophobic and super-lyophilic materials applied for oil/water separation: a new strategy beyond nature." *Chemical Society Reviews* 44 (1):336-361. doi: 10.1039/c4cs00220b.

Wang, F. H., H. P. Li, Q. Liu, Z. S. Li, R. M. Li, H. S. Zhang, L. H. Liu, G. A. Emelchenko, and J. Wang. 2016. "A graphene oxide/amidoxime hydrogel for enhanced uranium capture." *Scientific Reports* 6. doi: 10.1038/srep19367.

Wang, H. J., W. Y. Wang, H. Wang, X. Jin, J. L. Li, and Z. T. Zhu. 2018. "One-way water transport fabrics with hydrophobic rough surface formed in one-step electrospray." *Materials Letters* 215:110-113. doi: 10.1016/j.matlet.2017.12.066.

Wang, L., L. Y. Yuan, K. Chen, Y. J. Zhang, Q. H. Deng, S. Y. Du, Q. Huang, L. R. Zheng, J. Zhang, Z. F. Chai, M. W. Barsoum, X. K. Wang, and W. Q. Shi. 2016. "Loading Actinides in Multilayered Structures for Nuclear Waste Treatment: The First Case Study of Uranium Capture with Vanadium Carbide MXene."

Acs Applied Materials & Interfaces 8 (25):16396-16403. doi: 10.1021/acsami.6b02989.

Wang, Z. M., J. P. He, Y. F. Tao, L. Yang, H. J. Jiang, and Y. L. Yang. 2003. "Controlled chain branching by RAFT-based radical polymerization." *Macromolecules* 36 (20):7446-7452. doi: 10.1021/ma025673b.

WHO. 2005. Safe health-care waste management-policy paper by the World Health Organization. Waste Management

WHO. 2015. "Health-care waste Fact Sheet No 253." World Health Organisation.

Wiechert, Alexander I., Wei-Po Liao, Eunice Hong, Candice E. Halbert, Sotira Yiacoumi, Tomonori Saito, and Costas Tsouris. 2018. "Influence of hydrophilic groups and metal-ion adsorption on polymer-chain conformation of amidoxime-based uranium adsorbents." *Journal of Colloid and Interface Science* 524:399-408. doi: 10.1016/j.jcis.2018.04.021.

Windfeld, E. S., and M. S. L. Brooks. 2015. "Medical waste management - A review." *Journal of Environmental Management* 163:98-108. doi: 10.1016/j.jenvman.2015.08.013.

Wooley, K. L., J. M. J. Frechet, and C. J. Hawker. 1994. "Influence of Shape on the Reactivity and Properties of Dendritic, Hyperbranched and Linear Aromatic Polyesters." *Polymer* 35 (21):4489-4495. doi: 10.1016/0032-3861(94)90793-5.

Woranuch, S., A. Pangon, K. Puagsuntia, N. Subjalearndee, and V. Intasanta. 2017. "Starch-based and multi-purpose nanofibrous membrane for high efficiency nanofiltration." *Rsc Advances* 7 (56):35368-35375. doi: 10.1039/c7ra07484k.

Wu, F. C., N. Pu, G. Ye, T. X. Sun, Z. Wang, Y. Song, W. Q. Wang, X. M. Huo, Y. X. Lu, and J. Chen. 2017. "Performance and Mechanism of Uranium Adsorption from Seawater to Poly(dopamine)-Inspired Sorbents." *Environmental Science & Technology* 51 (8):4606-4614. doi: 10.1021/acs.est.7b00470.

Wu, J., N. Wang, L. Wang, H. Dong, Y. Zhao, and L. Jiang. 2012. "Electrospun Porous Structure Fibrous Film with High Oil Adsorption Capacity." *Acs Applied Materials & Interfaces* 4 (6):3207-3212. doi: 10.1021/am300544d.

Wu, J. Y., A. K. An, J. X. Guo, E. J. Lee, M. U. Farid, and S. Jeong. 2017. "CNTs reinforced super-hydrophobic-oleophilic electrospun polystyrene oil sorbent for enhanced sorption capacity and reusability." *Chemical Engineering Journal* 314:526-536. doi: 10.1016/j.cej.2016.12.010.

Wu, Jing, Nu Wang, Yong Zhao, and Lei Jiang. 2013. "Electrospinning of multilevel structured functional micro-/nanofibers and their applications." *Journal of Materials Chemistry A* 1 (25):7290-7305. doi: 10.1039/c3ta10451f.

Xiao, C. M., L. X. Si, Y. M. Liu, G. Q. Guan, D. H. Wu, Z. D. Wang, and X. G. Hao. 2016. "Ultrastable coaxial cable-like superhydrophobic mesh with self-adaption effect: facile synthesis and oil/water separation application." *Journal of Materials Chemistry A* 4 (21):8080-8090. doi: 10.1039/c6ta01621a.

Xie, X. L., Q. X. Liu, R. K. Y. Li, X. P. Zhou, Q. X. Zhang, Z. Z. Yu, and Y. W. Mai. 2004. "Rheological and mechanical properties of PVC/CaCO3 nanocomposites prepared by in situ polymerization." *Polymer* 45 (19):6665-6673. doi: 10.1016/j.polymer.2004.07.045.

Xu, L. X., Y. N. Chen, N. Liu, W. F. Zhang, Y. Yang, Y. Z. Cao, X. Lin, Y. Wei, and L. Feng. 2015. "Breathing Demulsification: A Three-Dimensional (3D) Free-Standing Superhydrophilic Sponge." *Acs Applied Materials & Interfaces* 7 (40):22264-22271. doi: 10.1021/acsami.5b07530.

Xu, Q. F., J. N. Wang, and K. D. Sanderson. 2010. "Organic-Inorganic Composite Nanocoatings with Superhydrophobicity, Good Transparency, and Thermal Stability." *Acs Nano* 4 (4):2201-2209. doi: 10.1021/nn901581j.

Xue, Z. X., Y. Z. Cao, N. Liu, L. Feng, and L. Jiang. 2014. "Special wettable materials for oil/water separation." *Journal of Materials Chemistry A* 2 (8):2445-2460. doi: 10.1039/c3ta13397d.

Yao, X., Y. L. Song, and L. Jiang. 2011. "Applications of Bio-Inspired Special Wettable Surfaces." *Advanced Materials* 23 (6):719-734. doi: 10.1002/adma.201002689.

Yi, L. M., X. M. Meng, X. P. Tian, W. Zhou, and R. W. Chen. 2014. "Wettability of Electrospun Films of Microphase-Separated Block Copolymers with 3,3,3-Trifluoropropyl Substituted Siloxane Segments." *Journal of Physical Chemistry C* 118 (46):26671-26682. doi: 10.1021/jp5065566.

Yoon, K., B. S. Hsiao, and B. Chu. 2008. "Functional nanofibers for environmental applications." *Journal of Materials Chemistry* 18 (44):5326-5334. doi: 10.1039/b804128h.

Yoon, K., K. Kim, X. F. Wang, D. F. Fang, B. S. Hsiao, and B. Chu. 2006. "High flux ultrafiltration membranes based on electrospun nanofibrous PAN scaffolds and chitosan coating." *Polymer* 47 (7):2434-2441. doi: 10.1016/j.polymer.2006.01.042.

Yue, Yanfeng, T. Mayes Richard, Jungseung Kim, F. Fulvio Pasquale, Xiao-Guang Sun, Costas Tsouris, Jihua Chen, Suree Brown, and Sheng Dai. 2013. "Seawater Uranium Sorbents: Preparation from a Mesoporous Copolymer Initiator by Atom-Transfer Radical Polymerization." *Angewandte Chemie International Edition* 52 (50):13458-13462. doi: 10.1002/anie.201307825.

Zacharides, A. E., R. S. Porter, J. Doshi, G. Srinivasan, and D. H. Reneker. 1995. "High modulus polymers. A novel electrospinning process." *Polymer News* 20:206-207.

Zander, N. E., D. Sweetser, D. P. Cole, and M. Gillan. 2015. "Formation of Nanofibers from Pure and Mixed Waste Streams Using Electrospinning." *Industrial & Engineering Chemistry Research* 54 (37):9057-9063. doi: 10.1021/acs.iecr.5b02279.

Zare, Y. 2013. "Recent progress on preparation and properties of nanocomposites from recycled polymers: A review." *Waste Management* 33 (3):598-604. doi: 10.1016/j.wasman.2012.07.031.

Zhang, H. T., H. L. Nie, D. G. Yu, C. Y. Wu, Y. L. Zhang, C. J. B. White, and L. M. Zhu. 2010. "Surface modification of electrospun polyacrylonitrile nanofiber towards developing an affinity membrane for bromelain adsorption." *Desalination* 256 (1-3):141-147. doi: 10.1016/j.desal.2010.01.026.

Zhang, L. F., T. J. Menkhaus, and H. Fong. 2008. "Fabrication and bioseparation studies of adsorptive membranes/felts made from electrospun cellulose acetate nanofibers." *Journal of Membrane Science* 319 (1-2):176-184. doi: 10.1016/j.memsci.2008.03.030.

Zhang, M. X., Q. H. Gao, C. G. Yang, L. J. Pang, H. L. Wang, H. Li, R. Li, L. Xu, Z. Xing, J. T. Hu, and G. Z. Wu. 2016. "Preparation of Amidoxime-Based Nylon-66 Fibers for Removing Uranium from Low-Concentration Aqueous Solutions and Simulated Nuclear Industry Effluents." *Industrial & Engineering Chemistry Research* 55 (40):10523-10532. doi: 10.1021/acs.iecr.6b02652.

Zhang, W. B., F. Zhang, S. J. Gao, Y. Z. Zhu, J. Y. Li, and J. Jin. 2015. "Micro/nano hierarchical poly(acrylic acid)-grafted-poly(vinylidene fluoride) layer coated foam membrane for temperature-controlled separation of heavy oil/water." *Separation and Purification Technology* 156:207-214. doi: 10.1016/j.seppur.2015.09.076.

Zhang, X., F. Shi, J. Niu, Y. G. Jiang, and Z. Q. Wang. 2008. "Superhydrophobic surfaces: from structural control to functional application." *Journal of Materials Chemistry* 18 (6):621-633. doi: 10.1039/b711226b.

Zhang, Y. Z., Y. Feng, Z. M. Huang, S. Ramakrishna, and C. T. Lim. 2006. "Fabrication of porous electrospun nanofibres." *Nanotechnology* 17 (3):901-908. doi: 10.1088/0957-4484/17/3/047.

Zhao, W., E. van der Voet, G. Huppes, and Y. F. Zhang. 2009. "Comparative life cycle assessments of incineration and non-incineration treatments for medical waste." *International Journal of Life Cycle Assessment* 14 (2):114-121. doi: 10.1007/s11367-008-0049-1.

Zhao, Y. G., J. X. Li, L. P. Zhao, S. W. Zhang, Y. S. Huang, X. L. Wu, and X. K. Wang. 2014. "Synthesis of amidoxime-functionalized Fe3O4@SiO2 core-shell magnetic microspheres for highly efficient sorption of U(VI)." *Chemical Engineering Journal* 235:275-283. doi: 10.1016/j.cej.2013.09.034.

Zhao, Y. G., X. X. Wang, J. X. Li, and X. K. Wang. 2015. "Amidoxime functionalization of mesoporous silica and its high removal of U(VI)." *Polymer Chemistry* 6 (30):5376-5384. doi: 10.1039/c5py00540j.

Zheng, J. F., A. H. He, J. X. Li, J. A. Xu, and C. C. Han. 2006. "Studies on the controlled morphology and wettability of polystyrene surfaces by electrospinning or electrospraying." *Polymer* 47 (20):7095-7102. doi: 10.1016/j.polymer.2006.08.019.

Zhou, S. K., P. P. Liu, M. Wang, H. Zhao, J. Yang, and F. Xu. 2016. "Sustainable, Reusable, and Superhydrophobic Aerogels from Microfibrillated Cellulose for Highly Effective Oil/Water Separation." *Acs Sustainable Chemistry & Engineering* 4 (12):6409-6416. doi: 10.1021/acssuschemeng.6b01075.

Zhou, Z. P., and X. F. Wu. 2015. "Electrospinning superhydrophobic-superoleophilic fibrous PVDF membranes for high-efficiency water-oil separation." *Materials Letters* 160:423-427. doi: 10.1016/j.matlet.2015.08.003.

Zhu, Q., Q. M. Pan, and F. T. Liu. 2011. "Facile Removal and Collection of Oils from Water Surfaces through Superhydrophobic and Superoleophilic Sponges." *Journal of Physical Chemistry C* 115 (35):17464-17470. doi: 10.1021/jp2043027.

Zhuang, G. L., H. H. Tseng, and M. Y. Wey. 2016. "Feasibility of using waste polystyrene as a membrane material for gas separation." *Chemical Engineering Research & Design* 111:204-217. doi: 10.1016/j.cherd.2016.03.033.

Ziabicki, Andrzej. 1976. *Fundamentals of Fibre Formation: The Science of Fibre Spinning and Drawing*: John Wiley and Sons.

Zulfi, A, A Fauzi, D Edikresnha, M M Munir, and Khairurrijal. 2017. "Synthesis of High-Impact Polystyrene Fibers using Electrospinning." The 4th International Conference on Advanced Materials Science and Technology.

Zuo, W. W., M. F. Zhu, W. Yang, H. Yu, Y. M. Chen, and Y. Zhang. 2005. "Experimental study on relationship between jet instability and formation of beaded fibers during electrospinning." *Polymer Engineering and Science* 45 (5):704-709. doi: 10.1002/pen.20304.

VITA

PERSONAL INFORMATION

Surname, Name: ISIK TUĞBA
Date and Place of Birth: 16.08.1989 – Konak/İZMİR

EDUCATION

Degree	Institution	Year of Graduation
MSc	İzmir Institute of Technology	2015
BSc	İzmir Institute of Technology	2013

WORK EXPERIENCE

Year	Place	Enrollment
2013-2018	İzmir Institute of Technology	Research Assistant
2012	TUPRAS Izmir Refinery, Izmir (Turkey)	Trainee

PUBLICATIONS

- Tuğba Isık, Nesrin Horzum, Mustafa M. Demir, *A Recycling Route via Electrospinning: From Daily Wastes To Functional Fibers,* In Progress for DeGruyter 'Green Electrospinning ' Book (publication date: **2019**)
- Bekir Satilmis, Tuğba Isık, Mustafa M. Demir, Tamer Uyar, *Amidoxime functionalized Polymers of Intrinsic Microporosity (PIM-1)*, Applied Surface Science, 467-468, 648-657 **(2019)**
- Tuğba Isık, Mustafa M. Demir, *Tailored electrospun fibers from waste polystyrene for high oil adsorption,* Sustainable Materials and Technologies, 18, e00084 (**2018**)
- Oktay Acar, Serhat Varis, Tuğba Isık, Seha Tirkes, Mustafa M Demir, *Synthesis and characterization of novel high temperature structural adhesives based on nadic end capped MDA-BTDA-ODA copolyimide,* Materials Research Express, 5, 105305 **(2018)**
- Mohamed El Housseini Hilal, Tuğba Isık, Nesrin Horzum, *Enhanced Bactericidal and Photocatalytic Activities of ZnO Nanostructures through Annealing and Controlled Cooling Rate,* New Journal of Chemistry, 42, 11831-11838 (**2018**)
- Tuğba Isık, Mustafa M. Demir, *Medical waste treatment via electrospun mat obtained from waste polystyrene,* Fibers and Polymers, 19 (4), 767-774 (**2018**)
- Aslı Çelik, Gökhan Topçu, Tuğba Isık, Nesrin Horzum, Mustafa M. Demir, *Investigation of Lithium Sorption Efficiency Using SWCNT Functionalized Electrospun Fiber Mats from the Hypersaline Geothermal Brine,* Materials Science Forum, 915, 121-126 (**2018**)
- Tuğba Isık, Mustafa M. Demir, Cansu Aydogan, Mustafa Ciftci, Yusuf Yagci, *Hydrophobic coatings from photochemically prepared hydrophilic polymethacrylates via electrospraying*, Journal of Polymer Science A: Polymer Chemistry, 55, 1338–1344 (**2017**)
- Tuğba Isık, Nesrin Horzum, Ü. Hakan Yıldız, Bo Liedberg, Mustafa M. Demir, *Utilization of Electrospun Polystyrene Membranes as a Preliminary Step for Rapid Diagnosis,* Macromolecular Materials and Engineering, 301, 827–835 (**2016**)

BACK COVER